POLITECNICO DI MILANO

Scuola di Ingegneria dei Sistemi

Corso di Laurea Magistrale in
Ingegneria Gestionale

In-Process Quality Monitoring via sensor data fusion: chatter control in grinding.

Relatore: Ch.ma Prof.ssa Bianca Maria Colosimo

Correlatore: Ing. Marco Grasso

Tesi di Laurea Magistrale di:

Matteo F. Maggioni Matr. 783979

Elena Marzorati Matr. 783978

Anno Accademico 2012 – 2013

Ai miei genitori, per avermi supportato.

A mia sorella, perché le sia di spunto per il futuro.

Ai miei genitori, per avermi supportato.

A mio fratello, per avermi motivato verso questo percorso.

Ringraziamenti

Desideriamo ringraziare in primo luogo la Prof.ssa Bianca Maria Colosimo per l'opportunità offertaci di cooperare all'interno di un importante progetto industriale.

Ringraziamo sentitamente l'Ing. Marco Grasso per la disponibilità, il supporto e le competenze che ci ha trasmesso in questo percorso.

Inoltre vorremmo ringraziare il team di ricercatori ITIA–CNR, Prof. Giacomo Bianchi, Ing. Marco Leonesio, Ing. Paolo Parenti e Ing. Alberto Cassinari, per la disponibilità e il supporto tecnico.

Ultimi, ma non meno importanti, siamo grati alle nostre famiglie e ai nostri amici che ci hanno supportato ma soprattutto sopportato durante questa esperienza.

Contents

List of Figures

List of Tables

Abstract

This work summarizes the results of a research project involving a world-leader producer of grinding systems for rolls to be used in hot and cold rolling. The main aim of the research project was to develop an innovative software aimed at controlling the grinding process to avoid vibrations (namely chatter) occurrences, which result is a bad quality of the surface of the ground rolls. In this project we proposed an *in-process* quality monitoring approach for chatter identification to be used in the machine control software.

The traditional quality monitoring approach consists in the inspection of the final product. However, in this way the identification of any problem or deviation, that may occur during the process, takes place downstream of the sampling of the produced parts, resulting in a consequent delay in response to process errors. In recent years, the study of in-process SPC, i.e. based on the analysis of sensor signals and data acquired during the process, has received considerable attention. The analysis of in-process signals rather than post-process measures gives the ability to quickly recognize deviations from normal working conditions. However, this paradigm shift requires the use of more sophisticated techniques rather the ones used in traditional SPC.

In this framework the SPC signals-based requires the adoption of multivariate techniques to summarize information content of the signals to quickly detect a variation in the working conditions (i.e., a degradation in the quality of the output). The idea of the work is to make use of different accelerometric signals to identify the *technological 'signature'*, which represents the process behavior under normal working conditions. The approach to identify this technological signature relies on the use of multivariate statistical analysis, based on the principal component analysis technique (PCA).

Having defined the process signature, the control system reports alarms when a change in the signature occurs, leading to a degradation of the output quality. Great efforts have been done in finding an approach that is *robust* to the variation of the process parameters (determined for example by the control parameters) which don't affect the quality of the final product. Actually, many techniques that ignore the robustness analysis as a key characteristics of a quality control system, generate false alarms when process parameters are varied, even if this variation doesn't affect the output quality. The high rate of false alarms, typical of these approaches, is the main cause of the monitoring system's deactivation. The thesis work is based on real industrial data on which a comparison with different approaches has been conducted to prove the effectiveness of the proposed approach.

Sommario

Questo lavoro riassume i risultati di un progetto di ricerca che ha coinvolto un leader mondiale nella produzione di sistemi di rettifica per cilindri impiegati in laminazione a caldo e a freddo. Lo scopo del progetto consisteva nel realizzare un software innovativo per controllare che, durante il processo di rettifica, non si sviluppino vibrazioni (*chatter*) che causano una scarsa qualità superficiale del cilindro rettificato. Abbiamo contribuito in questo progetto proponendo un approccio di monitoraggio *in-process* da implementare nel software di controllo della macchina per identificare il chatter.

L'approccio tradizionale del monitoraggio della qualità consiste, tipicamente, nell'ispezione del prodotto finale. Tuttavia, in questo modo l'identificazione di una variazione nel processo avviene a valle del campionamento delle parti prodotte, che si traduce in un ritardo nella correzione dei problemi di processo. Recentemente lo studio dell'SPC applicato ai processi, ovvero basato sull'analisi di segnali acquisiti durante il processo produttivo, ha ottenuto notevole attenzione. L'analisi dei segnali durante il processo, a differenza delle misure a valle, offre la possibilità di identificare più velocemente variazioni nelle condizioni nominali di lavoro. Questo cambio di approccio comporta una rapida e tempestiva risposta a situazioni di fuori controllo ma chiede un salto di qualità nelle tecniche tradizionalmente usate in ambito SPC. Implementare approcci SPC su segnali richiede tecniche multivariate che consentano di sintetizzare il contenuto informativo presente nei segnali per individuare rapidamente condizioni di funzionamento degradato.

L'idea del lavoro è quindi partire da diversi segnali (provenienti da accelerometri) e identificare la firma tecnologica, cioè il comportamento sistematico che caratterizza il processo in condizioni di funzionamento nominale. Questa firma tecnologica nel lavoro è identificata attraverso l'uso di tecniche di analisi statistica multivariate basate sull'analisi delle componenti principali.

Nota la firma tecnologica, il sistema identifica con allarmi i cambiamenti della firma che comportano il peggioramento della qualità in uscita. Particolare enfasi è data nel lavoro all'identificazione di un approccio robusto a cambiamenti del processo (dovuti ad esempio a variazioni nei parametri di controllo) che non inducono cambiamenti nella qualità del prodotto. Infatti, molte tecniche che non considerano l'analisi di robustezza come aspetto rilevante di un sistema di controllo qualità, segnalano allarmi al variare delle condizioni di processo anche quando questa variazione non si traduce in un peggioramento della qualità. Il rischio di questi approcci è un eccessivo tasso di falsi allarmi che porta alla disattivazione del sistema di monitoraggio.

La tesi si basa su dati reali e su un confronto di prestazioni con metodi alternativi esistenti per dimostrare l'efficacia del metodo proposto.

Introduction

'It is dark in front of the grinding grain'
Toenshoff & Grabner

The traditional quality control approach consists in the inspection of produced parts, typically sampled at regular intervals, evaluating the product's characteristics of interest. By monitoring the evolution of these characteristics it is possible to verify if the process is actually in control. Monitoring done in this way, is, however, focused on the inspection of the final product, that is the final result of the production process, although the objective of quality monitoring is to maintain the process itself under control.

This type of approach is commonly used in industry, but in some applications it may present some limitations. The identification of any problem or deviation that may occur during the process only takes place downstream of the sampling of the produced parts. The result is a consequent delay in the response to process errors, which, in the meantime, has continued to produce parts that may not be acceptable. This delay leads to a waste of time and materials, resulting in cost increase and productivity reduction for the enterprise.

Statistical Process Control (SPC) has had a long history of successful use in discrete parts manufacturing. Indeed in continuous processes, such as those found in the chemical and process industries, or in long-run manufacturing processes, the Engineering Process Control approach (EPC) is often used to reduce variability. This approach is based on process compensation and regulation, in which some manipulatable process variable is adjusted with the objective of keeping the process output on target.

In recent years, the study of in-process SPC, i.e. SPC procedures based on the analysis of sensor signals and data acquired during the process, has received considerable attention. This is mainly due to an important factor: be more competitive. This, coupled with the advent of improved on-line sensor technology and automation and the increase of on-board computational capability has led to a continuous growth of studies on the in-process monitoring

and controlling.

The analysis of in-process signals rather than post-process measures gives the ability to quickly recognize deviations from normal working conditions which may result into lower costs and less wastes, thanks to possible automated corrective actions applied during the process.

Our works takes place in this frame of in-process monitoring of sensor signals. The aim of this work is to monitor the surface quality in cylindrical grinding process on rolls for hot rolling machines, by monitoring the signals acquired during the process. The final characteristics that distinguish a good roll from a not acceptable one include the surface roughness, the waviness, the presence of burned areas, and the presence of other anomalous surface patterns, in addition to large scale geometrical errors. Monitoring the surface of the roll is crucial; in fact, a milled roll which presents noncompliant values of roughness, is not suitable to be used in hot or cold roll milling. The presence of chatter marks on the roll's surface highly affects the performance of the rolling machines not only producing several wastes but also damaging the machine itself. The laminated parts, milled with a waved roll, present the same geometry on their surface and might be affected by dangerous internal stress that can be generated. These quality features are the result of the roll grinding process, that is why it is strategic to monitor the stability of the process itself. Currently, these quality characteristics are monitored by means of qualitative approaches. Usually, the operator observes during the grinding process the ripple of the current absorbed by the machine through time and derives a subjective consideration about the ongoing process stability. The experience allows him to know if anomalous vibrations have been established, however this monitoring approach is unreliable and stands only on empirical basis. Indeed, the major standardized controls are done post-process where a subjective analysis of the surface is coupled with a roughness measurement on the worked roll. To overcome the subjective in-process quality supervision, we propose an approach for monitoring a grinding process which, fusing informations from different process signals, detects variations from good working conditions. The purpose is the identification of process abnormalities, such as chatter development, that lead to rework a roll.

Chatter vibrations, Inasaki says [14], *of the various difficulties, is one of the most crucial ones because it hinders higher form accuracy as well as better surface finish of the parts ground, which both are the main objectives of grinding.*

Chatter is a vibrational phenomenon which arises in machining grinding processes for specific combinations of cutting parameters. It consists of unstable, chaotic motions of the tool or of the workpiece and by strong

anomalous fluctuations of cutting forces. The onset of chatter may cause abnormal tool wear or tool breakage, damage of both the tooling structure and the spindle bearings, poor surface roughness and poor dimensional accuracy of the workpiece [20].

According to Altintas, [2], *the most common vibrations are due to self-excited chatter vibrations, which grow until the tool jumps out of the cutting zone or breaks because of the exponentially growing dynamic displacements between the tool and workpiece.* The presence of chatter vibrations is a very important phenomenon because, when they are present, the process is very unstable, producing large-amplitude, oscillating cutting forces, greatly affecting the surface quality.

The chatter is of course an assignable cause-type disturbance which leads to an increase of the variability of the products. Poor surface roughness and poor dimensional accuracy mean wastes, which translates directly in costs.

The traditional SPC approach would have monitored the surface quality of the roll downstream all the operations, measuring the roughness obtained, building a control chart to monitor this quality characteristic. However, the new trend is to use sensors to monitor its state during the operations and our case study focuses in this area of interest. Specifically, our attention is focused on the integration of a chatter detection system into the control unit of machine tool. The integration of an SPC based approach, capable of detecting the chatter phenomenon, with an EPC module, that controls an intelligent grinding machine, leads to a great improvement in machining precision.

We will propose a method for extracting informations from the grinding machine, through the acquisition of the signals of the sensors mounted on the machine: these signals allow the monitoring of the process variables of interest that characterize both the behavior & the state of health of the machine, and the stability & quality of the process. As several sources of information will be used, we will face the problem of managing and organizing large amounts of data provided by the sensors, and finding the best way to put them together. The technique that helps to solve the problem of merging data from multiple signals is known in literature as *sensor fusion*. We consider an approach to integrate information from different sources, and, at the same time, to achieve a synthetic characterization of the process. It consists of an extension of *Principal Component Analysis (PCA)* that allows dealing with multi-channel signals. It works by transforming a set of data from multiple sources into a synthetic feature set that explains the correlation structure of original data. These data come from the accelerometers placed on the machine and from the CNC unit that controls it. Signals coming from a manufacturing process can be sampled at high frequency leading to a big

amount of data that has to be considered in the statistical analysis. For this reason, the common approach is to conduct the analysis not on the raw data but on a selected group of synthetic indicators that allow to catch and identify some interesting features [27].

Monitoring techniques based on *multivariate analysis* and *data fusion* allow to study the process, exploiting the relations between the characteristics of the process itself and the various sources of information, thus making the results of analysis more complete. It is known that process signals often present characteristics of dependency between them, which in most cases considerably affect the evolution of the overall system. For this reason it is interesting to identify and monitor these features in order to estimate the quality of the ongoing process.

An 'in process' monitoring system, based on the implementation of a multivariate control chart on signals process, will be designed. The SPC determines if any change occurs in the process or in the state of the machine.

The intent is then to provide a complete monitoring system, reliable and robust to external disturbances and to dependency on operating conditions of the process and, for this reason, we use different sources of information, i.e. sensors positioned in different points of the machine, which detect different characteristics.

One of the challenges that we faced during the monitoring system design has been trying to isolate the effect of chattering vibration from new modes of vibration induced by changing process input parameters. In fact varying process parameters, such as wheel speed or infeed, can cause a different ways in which the machine vibrates. A not sufficiently robust system could interpret any on-line parameter modification as a deviation from in-control conditions, leading to a large number of false alarms. To try to solve this problem, which is crucial for an industrial application, we looked for a subset of indicators that could be insensitive to the variation of process parameters but sensitive to chatter vibrations. By designing an experimental campaign, that we run on a grinding machine, we have been able to select a reasoned subset of indicators, suitable to be implemented in the monitoring approach. Thanks to the availability of real industrial data we actually tested and identified the behavior of these indicators during working conditions.

Fusing these indicators together, by means of multivariate statistical approach, we investigated the design of a more robust monitoring system then the one currently in use for chatter monitoring. It is cheaper because it doesn't require highly skilled human supervision and it is objective because it is based on a statistical model. Furthermore this approach is not only easier to be implemented, compared to what is currently proposed in the specific literature, but it represents a competitiveness driver for the machine

manufacturer and cost efficiency driver for the machine user. A machine that is able to identify process instability is a machine that reduces wastes of time and materials, then is a much valuable product to be sold on the market.

The document is organized according to the following structure:

Chapter 1 introduces the reader into the grinding process. Then a brief description of the chatter phenomenon and its origins is provided. Then, a review of approaches used in literature for chatter detection in grinding is proposed.

Chapter 2 explains the theoretical framework of the sensor fusion approach on which this work is based, providing a review of the technique and the assumptions adopted. Then, the development of the strategy used to monitor the process is proposed.

Chapter 3 describes the main points of the industrial case; first the machine set-up and the signals used for the process monitoring are explained; then the focus moves on the role of the signal-based SPC approach in the industrial application.

Chapter 4 discusses the strategy that is proposed to detect the development of the chatter phenomenon. The experiments made on the machine are explained and the assumption and methods used for the dataset characterization are summarized. Then, synthetic indicators calculated on the accelerometric signals are proposed.

Chapter 5 shows the results of the application of the proposed approach on some tests.

Chapter 6 shows a further approach that could be used in the analysis, and then it will be tested.

Chapter 1

A state of the art on chatter detection in grinding

1.1 Grinding process

Before explaining the industrial case it is important to briefly focus on the basics of the grind process and the specific issue for which the statistical process control has been developed.

Grinding is a term used in modern manufacturing practice to describe machining with abrasive wheels, pads, and belts. Grinding wheels come in a wide variety of shapes, sizes, and types of abrasive [28]. Grinding is essentially a chip-removal process where the cutting tool is the single abrasive grain. Abrasive are generally the last operations conducted on a workpiece. This type of process, however, is not only limited to the surface finishing or to small material amount removal; in fact, it can be used for the removal of relatively high quantity of materials. That is why it is important to separate two kind of grinding: *roughing* and *finishing*.

The common grinding operations are:

- surface grinding;
- cylindrical grinding;
- internal grinding;
- centerless grinding.

The selection of a grinding process for a particular application depends on the workpiece shape and features, size, ease of filtering, and production rate required [17]. Each of these typologies can be furthermore classified by the movement direction.

Surface grinding is one of the most common operations, generally involving the grinding of flat surfaces. Typically, the workpiece is secured on a

magnetic chuck attached to the worktable of the grinder. A straight wheel is mounted on the horizontal spindle of the surface grinder. Traverse grinding occurs as the table reciprocates longitudinally and is fed laterally (in the direction of the spindle axis) after each stroke.

In cylindrical grinding, the external cylindrical surfaces and shoulders of workpieces such as crankshaft bearings, spindles, pins, and bearing rings are ground. The rotating cylindrical workpiece reciprocates laterally along its axis to cover the width to be ground. In roll grinders used for large and long workpieces such as rolls for rolling mills, the grinding wheel reciprocates. The workpiece in cylindrical grinding is held between centers or in a chuck, or it is mounted on a faceplate in the headstock of the grinder. For straight cylindrical surfaces, the axes of rotation of the wheel and workpiece are parallel. The wheel and workpiece are driven by separate motors at different speeds. Long workpieces with two or more diameters can be ground on cylindrical grinders [17].

In internal grinding, a small wheel is used to grind the internal surface of the part. Centerless grinding is a high-production process for continuously grinding cylindrical surfaces in which the workpiece is supported not by centers or chucks, but by a blade.

In fig. 1.1 it is shown a scheme of surface grinding and cylindrical grinding.

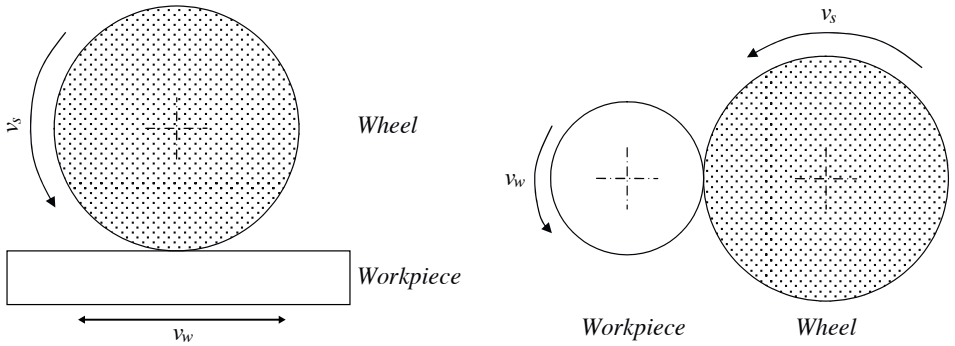

(a) Flat surface grinding (b) Cylindrical grinding

Figure 1.1: Two types of grinding: surface and cylindrical.

In this study, we will focus on the roughing phase in cylindrical grinding because this very first stage, that leads to the final product, may highly affects its quality and it may be affected by process instability phenomena. Grinding in fact is a strategic process for high-technology applications. It is in use in all the manufacturing processes that require high surface quality.

Tab. 1.1 shows the main four categories of roughness in which the grinding

Table 1.1: Surface roughness for grinding operations.

Precision [μm]	**Fine** [μm]	**Medium** [μm]	**Rough** [μm]
0.1	0.2 - 0.4	0.8 - 1.6	3.2 - 12.5

operations are divided. As it is possible to see, in this type of process the roughness moves in a large range. The grinding process can reach different levels of roughness, in function of the final application of the grinded piece. In some applications the required roughness is obtained with simple *roughing* passes, in other cases, when levels of roughness between 0.4 to 0.1 μm are required, *finishing* passes are performed. In this study, as it will be explained in chapter 3, the final roughness required is $R_a = 0.6\ \mu m \pm 10\%$, that calls for operations between the *medium* and *fine* range.

Roughness can be reduced down to mirror finishes and optical quality of flatness. The achievement of this quality depends on the roughness of the abrasive, the quality of the grinding machine and the removal rates employed. Grinding can ensure good quality where other processes may have difficulty meeting specifications. Quality is a term that includes all aspects required for parts to function correctly, then accuracy of dimensions and surface finish are obvious aspects of quality of a grinding process.

Despite all this, the grinding process is frequently considered as one of the most complex and difficult to control manufacturing processes due to its complex, nonlinear and stochastic nature. We will discuss this complexity in the following section, focusing on the chatter phenomenon which is the main issue of this work.

1.2 The chatter phenomenon

Vibrations represent a very important problem that afflicts the grinding process, because they deteriorate the wheel conditions, decreasing its performance and directly affecting the surface finish. Many different factors can cause vibrations, for example components of machinery or even external sources, such as nearby machinery; moreover, the grinding operation itself can cause vibrations from the process, and this specific phenomenon is called *regenerative chatter* [17]. In Figure 1.2, are shown the types of vibration involved in this type of process. This kind of chatter is one of the most important cause of vibrations, generated by an excitation of the system that grows, and it occurs at the natural frequency of the spindle and workpiece.

Grinding chatter is one of the most critical errors in grinding operations

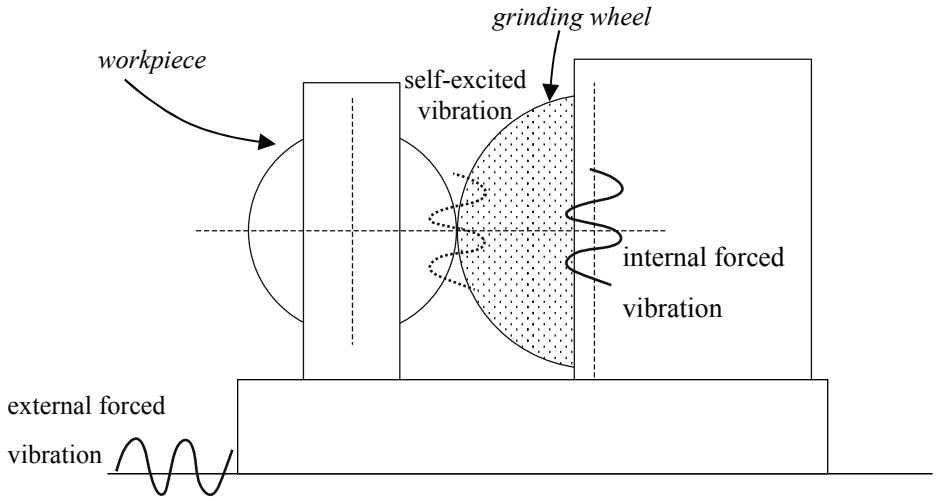

Figure 1.2: Chatter vibrations in grinding processes.

and one that has a strong impact on the ultimate geometrical workpiece accuracy [14]. In fact, chatter vibrations leads to poor surface quality, increased wheel wear and additional time and costs, due to the grinding passes aimed at removing the chatter marks on the part; moreover it can reduce the accuracy and the productivity of the machinery. For all these reasons, chatter continues to be a problem in grinding.

Vibrations generate *chatter marks* or *waviness* on the ground surfaces, as a light wave of the surface. The waviness is the effect of process vibration during grinding. When the system vibrates at a single frequency (as in the usual case of forced or chatter vibration) the wheel and the roll oscillates periodically in the radial direction modifying the actual depth of cut i.e. the actual infeed. Periodic surface defects are then generated in the form of waviness on the roll and, eventually, on the wheel surface. The theoretical shape of the waviness is sinusoidal. In Figure 1.3, it is shown a cylinder affected by waviness, where is visible that the cylindrical surface has alternate light and dark streaks.

General guidelines have been established to reduce the tendency for chatter in grinding, especially using soft-grade wheels, dressing the wheel frequently, changing dressing techniques, reducing the material-removal rate, and supporting the workpiece rigidly.

Generally, an experienced operator might detect, downstream of the process, if the chatter phenomenon was generated during the grinding operations, looking at the final roll surface. However, this procedure is often difficult; in fact, some times the waviness on the cylinder is visible with the naked

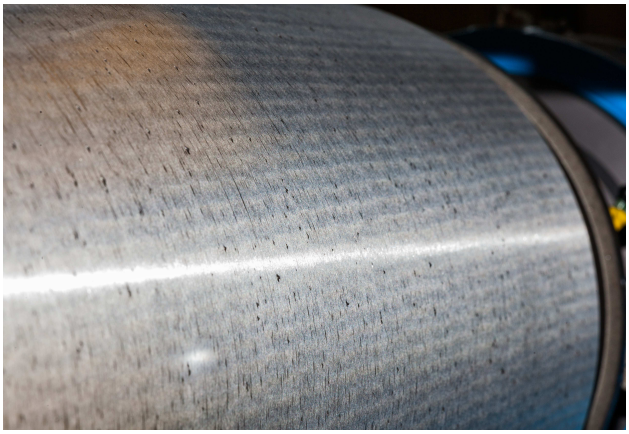

Figure 1.3: Chatter marks on a cylinder.

eye, while in other cases, observing the phenomenon requests the use of some lamps, oriented in a specific way. This approach however can only be used post-process. A second method currently used for chatter detection is the observation of some signals acquired in-process, through the man-machine interface. Despite this technical know-how developed by the single operator, it is not always easy to detect the growth of this phenomenon, which sometimes may be detected only when the job has been completed. However, both methods are subjective, qualitative and mainly unreliable. In any case, these detection capability requests proper skills and knowledge that the operator acquires during the time. Moreover, the show up of chatter marks on a cylinder represents a direct cost for the manufacturer which has to rework the workpiece leading to a waste of time and money. Recognizing as soon as possible the growth of the phenomenon is essential.

The development of accelerometric and acoustic emission sensors, and the continuous improvement of real-time computational capability offers the possibility to adopt other innovative techniques, that use specific sensors, to monitor the vibrations during the grinding process, helping the operator in reducing the variability of the final product. This possibility has become of great interest in many areas of manufacturing, and it has become a reality in some processes. For what concerns the grinding process, due to its complexity detailed before, this automatic monitoring and control is still on open project.

In this frame, the aim of our study is to fuse the large amount of data coming from a fully sensor-equipped grinding machine to try to achieve a robust, reliable and synthetic characterization of the process.

The goal is then to develop an SPC approach for the chatter monitoring that might be part of an EPC for grinding machines acting, for example, in hot rolling plants where the roll quality is mainly related to their surface waviness. SPC and EPC have to work together, the first monitoring the vibrations and the second suggesting or automatically adjusting, through a direct connection with the machine numerical controller, process parameters in order to maintain the waviness under a prescribed threshold.

1.3 State of art

In literature, it is possible to find a wide variety of studies that engage the problem of monitoring a grinding process. Analyzing the literature regarding these issues, different aspects can be distinguished with which to observe this process.

There are some studies that are focused on monitoring techniques to make the grinding process and the dressing process more reliable and economical. In this context, studies are concentrated upon the signals monitoring, to extend the wheel life and to optimize the grinding operations cycle, such as the works made by Inasaki [13], Tönshoff *et al.* [29] and Karpuschewski *et al.* [18]. Other authors have instead focused their studies on the vibrations monitoring during the grinding operations. Among these authors, the most important contributions were made by Inasaki [14], Gradišek *et al.*[9] and Gonzalez-Brambila *et al.* [8].

In the work of Tönshoff *et al.* [29] a review and classification of which signals and quantities are most suitable to fulfill a monitoring task is proposed. When choosing a suitable sensor, they advise that grinding process variants such as internal, external or surface grinding, the kind of material to be machined and its sensitivity to surface integrity, or the geometric quality which has to be achieved, have to be taken into consideration. Furthermore it is pointed out that monitoring the grinding process means generally that one or several output signals are observed to follow different targets such as optimizing the process with respect to machining costs or workpiece quality. Then a classification of process signals and output values that can be used for monitoring purposes is given in fig. 1.4a.

Moreover Tönshoff proposes a classification of the approaches that can be followed in process monitoring for modeling output quantities related to process quantities. As summarized in fig. 1.4b, models can be divided into two origins, those developed based on physical relationships and those based on empirical means. A physical model is developed from an understanding of the fundamental physical principles underlying the process. With spe-

cific objectives in mind, relevant physical processes are selected on the basis of process knowledge and a qualitative model is worked out. Based on the conformity to physical laws, the physical model is established using a mathematical function of the qualitative model. On the contrary, an empirical model is established by the means of measured values which have been obtained in grinding experiments. With respect to the objectives, relevant input and output quantities of the grinding tests are registered. Subsequently, a model type is chosen and the relationship between input and output of the model are identified using experimental data. The work concludes that a combination of physical and empirical models is of extremely high relevance for grinding.

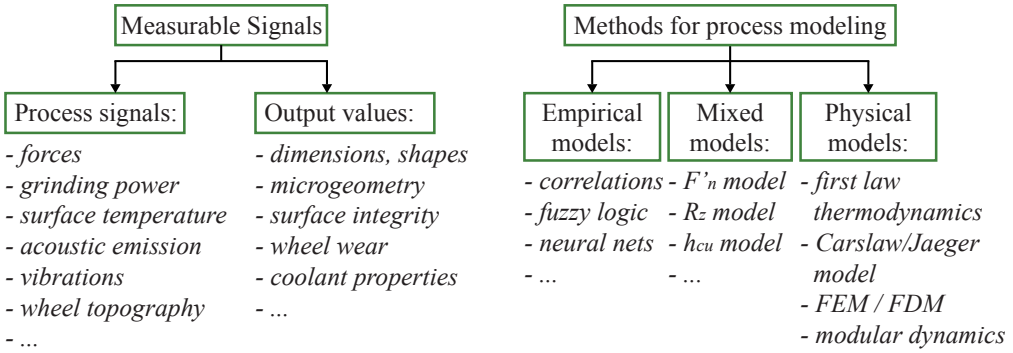

(a) Signals and quantities for monitoring purposes

(b) Methods of process modeling

Figure 1.4: Signals & methods for monitoring purposes by Tönshoff [29].

Inasaki in 1999 [13], proposed an approach for minimizing the grinding cycle time while meeting the requirements for the ground part quality, detecteding the problems in the grinding process. To do this, in his work, an approach to fuse two different types of sensors on the machine is carried out: the acoustic emission sensor (AE) with a power one. An intelligent grinding database, that makes use of Artificial Neural Networks (ANN), will automatically optimize the grinding cycle. Inasaki claims that there are many set-up parameters in addition to the grinding wheel and grinding fluid selection to be predetermined, such as wheel surface speed, workpiece speed and infeed-rate. It is pointed out in the paper that, among those parameters, the most influential on the grinding result is the infeed-rate. For these reasons the simultaneous use of two different sensors is proposed: the AE one will be used for the detection of contact between the grinding wheel and the workpiece, and the chatter vibration, which must include the high-frequency component of the signal, and the surface roughness deterioration. The other

one will be used for detecting grinding burn.

Karpuschewski *et al.* [18] discussed a monitoring approach based on data fusion from different sensors sources and artificial intelligence. They propose to provide with sensor the machine, getting more information of the process. They choose to implement an AE sensors and a power sensor. Monitoring the wheel life is very important, because when a grinding wheel exceeds its life time different kinds of disturbances, e.g. chatter or increased ground part surface roughness, may occur. To do this, in this paper the FFT of the enveloped AE signal is analyzed. To minimize the idle time instead, a fuzzy based system is used, built on power parameters and the low frequency component of the AE signal. The AE signal and the power signal are effectively fused for optimizing the grinding cycle. For example, the AE signal is used for minimizing the time constant, while the power signal is used for maximizing the infeed rate of the rough grinding process.

Until now, we have proposed a review of the literature that takes into consideration many general aspects on the grinding monitoring; we will focus now on a specific review of the works regarding the chatter detection and monitoring.

Inasaki [14], shows in his work that there are many input parameters that might affect the chatter generation; on the other hand, he illustrates that there are many different measurement tools that can be used to detect the chatter phenomenon. A distinction between different sensors is made:

- *Sensors for process quantities*: forces, power, acceleration, temperature or acoustic emission are quantities that, with dedicated sensors, is possible to monitor during the grinding operations. For chatter detection, the most appropriate to apply are accelerometer, force and acoustic emission sensors. For these kind of three sensors usually a FFT analysis of the recorded signals is conducted.
- *Sensors for the grinding wheel*: during the process, it is possible to monitor the state of the wheel with a laser triangulation sensor. In fact, the macro geometry of the grinding wheel plays a major part in the occurrence of chatter.
- *Sensors for the workpiece*: to monitor the chatter generation, many approaches to directly measure the waviness on the roll during the process are studied. However the detection of waviness in the circumference of symmetrical rotation parts during grinding is more complex due to the demand for a significantly higher scanning frequency. For this reason some studies introduce innovative contact measurement methods, other studies instead propose optical measurement approaches.

In 2003, Gradišek *et al.* [9] suggest a method to automatically detect

chatter in grinding. In this study, they compare the performance of two different indicators of chatter: the coarse-grained information rate (CIR) indicator, calculated from fluctuations of the normal grinding force F_n, and the entropy indicator, calculated from a power spectrum. In conclusion of the work, Gradišek *et al.* show that the performance of the proposed indicators is comparable, and they both are suitable for chatter detection. In contrast with the calculation of the RMS acoustic emission signals, that indicate only the cases of strong, fully developed chatter, CIR and entropy indicators detect chatter already in its early, developing stage, even before the workpiece has been damaged. However, this method, even if based on a threshold approach and not a statistical one, it is not free of false alarms. This false alarms are caused by harmonic vibrations in the measured signals which become pronounced in the absence of chatter vibrations but are not associated with them.

Another different approach, that has the same aim of chatter detection, has been studied by Gonzalez-Brambila *et al.* [8]. In this work, a technique for chatter detection by means of waviness on-line measuring is presented. Waviness is measured with a mechanical stylus profiler featuring a diamond tip; the output signal is later converted to digital form and transformed to the time–frequency domain by means of the wavelet transform, allowing its coefficients to grow as a function of surface defects and highlighting chatter marks. The signal is analyzed with a Daubechies 4 wavelet. The fourth level is used for chatter detection. The method was validated by extensive experimentation with actual production parts, and the authors claim that it can be easily integrated into the production process for manufacturing and quality control. This approach is not process quantities oriented but feature dimension oriented and then it doesn't monitor the growth of chatter but only the actual presence.

A second approach that uses the wavelet decomposition is used by Yao *et al.* [31]. Differently from the previous work, in this case the identification of chatter is based on accelerometric data and then is considered to be a process quantities oriented model. The authors present an intelligent chatter detection system based on signal analysis through wavelet decomposition and chatter condition identification through Support Vector Machine (SVM). After wavelet decomposition of the accelerometric data, two indicators are calculated: standard deviation of wavelet transform and wavelet packet energy ratio. Making use of these two indicators, a method based on chatter recognition with SVM is built. After that, a training phase is realized, which is followed by a testing phase, which shows an accuracy rate of about 95% for machining state recognition.

Chapter 2

The PCA Approach: a theoretical framework

2.1 PCA as a multi-sensor fusion approach

In the previous chapter we have seen some approaches followed in the chatter monitoring literature. Many authors proposed the usage of multiple sensors to detect the chatter phenomenon, but in most of the case empirical threshold methods are considered to identify the growth of vibrations during the grinding process. Thanks to the continuous evolution of integrated sensor equipments, together with the increase of on-board computational capability, we have achieved the possibility of *in-process* data analysis to monitor and control manufacturing processes evolution such as the development of chattering in grinding. Machines are being equipped with different sensors capturing various process features during working conditions, because making use of a signal from a single drive might not be reliable. On the other hand the sensitivity of signals from different drives may change depending on several process factors; for these reasons the integrated monitoring of multiple signals with multivariate techniques allows capturing correlation among different sources, leading to a more effective process monitoring during different operative conditions.

The main goal of multi-sensor data fusion for process monitoring consists, then, in extracting the knowledge about the working conditions of the machine and the quality and stability of the process, which is somehow better than the one which could be provided by a single signal, or by multiple signals when no actual data integration is applied [10].

The integrations of these multi-sensor data, acquired during a roll grinding process, will be based on an extension of the Principal Component Analysis (PCA) technique, called vectorized PCA. With PCA, informations coming from machine sources will be fused to identify good working condition

patterns. These patterns will be monitored through a multivariate control chart with empirical control limits with the purpose of detecting a precise process cause of variation: the chatter phenomenon.

Along this analysis important issues have to be faced with, such as the time-varying nature of grinding processes, the modification of the wheel geometry, the change of cutting conditions and other working parameters. PCA can be an appropriate methodology to investigate correlations between signals pattern on which a robust monitoring process can be built.

Before explaining the industrial case on which this approach is intended to be tested, we will briefly provide a review of the technique and its assumptions adopted in this work. Hence the monitoring strategy, that has been applied on real industrial data, is detailed.

2.2 The fundamentals of the PCA technique

Principal Component Analysis is probably the oldest and best known of the techniques of multivariate analysis. It was first introduced by Pearson (1901), and developed independently by Hotelling (1933). Even if we make use of an extension of the traditional PCA, the basic technique remains the same. The central idea of Principal Component Analysis is to reduce the dimensionality of a data set in which there are a large number of interrelated variables, while retaining as much as possible of the variation present in the data set [16]. This reduction is achieved by transforming the data set to a new set of variables, the principal components, which are uncorrelated, and which are ordered so that the first few retain most of the variation present in all of the original variables. Computation of the principal components reduces to the solution of an eigenvalue-eigenvector problem for a positive-semidefinite symmetric matrix.

This apparently simple technique has a wide variety of different applications, and it has been used even in many industrial applications as a support for on-line monitoring of multivariate processes. For example Nomikos and MacGregor in 1995 proposed an approach for monitoring batch processing using an extension of the PCA called Multiway PCA [24]. In 2007, Colosimo and Pacella proposed a method that uses Principal Component Analysis instead of regression to identify patterns in geometric profile data [5]. Further development of PCA are in the approach of Colosimo and Grasso where a PCA-based multivariate SPC approach to auto-correlated data is proposed, making use of a Moving PCA based on the "moving time window" concept [11]. Recent works make still use of the PCA technique, extended to be used in a multi-sensor based condition monitoring approach for tool breakage detection in milling of hard-to-cut materials. [10].

Despite the different extensions of the principal component analysis techniques that are proposed in literature, they are based on the same idea of making use of orthogonal linear transformations that transforms the data to a new coordinate system such that the greatest variance by any projection of the data comes to lie on the first coordinate, the second greatest variance on the second coordinate, and so on. A complete description and further developments of this technique can be in found in [16] and [15].

To introduce the basis of the PCA theory we refer to $\mathbf{x}$ as a vector of p random variables. These variables are, in this case study, observations of different signals sources. The variances of the p random variables and the structure of the covariances or correlations between the p variables are of interest and we want to monitor their evolution during the process.

We refer then to

$$X = [X_1, X_2, \ldots, X_k, \ldots, X_N]^T$$

as a matrix of N observations of multivariate vectors X_k collected during the process where

$$X_k = [X_{k,1}, X_{k,2}, \ldots, X_{k,P}]^T$$

where $p = 1, \ldots, P$ is the number of monitored variables at the time $k = 1 \ldots N$.

We make use of a portion of X that we define $X_{\{1:M\}}$ as $(M \times P)$ matrix of $M < N$ in control observations that are used to generate the reference PCA model:

$$X_{\{1:M\}} = \begin{bmatrix} X_{1,1} & \ldots & X_{1,p} & \ldots & X_{1,P} \\ \vdots & \ddots & \vdots & \ddots & \vdots \\ X_{k,1} & \ldots & X_{k,p} & \ldots & X_{k,P} \\ \vdots & \ddots & \vdots & \ddots & \vdots \\ X_{M,1} & \ldots & X_{M,p} & \ldots & X_{M,P} \end{bmatrix}$$

Dealing with different sources of informations to be analyzed with PCA, it is a common practice, when columns of the X matrix are referred to different quantities, to work with the standardized $\tilde{X}$ matrix that can be easily calculated as follows:

$$\tilde{X}_{k,p} = \frac{X_{k,p} - \bar{X}_{\{1:M\},p}}{\sigma_{\{1:M\},p}}$$

where $\bar{X}_{\{1:M\},p}$ is the mean value of the p^{th} variables and $\sigma_{\{1:M\},p}$ is the standard deviation of the p^{th} variables from the same data matrix.

The first step after having standardize our values is to look for a linear function $\boldsymbol{\alpha}_1{}'\mathbf{x}$, of the elements of $\mathbf{x}$, having maximum variance, where $\boldsymbol{\alpha}_1$ is a vector of p constants $\alpha_{1,1}, \alpha_{1,2}, \ldots, \alpha_{1,p}$ so that:

$$\boldsymbol{\alpha}_1{}'\mathbf{x} = \alpha_{1,1}x_1 + \alpha_{1,2}x_2 + \ldots + \alpha_{1,p}x_p = \sum_{k=1}^{p} \alpha_{1,k}x_k$$

The procedure goes on looking for a linear function $\boldsymbol{\alpha}_2{}'\mathbf{x}$, uncorrelated with $\boldsymbol{\alpha}_1{}'\mathbf{x}$ having maximum variance, and so on, so that at the k^{th} stage a linear function $\boldsymbol{\alpha}_k{}'\mathbf{x}$ is found that has maximum variance subject to being uncorrelated with $\boldsymbol{\alpha}_1{}'\mathbf{x}, \boldsymbol{\alpha}_2{}'\mathbf{x}, , \ldots, \boldsymbol{\alpha}_{k-1}{}'\mathbf{x},$. The k^{th} derived variable, $\boldsymbol{\alpha}_k{}'\mathbf{x}$ is the k^{th} PC. Up to p PCs could be found, but it is hoped, in general, that most of the variation in x will be accounted for by m PCs, where $m \ll p$.

In practice it is quite usual that the vector of random variables $\mathbf{x}$ has an unknown covariance matrix $\boldsymbol{\Sigma}$, for this reason it is replaced by the sample covariance matrix $\mathbf{S}$ that can be calculated as follows:

$$\mathbf{S}_{\{1:M\}} = \frac{1}{M-1} X^T_{\{1:M\}} X_{\{1:M\}}$$

For $k = 1, 2, \ldots, p$ then the k^{th} PC is given by $z_k = \boldsymbol{\alpha}_k{}'\mathbf{x}$ where $\boldsymbol{\alpha}_k$ is an eigenvector of $\mathbf{S}$ corresponding to its k^{th} largest eigenvalue λ_k.

To derive the form of the k^{th} PC $\boldsymbol{\alpha}_k{}'\mathbf{x}$, we have to find the vector $\boldsymbol{\alpha}_k$ that maximizes $var(\boldsymbol{\alpha}_k{}'\mathbf{x}) = \boldsymbol{\alpha}'_k\mathbf{S}\boldsymbol{\alpha}_k$. It is clear that the maximum can not be achieved for finite $\boldsymbol{\alpha}_k$ so a normalization constraint must be imposed. The constraint used in the derivation is $\boldsymbol{\alpha}'_k\boldsymbol{\alpha}_k = 1$, that is, the sum of squares of elements of $\boldsymbol{\alpha}_k$ equals to 1.

As a result, in other words, the PCA consists then in performing a spectral decomposition of the sample correlation matrix $\mathbf{S}_{\{\mathbf{1:M}\}}$ which means computing the $(P \times P)$ diagonal eigenvalue matrix Λ and the $(P \times P)$ eigenvector matrix $\mathbf{A}$ satisfying the relationship:

$$\mathbf{A}^T\mathbf{S}_{\{1:M\}}\mathbf{A} \quad = \quad \Lambda$$

$$where\ A = \begin{bmatrix} \alpha_{1,1} & \ldots & \alpha_{1,p} \\ \vdots & \ddots & \vdots \\ \alpha_{p,1} & \ldots & \alpha_{p,p} \end{bmatrix} \quad and \quad diag(\Lambda) = [\lambda_1, \lambda_2, \ldots, \lambda_p]$$

In this work we will use the term 'principal components' for the derived variables $z_k = \boldsymbol{\alpha}_k{}'\mathbf{x}$, and refer to $\boldsymbol{\alpha}_k$ as the vector of coefficients or loadings for the k^{th} PC.

The k^{th} eigenvalue λ_k represents the variability described by the k^{th} PC, whereas the k^{th} column of the eigenvector matrix $\mathbf{A}$ represents the unit vector

of the k^{th} PC bearing orthogonal directions in the transformed variable space. Then, the k^{th} PC is defined as follows:

$$\mathbf{Z}_k = \mathbf{A}^T X_k = [z_{k,1}, \ldots, z_{k,p}, \ldots, z_{k,P}]^T$$

The goal of this approach is to retain just the most important PCs in order to reduce the dimensionality of our input channels and fuse them in an appropriate way. This can be done selecting the m PCs associated with larger variance. The selection of number is a key topic in literature dedicated to PCA [16] [15], and several approaches have been proposed. Two simple methods that will be followed and considered in this selection procedure are:

- Computing a Pareto chart on the eingenvalues and using a threshold to select the m PCs;
- Kaiser's rule which suggest to choose the number m by retaining the PCs with corresponding eigenvalue larger than the overall eigenvalues average.

Having selected m PCs, we can reconstruct the original standardized $\tilde{X}_k$ vector by computing:

$$\widehat{\tilde{X}_k} = \sum_{p=1}^{m} z_{k,p} \boldsymbol{\alpha}_p$$

where $\boldsymbol{\alpha}_p$ is the p^{th} eigenvector i.e. the p^{th} column of the $\mathbf{A}$ matrix.

2.3 Development of the statistical monitoring strategy

The PCA allows to represent the correlation between the different signals and to summarize the important informations that are captured in a limited number of new features. A key factor of the PCA is that it provides the possibility of results interpretations, since the results are linear combinations of the original variables.

We believe that a multichannel extension of the PCA represents an efficient sensor fusion approach that is able to deal with different sources of informations. We propose then to use an extension of the traditional PCA, that is called vPCA, which, in this case, is based on the transformation of multi-dimensional dataset in a two-dimensional matrix by concatenating the variables associated to the channels.

The statistical techniques, which come from PCA and the control charts that are based on it, request the hypothesis of temporal independence between the observed samples. Of course in our application this hypothesis is violated due to the nature of the *in-process* approach. We still use this technique

because in many industrial applications, such as the one we are working on, there is the need of detecting unexpected changing in the process conditions while long term oscillations are considered as normal working fluctuations.

The Principal Component Analysis is normally applied directly to raw data channels, but, in this framework of vectorized PCA, we propose to pre-process the signals, extracting synthetic indicators, so that they can identify specific process features. Furthermore these indicators may reduce the problem of the outliers, typical of the signals data, and may represent a smart summarization to deal with high frequency rates of information when building a control charting system. In general, the extraction of synthetic indicators can lead to possible losses of information, in addition to requiring a further step in pre-processing raw data. Despite this, in some situations of practical interest, a good choice of indicators can provide acceptable performance. For this reason we will discuss in section 4.5.1 the performance of the indicators proposed in sections 4.4.1 and 4.4.2, because selecting an inappropriate set of them may lead to detect sources of informations that are not related to the purpose of the system. On the other hand, a reasoned selection of indicators may resolve a typical issue faced during the design of a statistical in-process control approach: the dependency of the process output signals from the variation of the process input parameters.

The statistical monitoring strategy that we propose can be summarized in fig. 2.1, where we present the sequential steps that bring from the grinding operation data acquisition to the control charts that monitors the process. These steps are performed in real time during the grinding operation.

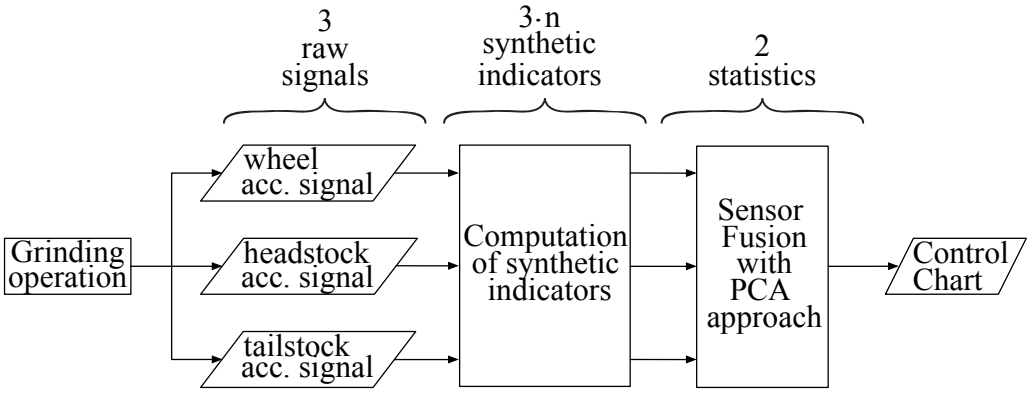

Figure 2.1: Statistical monitoring approach.

In step one the accelerometers channels are acquired and stored in the 'raw data matrix'. Every accelerometer's channel is acquired and divided in windows of amplitude w, each of them is constituted by p data points.

During the grinding cycle, J windows of p data points are stored in the 'raw data matrix'. This matrix has a dimension of $(N \times p \times J)$ where N is the number of accelerometers channels, p is the number of data point of each window, acquired for every single channel, J is the number of consecutive windows acquired during a grinding cycle. Our approach suggests to divide the original signal in overlapping windows to avoid spectral leakage during the indicators calculation, where a typical value of overlap is 90%.

In step two, according to the framework of fig. 2.1, we calculate the 'synthetic indicators matrix' starting from the data stored in the raw data matrix. The p data points constituting every window of the accelerometric data are summarized by means of the chatter indicators developed in section 4.4.1 and 4.4.2. On each window, n different indicators can be calculated for everyone of the N accelerometers channels. To clarify with an example, if we have $N = 3$ accelerometers in the raw data matrix and we choose to consider three synthetic indicators for every single accelerometer channel, we then have $N' = 3 \cdot 3 = 9$ *indicators channels*. The number of data points that constitute every indicator channel is equal to the number w of windows acquired. Every single point of the indicators channels summarizes the p original data points that are part of every window. The results are organized then in the 'synthetic indicators matrix' which has a dimension of $(n \times w)$ where n is the number of indicators channel previously introduced and w is the number of sequential windows. A diagram of the PCA input matrix organization is shown in fig. 2.2.

In step three the extended version of the PCA, called vectorized PCA, is performed on the synthetic indictors matrix; to refer to the theory we can call it $\mathbf{X}$ matrix. The X matrix collects indicators values calculated on windows of phase I and phase II working cycles. Only the $\{1 : M\}$ samples of phase I are used for the PCA model identification. As the columns of the X matrix are referred to different quantities, it is better to work with the standardized $\tilde{X}$ matrix where the sample mean on each $X_{\{1:M\}}$ column is subtracted to the entire X matrix and then divided by the sample standard deviation. The output of the PCA is then a matrix of m principal components that we call PCs.

In step four the monitoring strategy requests the calculation of two statistics on the first PCs that have been retained: the T^2 *Hotelling* and the Q statistics.

- The *Hotelling's statistics* is used to detect possible deviations along the directions of the first m PCs [24, 5].

- The Q statistics is used to detect possible deviations in directions orthogonal to the ones associated to the first PCs.

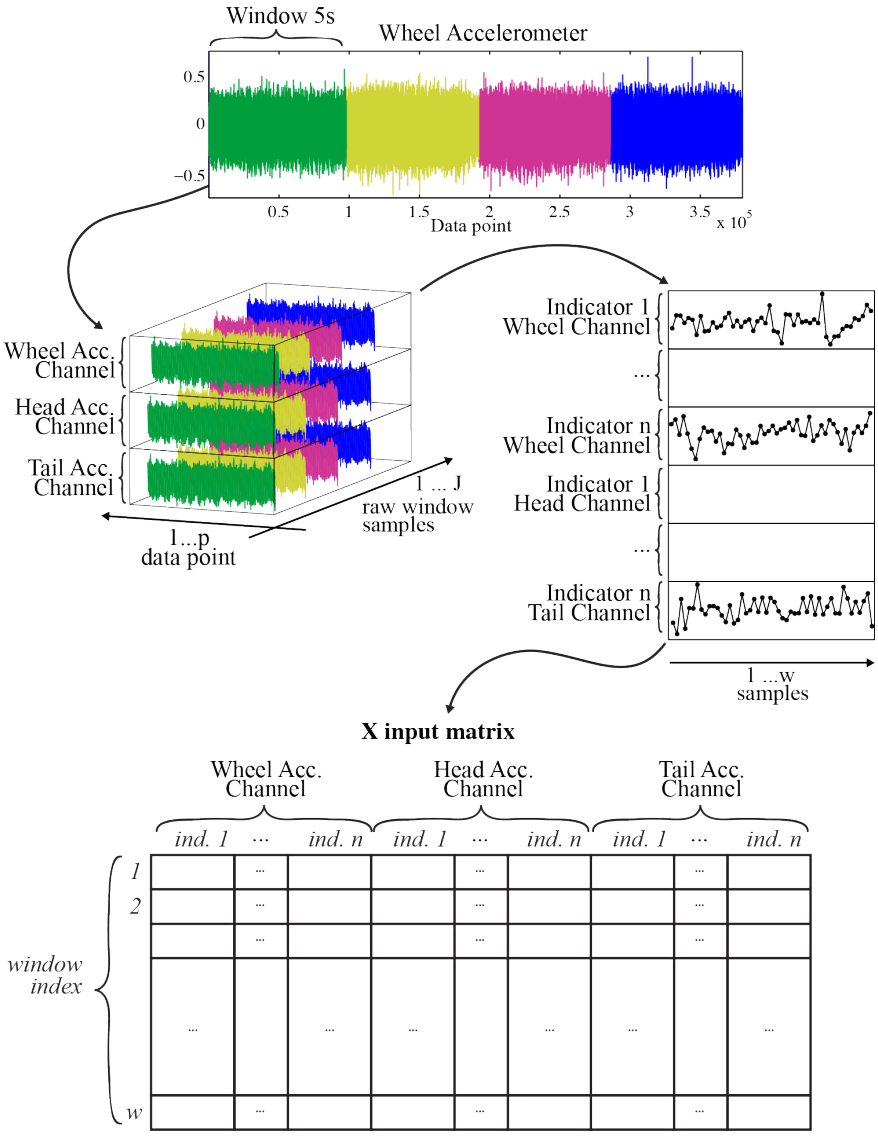

Figure 2.2: From raw data matrix to the vPCA input matrix.

The Hotelling's statistics is the sum of squared principal components weighted on their explained variance:

$$T_k^2(m) = \frac{z_{k,1}^2}{\lambda_1} + \frac{z_{k,2}^2}{\lambda_2} + \ldots + \frac{z_{k,m}^2}{\lambda_m}$$

while the Q statistics is the Sum of Squared Errors computed as:

$$Q_k(m) = \left(\tilde{X}_k - \widehat{\tilde{X}}_k\right)^T - \left(\tilde{X}_k - \widehat{\tilde{X}}_k\right)$$

Each new observed X_k vector, constituted by the various indicators channels, is monitored by using the reference PCA model based on the $X_{\{1:M\}}$ Phase I data set, then on the PCA estimates results T^2 and Q statistics are calculated.

The two statistics are then monitored with an SPC control chart approach, performing two separate control charts. Two control limits have to be defined, based on a selected $\alpha_{overall}$ type I error. On each chart a single α value is considered according to the Bonferroni approach applied to type I error which results in taking $\alpha = 1 - \sqrt{1 - \alpha_{overall}}$ for every single chart.

Control limits typically used in multivariate analysis are all based on the assumption of approximate multivariate normality. However, it is quite common that working with variables coming from signals or indicators calculated on them, means dealing with non-normal distributions, which violated the multi-normality assumption of the traditional control limits. Due to the presence of time dependency and non-normality of the dataset of input, the usage of empirical control limits has been suggested. This is a frequently encountered situation in practice and different authors have discussed available solutions to face such an issue, for example calculating the percentile estimating the Kernel Density distribution or making use of bootstrap techniques to determinate statistics estimates when the population distribution is not known.

2.3.1 Boostrap methods for empirical limits calculation

In this framework we follow the bootstrap based approach for the estimation of control limits, according to [25, 16]. The bootstrap is a method for estimating the distribution of an estimator or test statistic by resampling one's data or a model estimated from the data. The bootstrap provides approximations to distributions of statistics, coverage probabilities of confidence intervals, and rejection probabilities of tests that are at least as accurate as the approximations of first-order asymptotic distribution theory [12]. Different bootstrap techniques have been developed in literature, and there are many different versions that can be used for empirical limits estimations.

Two approaches of empirical control limits estimation have been followed so far:

- Moving Block Bootstrap control limit;
- Bootstrap T^2 & Q Percentile Approach control limit.

In the moving block bootstrap, introduced by Künsch [21], the original matrix of input of the PCA X is split into $n-b+1$ overlapping blocks matrix of length b. The observations 1 to b will be organized in block matrix 1, observations 2 to b+1 will be block 2 and so on. Then from these n-b+1 matrix blocks, n/b matrix blocks will be drawn at random with replacement realizing a new matrix $\tilde{X}$. On this $\tilde{X}$ matrix a PCA analysis is conducted, and T^2 and Q statistics are calculated. For both of this two statistics, two upper control limits corresponding to the $100 \cdot (1-\alpha)^{th}$ percentile are identified. This procedure is replicated $B = 1000$ times, identifying 1000 UCL for T^2 and 1000 UCL for Q empirical limits. Then averaging the 1000 values, one UCL for every single chart is defined. This approach is computationally more intensive than the following one as it has to compute B PCA and then average the empirical limits. The reason why we implemented this approach is because this bootstrap works with dependent data and it capable of dealing with time correlation better than the other bootstrap approaches.

The bootstrap percentile approach, proposed in the work of Phaladiganon *et al.* [25], is based on the computation of the empirical limits starting directly from the T^2 and Q statistics calculated on n observations from an in-control dataset.

Then the approach suggests to select $T^{2(i)}_{(1)}, T^{2(i)}_{(2)}, \dots T^{2(i)}_{(n)}$ as a set of n T^2 values from *i-th* bootstrap sample ($i = 1, \dots B$) randomly drawn from the initial T^2 statistics with replacement. In each of B bootstrap samples, the $100 \cdot (1-\alpha)^{th}$ percentile value is determined, given a users-specified value α with a range between 0 and 1. The control limit is defined by taking an

average of B $100 \cdot (1-\alpha)^{th}$ percentile values $\bar{T^2}_{100\cdot(1-\alpha)}$. The same approach is followed for the definition of the Q control limit. The established control limits are then used to monitor new observations.

This approach is easier and computationally less intensive but relies the definition of the control limits directly on the T^2 and Q statistics and might be less robust than the moving block bootstrap approach.

After having explained the approach followed in the development of the SPC method and its assumption, it is important to briefly describe the configuration of the grinding machine and some details of the real industrial case. The main problem that has to be tackled, is represented by detecting on-line the growth of waviness on the roll surface generated by the process vibration; to do this it is very important to define what we mean by a chattered cylinder and what is a good one. For this reason it will be of a crucial importance identifying the machine vibration related to an 'in control' or an 'out of control' cylinder surface. To correctly identify the growth of this phenomenon is important to know the machine dynamics and setup which will be synthetically described in the next chapter.

Chapter 3

Industrial Case

3.1 Machine Set-up

The case study takes part in developing an intelligent grinding machine that will be acting in hot rolling plants. As mentioned before, to explain the monitoring system proposed, it is better to understand the basic parts of the machine on which it will be tested and the sources from where the SPC will acquire data.

Four are the main parts that needs a brief overview: the structure of the machine, the workpiece, the wheel and the sensors from which we will acquire the data.

The principal components of the structure of this type of machinery are:

- headstock: the part of the machine that puts the roll in rotation;
- joined bed: part connected to the foundation of the machine where the carriage moves and the lubrication flows. Stability and rigidity are essential to maintain alignment and precision work;
- tailstock: opposite to the headstock, avoids backwards movement and has other features not relevant for this analysis;
- wheel head: part essential for the transversal translation towards and away from the roll and allows the wheel grinding the roll;
- hydrostatic spindle: part that generates the profile on the roll barrel and it allows continuous infeed for the compensation of the wheel wear.

The machinery is completely controlled by a control system, that allows an high level of automation. The CNC system is used, mainly, for:

- Regulation of the axes speeds and positions.
- Speed regulation of the spindles.

Table 3.1: The range of the parameters in our case study.

Parameter	**Min. value**	**Max. value**	**Units**	**Effects**
Wheel speed	15	50	m/s	Reduce forces, increase wheel wear, increase burning risks.
Roll speed	20	50	rpm	Increase forces, chatter tendency productivity, decrease burining risks.
End infeed	0.001	0.05	mm	Increase power, forces, roughness, wheel wear, productivity; chatter tendency may be affected.
Continuous infeed	0	0.05	mm/min	Compensate wheel wear
Wheel width	Slim (about 60)	Large (about 120)	mm	Increase forces, productivity, chatter tendency (if dynamic nonlinearities can be neglected)
Wheel diameter	Small	Large	mm	Increase forces, productivity, chatter tendency.

- Management and implementation of programs containing the commands for sequential operations and movements of grinding cycles, measuring and works.

Moreover the computer makes available in real time a large number of input & output variables available to be used for the process control and for the adjustment of the machine. These variables coming from the machine will be part of our analysis to design a robust chatter monitoring system.

The workpiece considered in this project is a roll for hot rolling mills that produce steel plates. Rolls size can vary significantly between $400 - 600\ mm$ for the work roll; the roll's width is spacing from 1800 to 2000 mm. Roll materials are special alloyed steel or spheroidal graphite cast iron.

Roll quality is mainly linked to its surface waviness and the typical prescribed roughness is $R_a = 0.6\mu m \pm 10\%$.

Grinding wheels used during the process monitored are of three types:

- for cast iron rolls: silicon carbide;
- for steel rolls: aluminum oxide.
- for difficult cutting conditions: diamond grinding wheel.

The technological boundaries for the machine used in this case are summaries in tab. 3.1.

Table 3.2: Accelerometric sensors.

Signal	**Source**	**Machine & Process Feature**
Vibration	Wheel head	Chatter, waviness
Vibration	Headstock	Chatter, waviness
Vibration	Tailstock	Chatter, waviness
Vibration	Joined bed	Chatter, waviness
Acoustic Emission	Wheel hub	Process vibrations, wheel touch

Omitting the other technical details on the machine structure, it is important to focus on the specific hardware on which relies our project: sensors attached to the grinding machine.

To perform an online process monitoring, it is necessary to have access to a lot of data from the machine in real time so that we can have full knowledge of the ongoing process. We can divide this class of data in three main categories:

- accelerometric data: for vibration and wheel status monitoring;
- data of forces, speeds and current monitoring;
- data of input parameters monitoring.

The most important sensors are the accelerometers installed on the machine that can be analyzed to reconstruct the vibration state of the machine which is directly connected to the scope of the project: detect the waviness generation. The accelerometric data come from three tri-axial accelerometers (see tab. 3.2), placed on the machine body, and one acoustic emission encoder, placed inside the grinding wheel. In fig. 3.1 is shown an accelerometer placed on the machine, specifically the tailstock one. The sampling rate of the accelerometers is 2000 Hz.

In fig. 3.2, it is possible to see the machine layout and the position of the three accelerometers and the AE encoder.

In fig. 3.3, the orientation of the accelerometers axes is visible. The wheel accelerometer *x-axis* is opposed to the headstock and tailstock ones. The *y-axis* is oriented in the same direction for all accelerometers.

The acoustic emission sensor is placed in the wheel hub and it will be mainly used to detect whether the wheel is touching the workpiece or not. On the other hand the scope of the accelerometers is to monitor the growth of vibration during the grinding process. These accelerometers have been placed in the main three parts of the previously described machine structure, so that we can acquire space variant data of the process.

Figure 3.1: A detail of one of the accelerometers placed on the machine.

The wheel accelerometer is the 'closest' to the process source of data and the one that should easily detect the bouncing of the wheel towards the cylinder. This accelerometer follows the wheel axial movement differently from the head and tail ones which will have a different intensity based on the axial location of the grinding wheel on the cylinder. The headstock and tailstock accelerometers will be sensible more to the vibrations of the body and the workpiece adding informations about the whole structure dynamics.

There is also another accelerometer that is placed on the basement of the machine that should detect the external vibrations, but as we will detail in the next sections, this accelerometer is much less sensible to detect the chattering and it is useful for other purpose that are not linked to our aim.

Together with the accelerometric data, we can get information directly from the machine sensors. As listed before we have two main classes: the high frequency data and the low frequency. The first class (Tab.3.3) contains all the drives, speeds, forces and currents data which are sampled at 250 Hz and represent an output source of the ongoing process.

The second class, with a sampling rate of only 2 Hz, collects the input data of process that don't change frequently during working conditions, such as continuous infeed, end infeed, wheel and roll dimensions.

Designing the SPC monitoring approach is it very important to take a look not only to the accelerometric data but also the machine sensors, to correlate vibrations to the working conditions. The most important parameters are the rotational speeds of the roll and the wheel, including the continu-

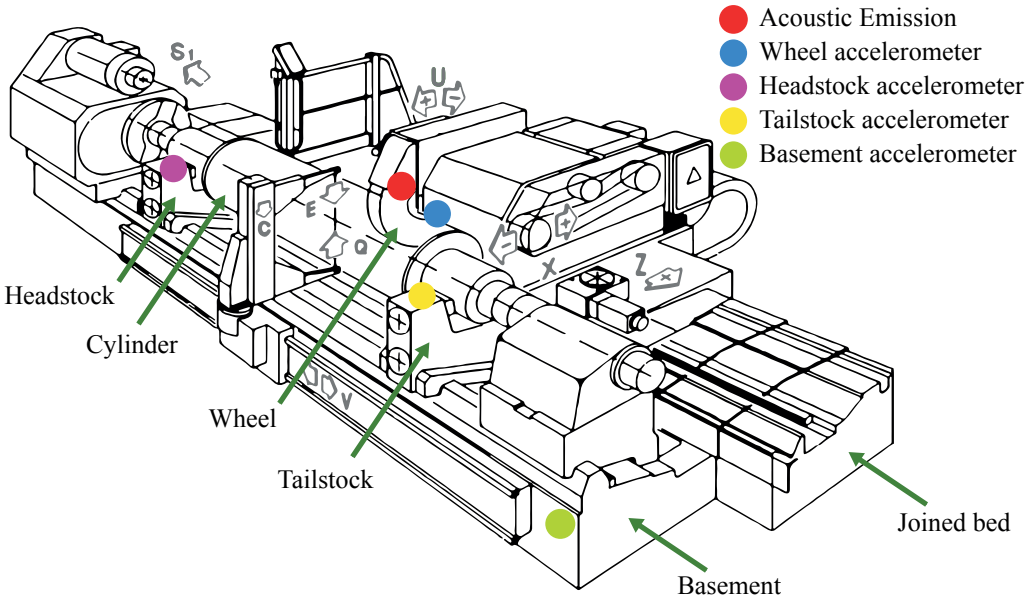

Figure 3.2: Position of additional sensors on the machine.

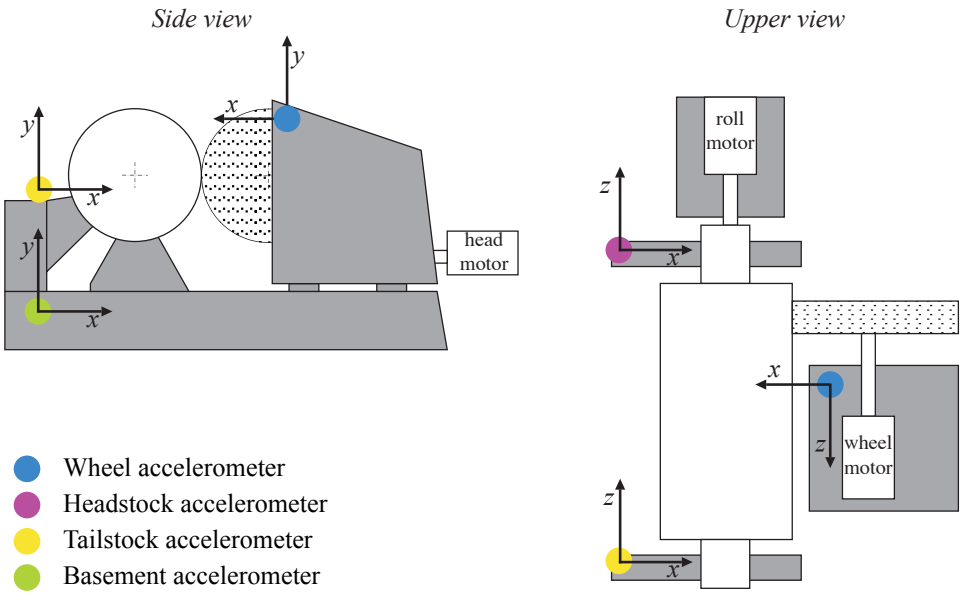

Figure 3.3: Axes of accelerometric sensors.

Table 3.3: Machine sensors.

Signal	**Source**	**Machine & Process Feature**
Current	Headstock motor	Cutting forces
Current	Wheel motor	Cutting forces
Current	Micrometric infeed axis (U)	Cutting forces
Current	Infeed axis (X)	Cutting forces
Displacement	Infeed axis (U)	Actual infeed
Displacement	Infeed axis (X)	Actual infeed
Displacement	Carriage axis (Z)	Axis positioning, cycle time estimation
Velocity	Headstock (HD)	Grinding parameter, roll speed variation, waviness measure
Velocity	Wheel head	Wheel velocity, grinding cycle

ous speed variation parameters. In fact they are directly related with the waviness generation process and with the vibration frequency of the system when chattered surface, both on the roll and the wheel, are present. Other important parameters are the radial infeed (i.e. end infeed and continuous infeed) since they are the main variables affecting the chip thickness and then the cutting forces.

3.2 The role of the SPC into the EPC

Until now we have seen almost all the sensor that are available, where they are placed and what do they measure; these sensors together with the machine and the workpiece itself, represent the input of our case study. In this session we will clarify the integration of our work, the development of an SPC monitoring approach into the Engineering process control, that has been developed to adjust the process if it reaches unstable conditions.

First of all, thinking back to the introduction, it is necessary to distinguish the roles of the SPC and the EPC (see fig.3.4). The Statistical Process Control consists of set of tools that have the aim of detecting deviations from good working conditions. The Engineering Process Control, on the other hand, represent a tool that is able to adjust unstable working conditions to get back to a new state of stability.

Briefly the SPC monitors the process and the ECP controls it. The joint

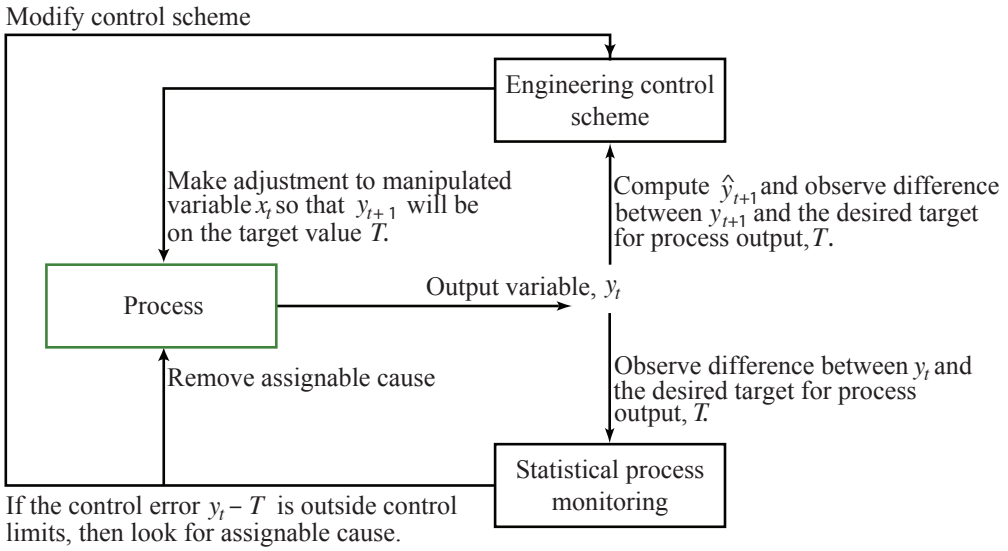

Figure 3.4: Roles of SPC and EPC towards the process.

of this tools is a system that is able to recognize deviations from good working conditions and suggest new process parameters to get back to stability. To be more specific, the SPC is integrated into the EPC because, after receiving the inputs, it analyzes the process with a specific statistical approach and if it detects a process drift it provides an alarm. This alarm, coming from the SPC, is the input of the EPC that will provide to change the process parameters.

This has been a general overview of the cooperation between SPC and EPC, but it shows how the SPC approach that we propose can be integrated into an EPC to control the grinding process. In Figure 3.5 it is possible to understand the connection between the machine and the Numeric Control Unit that runs the EPC.

During a grinding process, the plant operator sets the process parameters in the numerical control unit that is connected to grinding machine. The machine then starts grinding with the parameters set up by the operator and, as soon as the process gets out of the initial transient state, the SPC model begins to make use of the data coming from the different sources. Combining the accelerometric data and the output parameters, it is possible to verify if the present working condition follows the *in control model* designed by means of the SPC. The aim of the SPC is to detect the chatter phenomenon, which can occur at different working conditions; for this reason the challenge of the statistical model is to be robust to the process parameters and detect the phenomenon without being influenced by the manipulation of the working

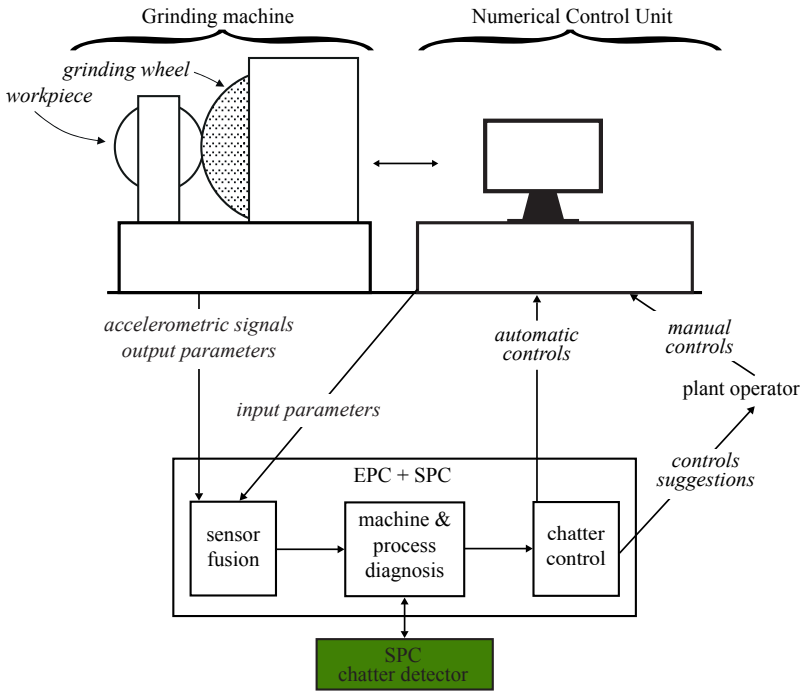

Figure 3.5: Integration of the SPC chatter monitoring approach into the EPC.

condition. To be more specific, a 'weak model' that analyze vibrations may incorrectly indicate the presence of chattering when the amount of vibration is increased not due to the presence of chatter, but, for example, when the operator has set different wheel speed which translates in more vibrations.

If the statistical model is robust and capable of detecting the chatter, then the EPC can control and reduce the chatter, suggesting to the operator or automatically changing the wheel and the workpiece speed.

What described before can be summarized in the flowchart of fig. 3.6 where the role of the *chatter detector* is underlined. By chatter detector we mean the monitoring of the process conditions, and it is possible to see that if the process remains in an *in control state* the loop brings to the grinding cycle end. On the other hand, if the detector shows that the process has gone *out of control*, the EPC strategy for controlling chatter comes in action. After having detailed the role of our work into the EPC framework, is now time to explain in a proper way the basis of the SPC approach on which the chatter monitoring relies.

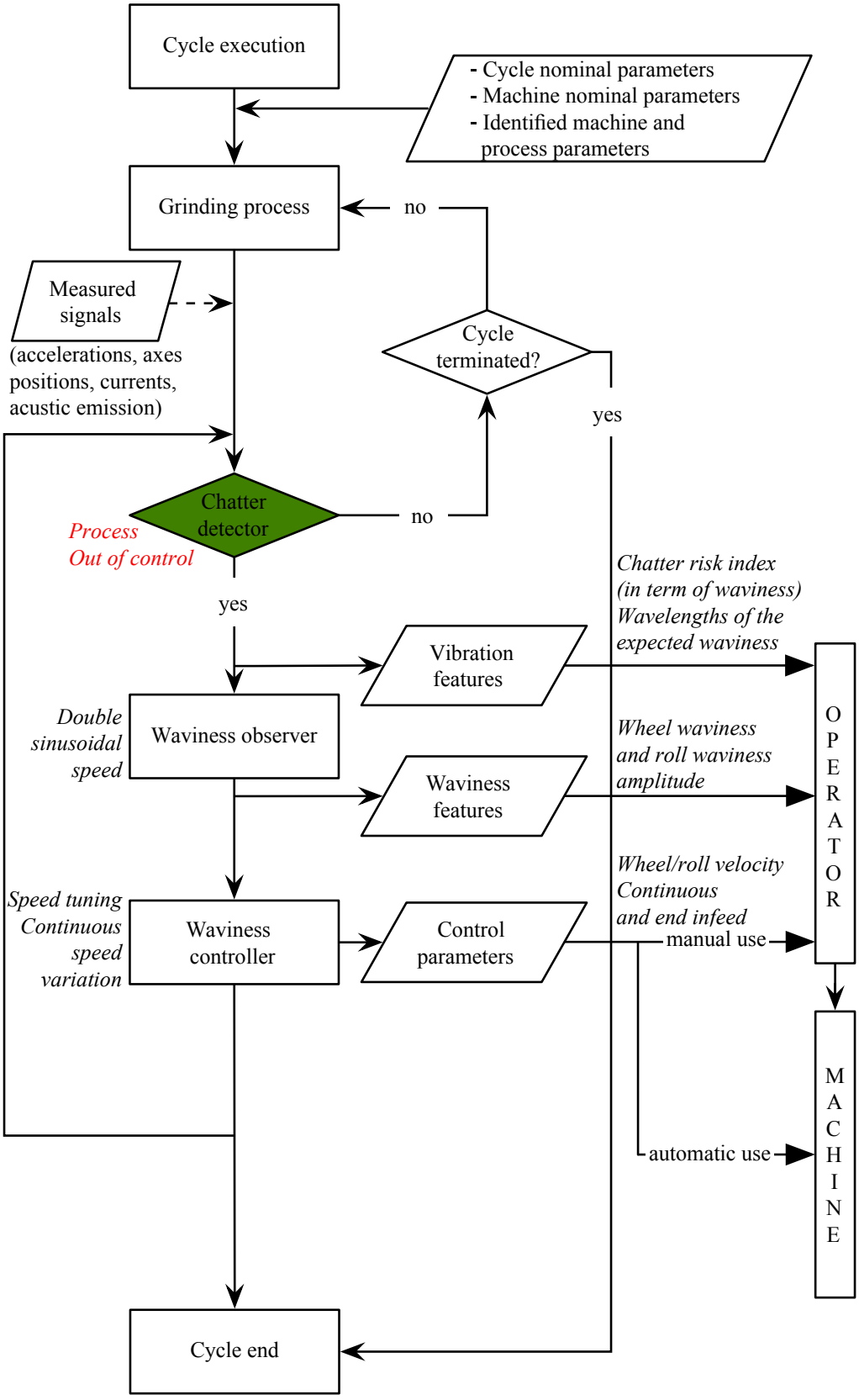

Figure 3.6: Process monitoring & control flowchart.

3.3 Signal-based SPC

A statistical process control approach, as we have anticipated in the previous section, is a statistical method for quality monitoring, and as any method, it relies on some hypothesis. The main hypothesis of the SPC approach is that it is impossible to inspect or test quality into a product without having the product built right the first time. This implies that the manufacturing process must be stable and that all individuals involved with the process (including operators, engineers, quality-assurance personnel, and management) must continuously seek to improve process performance and reduce variability in key parameters [23].

The SPC approach permits to obtain this results and the control charts are useful to define an on-line statistical process control procedure. In any kind of production process, there are essentially two types of causes that affect the output:

- a lot of small unremovable causes, always present, which cumulative effect is the natural variability of the process;
- other kinds of variability that affect, when they are present, the finished quality of the product. Examples could be operator errors, defective raw materials or machinery not properly working

The first group of causes is called *normal process variation* or natural variability, the second group is known in literature as assignable causes of variation. If a process is affected only by natural variability, the process is defined in statistical control. When in the process there are the other sources of variability, the process is defined *out of control*, because generally this type of causes lead to unacceptable levels of process performances.

Quality monitoring via statistical process control can be used for quickly detecting any change from the in-control behavior in order to avoid deteriorated process performance. In traditional SPC, the quality characteristic is usually off-line inspected (by using traditional measuring systems, as coordinate measuring machines) without requiring on-line sensing [6].

Usually, a process that is in a in control state, produces acceptable workpieces with known quality variability. When an assignable cause of variation affects the process, the workpieces produced will not be likely more accepted, but they will be refused. To avoid to have many scraps, it is necessary to quickly identify when a assignable cause occurs and set the process back to an in control state. The control chart is an on-line tool, that relies on a statistical model and allows to:

- monitor and control the process;

- reduce the process variability.

Traditional SPC approaches based on control charts can easily deal with quality characteristics that are related to dimensions. In our case the quality of the manufactured product is related to surface texture (the waviness of the cylinder) and not to a dimension. Furthermore this characteristic will not be inspected offline, but the aim of the project is to find a proxy that is related to cause of waviness so that it can be evaluated during the process.

For these reasons, the first step to do is to define, for the process we are studying, what can be considered as 'in control' and what 'out of control'. Only after having clarified the in and out control states it is possible to design the control chart with 'in control' operations and test it with both 'out of control' and 'in control' operations.

As mentioned before, the SPC approach will focus on the identification of the problems that cause waviness on the cylindrical surface. Until now, in hot rolling plants, a workpiece is considered a production scrap if it presents waviness on its surface, and can be considered a good one if the amount of waviness is under a defined threshold. In fig. 3.7 is possible to see a portion of a cylinder that doesn't present waviness in the first half while is visible in the second half. The first part of the roll has been milled with an 'in control' process while the second one with an 'out of control' one.

Figure 3.7: Example of a cylinder presenting chatter marks only on the right side.

To relate chatter vibrations with the waviness on the cylinder's surface, it is important to understand which are the states that a grinding machine can take on. During a grinding operation, the machinery can mainly assume four different states of working conditions:

- good or stable cutting;
- anomalous vibrations (for example external vibrations);
- chatter vibrations;
- lobed roll and wheel.

The first condition is the ideal one, and it produces a workpiece that is likely to be considered in control and then accepted by the quality inspector. The other conditions may lead the production to an out of control state. Our focus will be on two of these states: good or stable cutting and chatter vibrations. In fact, anomalous vibrations are not related to wrong process parameters but they are caused, for example, by the presence of other machineries. Working with a lobed roll or wheel, on the other hand, is a condition that should be avoided. The wheel and the roll present lobes when, during the process, bad cutting parameters are used; these parameters cause vibrations that generate lobes on the wheel or on the cylinder. For this reason, monitoring the vibrations should avoid this phenomenon.

However, up today, it is difficult to link the waviness on the worked roll perceived to naked eye with the process vibrations. There might be some rare cases in which the process signals the presence of chatter vibrations, but inspecting the worked roll the waviness is under the acceptability threshold. On the other hand, there are some sporadic cases where the cylindric surface presents chatter marks, but the process doesn't signal vibrations. Luckily, in most of the cases the existence of waviness on the cylinder is directly connected with the vibrations during the grinding process.

The discriminating factor between an in control or out of control workpiece is, so far, determined by the subjective judgment of the plant operator, that varies according to his experience and attention. Judging a workpiece of these dimensions as a scrap involves the need to rework it, which means additional costs. On the other hand, reworking a roll that could be marked as an acceptable one by an accurate skilled operator, causes extra-costs that are not necessary.

Up today it is difficult, for the skilled operator, to define during the process if the working cylinder will result acceptable or not, before viewing the final output. A competent operator might rely on an empirical analysis of the machine parameters and on his experience to estimate if the process will produce a scrap roll. But today, there isn't an objective and univocal framework to evaluate working conditions.

This problem doesn't result easily solvable with a traditional SPC approach, that expects the description of a quality's characteristic in different time instants [23]. The basic idea behind the traditional approach is in fact

to sample the output of a productive process and to measure its quality characteristic. If the measure is inside some defined control limits, the process will result in an 'in control state'; on the other hand, if the characteristic falls outside the control limits, an alarm will tell that something has happened in the process that modified the mean or the variance of the output. The evolution of statistical methods in quality monitoring started with univariate control charts on a single quality characteristic, has later moved to multivariate approaches, that allow simultaneous monitoring of several variables and characteristics, keeping the same efficiency of the univariate approach.

However, there are many industrial situation where the final quality of a product or a process is characterized by two or more variable relation. Sometimes these variables, that affect the quality of a product, are input parameters in the process; sometimes instead the product quality might be linked with the vibrations generated during the process. A further development, that is still in research, is then to use these multivariate methodologies not only on the characteristics of final product, but on the process characteristics that impact on the quality of the output. For these reasons, it is useful to monitor these specific signals, that can will be the base of the process monitoring.

Our goal is to introduce a method that, during the process, will understand if the machine is going in a 'chatter vibration' state. We will refers to this approach as *signal-based SPC*. For all the reasons explained in this section, the analysis of the available signals is linked to the roll evaluation by a subjective judgment of an expert. Further researches might determine a quantitative relation between the development of chatter vibrations and the presence of waviness on the roll. In this way, it will be possible to improve our approach, that would be based on a more objective characterization.

Chapter 4

Chatter monitoring strategy

4.1 Acquisition of industrial data

In this section we will detail the approach that we have followed in conducting grinding tests on the machine. The purpose of our work is, as said before, developing a statistical approach to identify the presence of chatter vibration during the grinding process. To do this it is necessary to understand in which conditions the phenomenon occurs and in which it doesn't. Distinguishing the states of *in control* and *out of control* by means of chatter presence it is fundamental for any statistical method based on control charting. The scope of the experiments is to obtain a dataset containing accelerometric data and parameters of various grinding passes so that a phase I and phase II for control charts can be defined. It is very important to have a dataset for 'phase I passes' that represents correct working conditions, where the roll is considered acceptable with an eye inspection by a grinding expert. This set will be used to train the model and test its behavior towards false alarms. On the other hand a set of 'phase II passes' will be necessary to see if the developed model correctly identifies the presence of chatter vibrations.

To set up an experimental plan which aim is to obtain the phase I & II dataset it is important to isolate the main parameters that affect the presence of chatter vibration. As seen in section 3.1 the most important parameters, which have a direct effect on the chatter dynamics, are the rotational speeds of the roll and the wheel. Other important parameters that can lead to the growth of chatter are the end infeed and continuous infeed because they affect the chip thickness and the cutting forces.

Selecting appropriate cutting parameters is strategic because, according to literature, the chatter phenomenon arises for example when the wheel speed is multiple to one of the machine mode shapes of vibrations.

For this reason the selection of cutting parameters has been based on the stability analysis of the machine conducted by *Engr.* Leonesio, M. who

Table 4.1: Main resonance of the system.

Structure $[Hz]$	**Relevance**	**Spindle** $[Hz]$	**Relevance**
43	minor	159	dominant
49	minor	168	important
57	minor	185	important
63	dominant		
67	important		

Table 4.2: Test for chatter frequency identification.

Test	**WH vel** $[rpm]$	**HD vel** $[rpm]$	**C.I.** $[mm]$	**E.I.** $[mm]$
1	700	26	0.06	0.01
2	729	26	0.06	0.01
3	901	26	0.08	0.01
4	725	30	0.06	0.01
5	910	30	0.01	0.01
6	630	30	0.02	0.02
7	631	30	0.01	0.01
8	721	30	0.02	0.02
9	929	30	0.02	0.02
10	1201	30	0.01	0.01
11	1215	30	0.01	0.01

performed a complete modal analysis of the grinding machine in order to evaluate the dynamic behavior of the system.

The impact testing technique has been used to excite the machine structure and the mode shapes have been extracted by the use of commercial SW for modal analysis. The results show that the main resonance of the machine is around 60 Hz, which is due to the machine structure, and another important compliance is found to be the one of the spindle system at around 200 Hz. In tab. 4.1 the main resonance of the system are identified.

The resonance at 63 Hz is strongly involved in the process vibration and it is the main cause of the waviness. To prove this a pre test is run with different wheel and roll speeds (see tab. 4.2) that may generate chatter marks on the cylinder.

As an example, considering a chatter frequency of 63 Hz and a wheel rotational frequency of 630 rpm (10.5 Hz) with a roll rotational frequency

of 30 rpm (0.5 Hz) the waves on the wheel will be $\frac{63}{10.5} = 6$ while the ones on the roll will be $\frac{63}{0.5} = 126$. The runs of tab. 4.2 have been carried out, evaluating the roll conditions after few passes. In all the runs chatter marks are visible on the roll, with different amount of waviness. A spectral analysis of the pre test is shown in fig. 4.1 where the component around 60 Hz is the dominant one and the main cause of chatter marks.

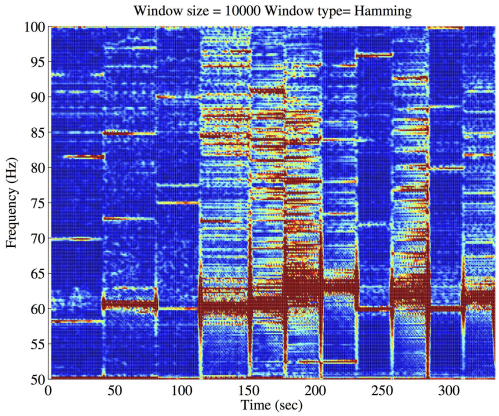

Figure 4.1: Spectrogram of runs in tab.4.2.

What comes out of the analysis is that chatter frequency is almost synchronous with wheel frequency, as verified experimentally. Starting from dynamic measurements and process parameters, *Engr.* Leonesio M. developed an experimental map indicating the unstable wheel velocities and the corresponding chatter frequencies (fig. 4.2 and fig. 4.3).

In the upper graphic of fig. 4.2 on the y axis is the width of the grinding wheel while on the x axis is the wheel speed expressed in rpm. This experimental diagram shows at which wheel speeds and wheel width corresponds the probability of lobes growth on the wheel which translates to possible presence of chatter. The green line indicates the wheel width used during the test conducted on this machine and will be a constant parameter which is 75 mm. The lower part of fig. 4.2 shows which is the chatter frequency known the number of the wheel lobes and the wheel speed. To make an example of how to use this diagram, if we want to select a bad cutting condition with a 75 mm wheel we could set a speed of 900 rpm which most likely generates 4 lobes on the wheel. This is know from the upper graph, where the instability for a speed of 900 rpm is obtained with a wheel width much lower than the one we have used for the experiments. From the lower part of the graph we can then see the chatter frequency that occurs at 900 rpm which is around 60 Hz. If, on the other hand, we would like to select a wheel

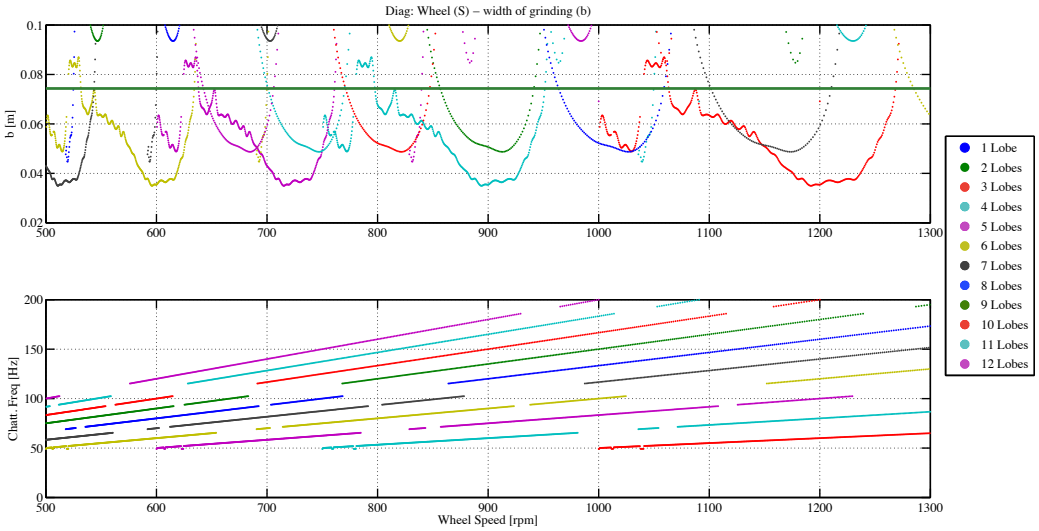

Figure 4.2: Lobes diagram showing chatter frequency and number of wheel lobes as a function of wheel speed and width of grinding. Courtesy of *Engr.* Leonesio M., CNR-ITIA, 2013.

speed that probably can produce a good workpiece, we can select a speed of 1050 *rpm* because for a wheel width of 75 *mm* the probability of lobes formation is very low.

Of course this diagram is based on the measured machine dynamics and it has still to be validated. The nature of this complex validation is that in chatter-free operation the cutting force can be assumed as a wide-band signal that excites the structure for a broad range of frequencies, including the system resonances, but with little amount of energy for each band. A good roundness of the roll and wheel assures limited variation of the force with the wheel and roll rotation. On the other side in case of process vibration (due to the wheel and roll wear), waviness on both surfaces are created influencing the roundness of the roll and wheel and thus affecting the cutting. The energy focalizes at the rotational frequency of the part that introduce more energy into the system: a lobed wheel, for example, introduces most of its energy at one of its harmonic. This energy, for wrong wheel speeds, can fall into a system resonance and then being amplified intensifying the problem of the waviness.

Even if still experimental, this diagram is a good starting point to design an experimental plan for obtaining a dataset of good and bad cutting conditions. To be sure to select runs for phase I that might not produce chatter marks on the roll we made use of another graph, called Forced Maps (see

fig. 4.3). Providing the system resonance measured with the modal analysis, this graphs shows with colored horizontal and vertical bands the speeds that make the wheel and roll harmonic to fall in a narrow band close to a machine resonance, thus increasing vibration and possibly leading to the chatter phenomenon. The red lines in fig. 4.3 indicate the workpiece and wheel velocities that are multiples: these values should be avoided in order to limit the regeneration effects. In this case wheel speed is expressed in m/s^2, and the bands are $\pm 4\%$ of the unstable wheel speeds.

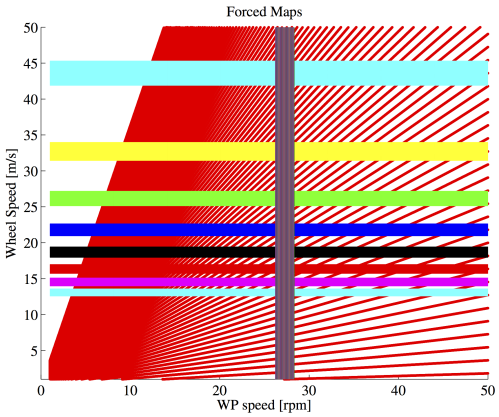

Figure 4.3: Forced Maps showing speeds that make the wheel and roll harmonic to fall in a narrow band close to a machine resonance. Courtesy of *Engr.* Leonesio M., CNR-ITIA, 2013.

It is worth to notice that this approach was used to help us in identifying the sets of parameters to design the experiments. However, the complexity of the machine dynamics characterization and the need for reliable validation of such a method motivate the investigation of process monitoring solutions that do not require such a complex and time-demanding pre-process characterization.

Having defined the procedure used to identify phase I and phase II passes, it's now important to specify how the test have been performed.

- The tests have been conducted according to the technological range of the machine which is smaller than the range showed in fig. 4.3.
- For an initial model identification and evaluation a set of run with constant roll speed and two levels of end infeed is performed.
- The continuous infeed has been kept equal to the end infeed for all this batch of tests.

- The nominal wheel diameter is 700 mm with a width of 75 mm, while the initial roll diameter is around 500 mm and its axial length is 1700 mm.
- Wheel, headstock, tailstock accelerometers data together with acoustic emission and CNC unit parameters have been recorded at a sampling rate of 2000 Hz.
- For every single wheel speed run which should not cause chatter vibrations, 8 passes of roughing grinding without overlap have been conducted.
- For bad cutting conditions the number of passes have been stopped just before the phenomenon reaches dangerous conditions.
- After every run conducted with bad cutting parameters the roll is set back to good starting conditions milling it with known good cutting parameters.
- The test for model identification and evaluation is shown in fig. 4.4.

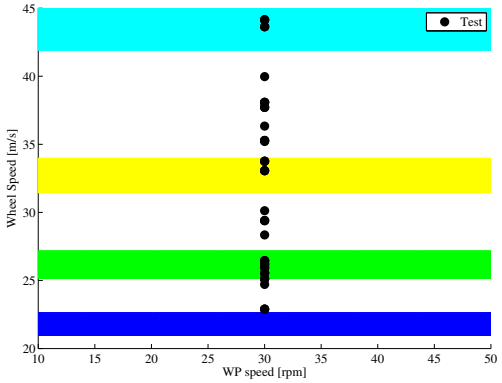

Figure 4.4: Experimental Plan designed on the basis of the Forced Maps.

One of the purpose of the monitoring approach is to be robust to process parameters variations. For this reason, in this first batch of test, we have kept the roll speed constant and varied only the wheel speed and the infeed because they are supposed to be the most influencing factors connected to chatter vibrations. The dependency of the monitoring approach towards variations of wheel speed and infeed rate will be investigated. Unfortunately running a DoE with different workpiece speed, wheel speed and infeed rate would have requested too many hours of machining, which were not available. For this reason we have decided to reduce the experimental plan, and pick

up in a second run of test some working conditions with different values of cutting parameters to be tested with the designed monitoring system.

The experimental plan parameters are shown in section 4.3.3 tab. 4.3.

4.2 Pre-processed data analysis

Before carrying out the tests scheduled in section 4.1, preliminary tests are realized. In fact, due to the experimental nature of this project, we must ensure that data are recorded correctly; then, on these data, preliminary analysis will be made to understand the process behavior and how the accelerometers react.

Observing the accelerometric signals, the presence of peaks with random intervals emerges; so it is necessary to investigate the cause that led to the creation of those peaks, to see if they are caused by the process or by another type of cause. A brief analysis led us to say that these peaks can be considered true *outliers*, as they are due to electrical problems, related to the grounding system of the devices which acquire the data.

For this reason, because they are definable as *assignable causes*, it is important to 'delete' them. However, we have chosen not to simply remove the data outliers in order to perform an analysis in the frequency domain. We have opted for a reduction of the energy content of these peaks, reducing their level with a local smoothing. The peaks are weighted according to the local variability. In fig. 4.5a an accelerometric signal with spikes is compared with the same signal cleaned out. In fig. 4.5b instead a detail of the comparison between the signal with and without the spikes is shown.

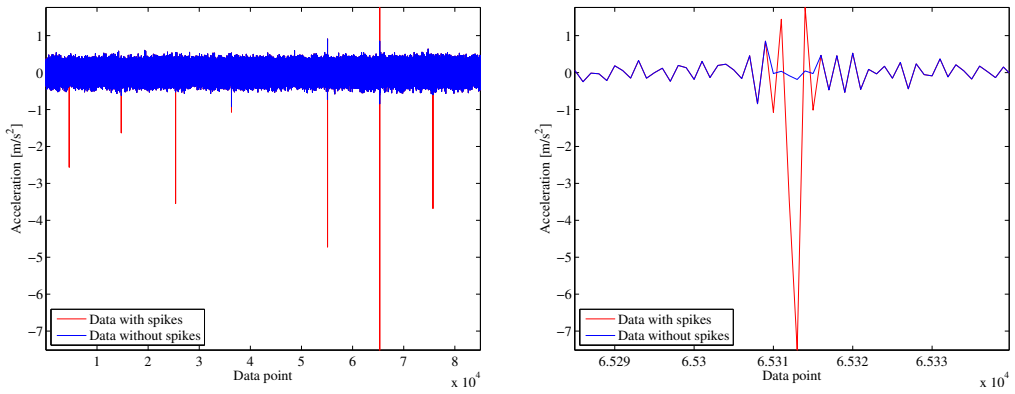

(a) Signal of an whole operation.

(b) Details of a spike.

Figure 4.5: Comparison between data with and without electrical spikes.

Using this approach, we noticed that there aren't significant impacts in the frequency domain after the reduction; in other words the signal spectrum and its harmonics are not affected by these correction. In fig. 4.6 the comparison between the FFT calculated on a window of 1 s of a signal containing a peak and the FFT with the data correction, is proposed. What is observed is the presence of an initial decay in the signal with the spike, significantly reduced in the same signal without the peak. The presence of the decay in fact is precisely caused by the presence of a peak, which increases the noise of the spectrum. The FFT are shown for velocity and displacement; in acceleration FFT there isn't a an initial decay, but there is a different level of mean between the two spectra.

This approach will be applied to all signals that will be used in the following analysis; in this way, we eliminate the outliers that are not related to the process and may lead to false conclusions.

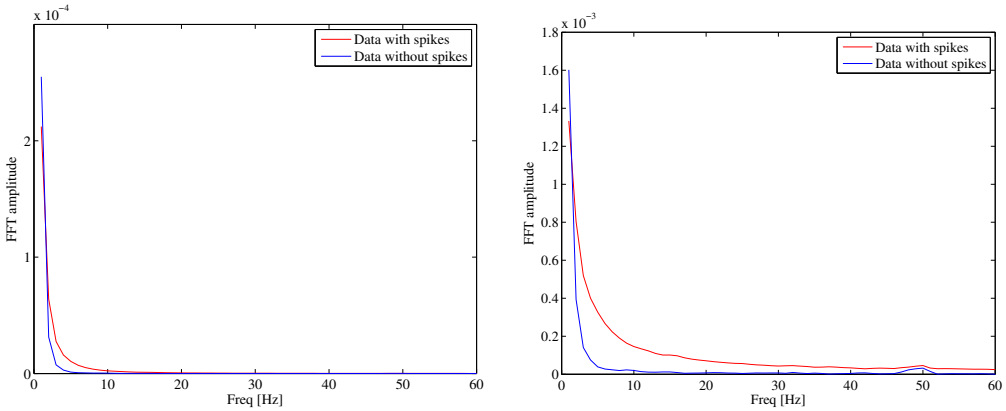

(a) Decay Displacement.

(b) Decay Velocity.

Figure 4.6: Comparison between decay of data with and without spikes.

The same preliminary tests are used to compare the sensibility to chatter phenomenon of the x, y and z *axis* of each accelerometer and then to analyze the sensibility of each accelerometer, in relation to the position on the machine.

Remember that the axes of the accelerometers, as shown in section 3.1 are the same of machine axes. In fig. 4.7, the signals of the four accelerometers for each axis have been plotted. These specific data were recorded during a process that has caused waviness on the cylinder. Between the four accelerometers, a first analysis displays that the basement one is less affected by the chatter phenomenon; on the contrary, the other ones seem to detect vibrations.

A further comparison can be made towards the three axes of each accelerometer. Indeed, it is possible to see that the x axis is strongly more sensitive than y and z axes. This is in accordance to the assumption of the chatter generation that, as has been said in section 1.2, arises when the grinding wheel and the roll oscillate periodically in the radial direction modifying the actual depth of cut. The main machining axis is exactly the x axis, which consistently turns out to be the most sensitive.

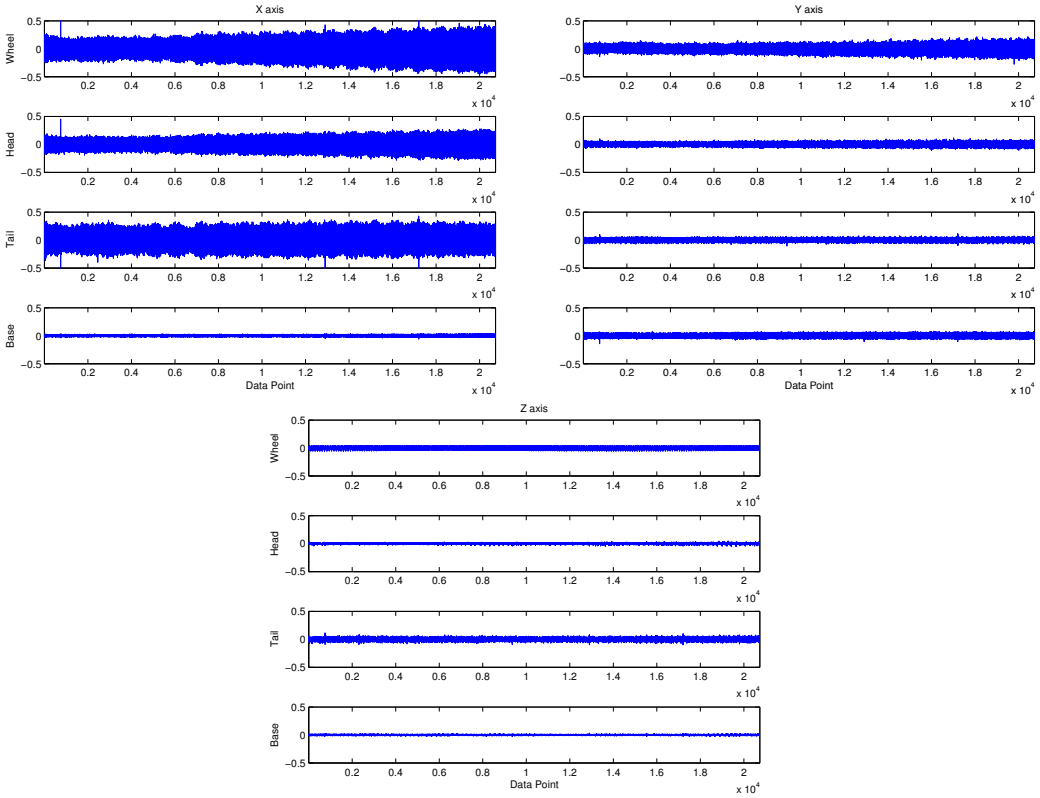

Figure 4.7: Accelerometric signal from four different points on the machine.

4.3 Dataset characterization: *in* and *out of control* experiments

Until now we have talked about the importance for control chart design of defining phase I and phase II:

- phase I: requires a set of process data that are analyzed in a retrospective analysis, to build control limits. These data must come from a process working under stable conditions and representative of good process performance. To qualify this process, we must define and understand what can be considered a good final workpiece.
- phase II: is composed by a set of data on which the control chart is tested.

The qualification of phase I data is made after the final product has been produced. During the process the accelerometer and the CNC unit data are acquired. To link the data recorded to the quality of the final product, three approaches have been followed:

- *By-eye inspection*: a skilled operator evaluates by eye the surface quality of the roll making a *go/no go* judgment.
- *Caliper measure*: the roll is measured with a caliper installed on the machine which can evaluate roundness, straightness and even roughness.
- *Spectral analysis*: the signals from the machine are analyzed in the frequency domain as an additional proof of the presence of anomalous vibrations.

4.3.1 Caliper analysis

When the grinding process is completed and the skilled operator has expressed a judgment about the surface quality of the milled roll, the surface is then analyzed by means of a caliper numerically controlled. The caliper is a fork moving along the horizontal axis. The fork is constituted by two arms, which can be moved independently on vertical axis. Each arm supports an high resolution displacement sensor, identified by axes E and Q which measures the vertical displacement of a cylindrical probe tip, which is in contact with either the upper or lower side of the roll. During measurement the fork is placed on the roll, and axis C is moved until the output of sensors on axes E and Q is equal to zero. Then the roll is rotated, and the two sensors simultaneously measure two diametrically opposed points of the roll.

As the purpose of these experiments is to acquire from the sensors a set of 'good process vibrations', it is sufficient to discriminate between a good quality surface and a bad one. No inference on the amount of waviness will be done during this work, and different amount of vibrations will not be connected to different levels of waviness. This link might be possible in a future work, but not in this case, because the purpose is just to detect the growth of anomalous vibrations which should lead to chatter phenomenon.

However, to discriminate between a good and a bad workpiece we have followed a precise measurement procedure of the surface of the roll. Five sections along the axial length of the roll has been acquired according to the model of fig. 4.8. Each section has been replicated 10 times and then averaged in order to smooth possible surface dirt or chip traces that can affect the data acquired. The analysis is then conducted on the resulting 5 sections of the roll.

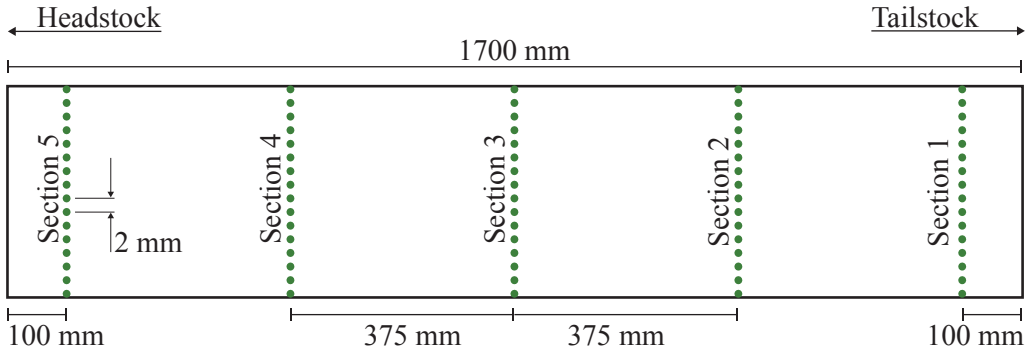

Figure 4.8: Location of caliper measures on the roll.

Caliper measures are analyzed in the frequency domain, where it easier to see the number of lobes that a bad cutting condition might have generated on the roll. During the analysis is important to distinguish between shapes feature and roughness. A common value for shapes feature is around 50 *upr* and it is indicated in fig. 4.9 and 4.10 with a red line. To detect waviness we should look in the range starting from the red line up to the end. If a spike occurs it is possible that the roll is lobed and chatter marks are visible on its surface. The number of lobes on the roll corresponds to the *upr* value of the spike, in the case of fig. 4.10 the number of lobes on the roll is 126. The number of lobes on the cylinder can be calculated if the chatter frequency is known as shown in section 4.1 where with wheel rotational frequency of 10.5 Hz (630 rpm) and a roll rotational frequency of 0.5 Hz (30 rpm) the waves on the roll will are 63/0.5=126, as it is in the case of fig. 4.10.

Even if used as a rough measure of the presence of lobes on the roll, this

analysis is enough for determining the presence of waviness on the roll, adding information about the number of marks present to the *go/no go* judgment expressed by the operator.

As an example of this analysis in fig. 4.9 is a plot of a workpiece after an in control roughing phase and in fig. 4.10 is a plot of an out of control surface.

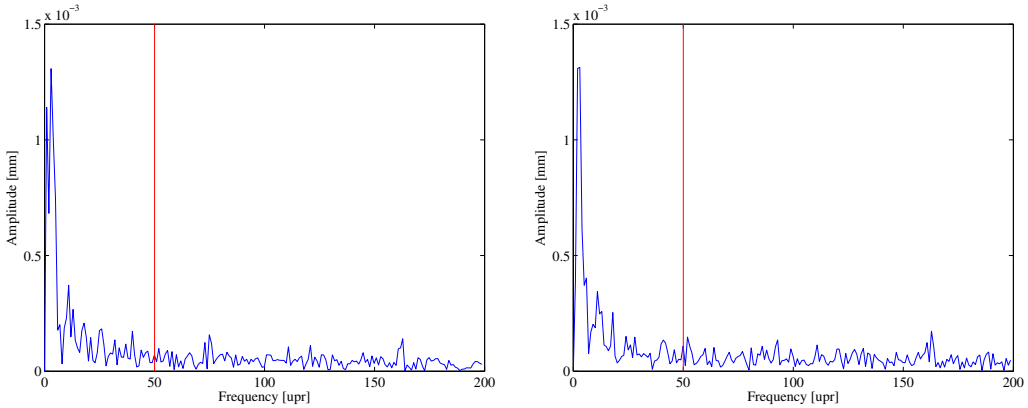

(a) Section 1 (b) Section 3

Figure 4.9: Caliper Analysis of an in control condition.

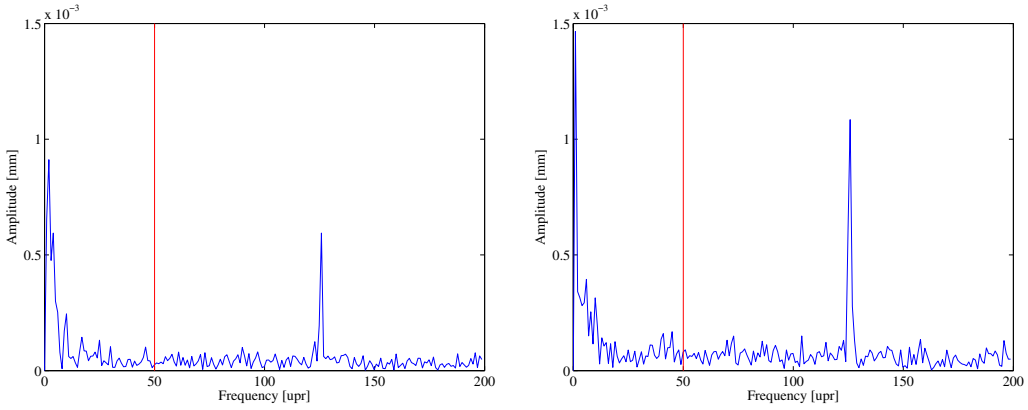

(a) Section 1 (b) Section 3

Figure 4.10: Caliper Analysis of an out of control condition.

4.3.2 Spectral analysis

In addition to the caliper analysis, to qualify the performed test in terms of in control or out of control, an analysis of the signals in the time-frequency domain is proposed. The aim of this analysis is to verify if the classification defined by the caliper is the same that is determined by the signals analysis. For this reason, the analysis will focus on the same tests used in the previous section. However, instead of using measures of the geometric shape of the roll, we will analyze the signals acquired during the process.

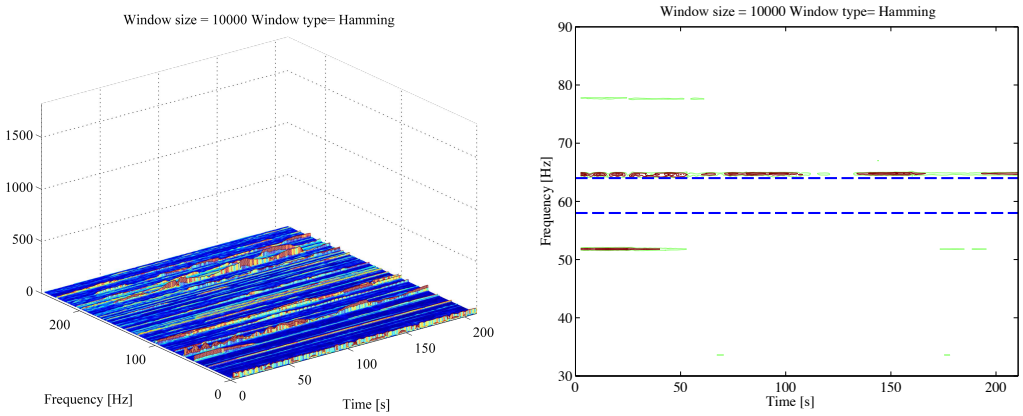

(a) Spectrogram. (b) Contour plot.

Figure 4.11: Spectrogram analysis of an in control operation.

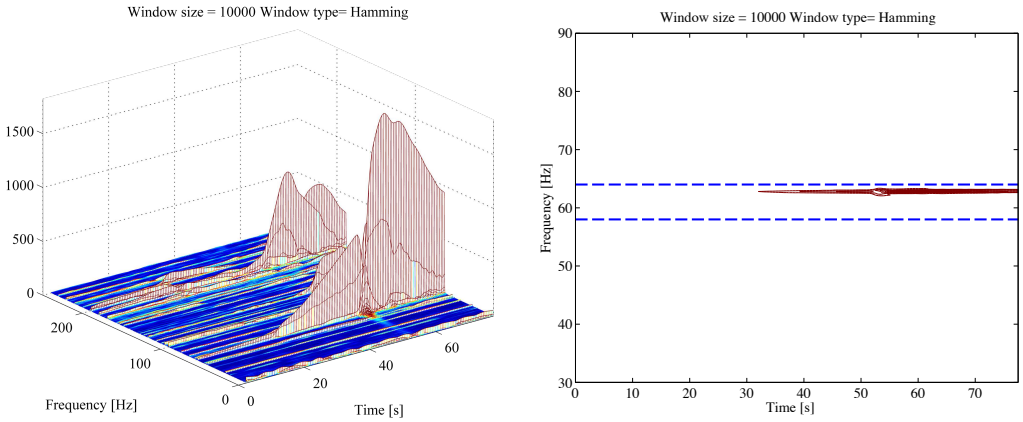

(a) Spectrogram. (b) Contour plot.

Figure 4.12: Spectrogram analysis of an out of control operation.

In fig. 4.11 and 4.12 there are the spectrogram and the contour plot of

two different operations: the first one is in a 'in control state' and the other one is in a 'out of control state'.

To realize the spectrogram and the contour plot, a Hamming window of 5 s with a 90% overlap is adopted. The spectrograms are limited at the 250 Hz frequency, in order to better visualize the behavior of the signals in the frequency range of our interest, between 58 Hz and 64 Hz.

Comparing the two spectrograms (fig. 4.11a and 4.12a), it is possible to notice the difference: in fact, if in the first one there is no frequency that dominates the others, in the second one there is a particular frequency that stands out compared to the others. To confirm that the predominant frequencies are those of our interest, the contour plots of the interest range frequency are shown, and they confirm that the more relevant frequency in fig 4.12b is precisely within the interest range; at the contrary, in the other contour plot (4.11b) there aren't frequencies within the interest range.

4.3.3 Test qualification

As said in section 4.1 an experimental plan has been conducted with two levels for the factor *infeed* and four levels for the factor *wheel speed* for the parameters that we expected to be 'in control' and then we picked up some test for out of controls parameters. It has been important to have a balanced plan for the 'in control' conditions to estimate the robustness of the statistical model that we want to use. At the end of every single test we evaluated the quality of the roll with the three methods explained before and then we divided them in tab. 4.3a and in tab. 4.3b according to their contitions.

4.4 Development of chatter indicators

The vibration signals usually present multiple harmonic components with different frequencies and phases. The representation of the vibrations in the time domain allows the estimation of some parameters in amplitude (Root mean square, peak to peak, *etc.*); instead a frequency analysis is essential to evaluate the contribution provided by different harmonic that compose the signal.

There are many different synthetic indicators that summarize the informations coming from the accelerometric signals and parameters. In this work, these synthetic indicators makes part of the 'sensor fusion module' of the EPC and they are analyzed by the 'machine & process diagnosis module' to identify process and machine state, related with vibration problems, e.g. identifying vibrations sources due to unbalance or other periodic excitations

Table 4.3: Test for model identification.

(a) Tests marked as 'in control'

Test n.	**WH vel** $[rpm]$	**Infeed** $[mm]$
1	680	0.01
2	680	0.02
3	780	0.01
4	780	0.02
5	830	0.01
6	830	0.02
7	1000	0.01
8	1000	0.02
9	1100	0.01
10	1100	0.02

(b) Tests marked as 'out of control'

Test n.	**WH vel** $[rpm]$	**Infeed** $[mm]$
1	630	0.01
2	630	0.02
3	720	0.01
4	720	0.02
5	730	0.01
6	910	0.01
7	930	0.02
8	970	0.02
9	1200	0.01
10	1230	0.01

or due to the grinding process interaction with the machine structure compliance.

Different synthetic indicators can be extracted from vibration signals to characterize the machine and process vibration states in order to perform an effective diagnostic and control. The most important condition that has to be monitored during grinding is the chatter onset. The result of this condition, the waviness, is generated by a single vibration component, that build up and keep up at high level during the cycle.

Below, both of the indicators in time-domain and frequency-domain will be proposed and analyzed.

4.4.1 Time-domain chatter indicators

The input for the calculation of chatter indicators in time-domain are only the accelerometric signals. In tab. 4.4 there are the five indicators that we propose to use, with the mathematical formula to calculate them.

- The *RMS* indicator is a standard measure that returns an evaluation in amplitude directly related to the energy content of the vibration.
- The *kurtosis* is defined as the fourth statistical moment divided by the square of the second statistical moment. This is done to remove variability due to waveform amplitude from the measurement. It is a compromise measurement between the insensitive lower moments and

Table 4.4: Time-domain indicators.

N.	Name	Outputs	Units
1	RMS[a]	$\sqrt{\frac{1}{N}\sum_{i=1}^{n}\lvert X_n\rvert^2}$	m/s^2
2	Kurtosis	$\frac{\frac{1}{N}\sum_{i=1}^{n}(X_i-\bar{X})^4}{\left(\frac{1}{N}\sum_{i=1}^{n}(X_i-\bar{X})^2\right)^2}$	-
3	Skewness	$\frac{\frac{1}{N}\sum_{i=1}^{n}(X_i-\bar{X})^3}{\left(\frac{1}{N}\sum_{i=1}^{n}(X_i-\bar{X})^2\right)^3}$	-
4	Peak to peak	$\lvert X_{max}-X_{min}\rvert$	m/s^2
5	Peak to RMS	$\frac{\lvert\lvert X\rvert\rvert_\infty}{\sqrt{\frac{1}{N}\cdot\lvert X_n\rvert^2}}$	-

[a] RMS: Root Mean Square.

the over-sensitive higher moments. It is particularly useful in the detection of bearing failure.

- The *skewness* indicator measures the relative energy above and below the mean level.
- The *peak to peak* indicator indicates the maximum excursion of the wave.
- The *peak to RMS*, or *crest factor* is the ratio between the peak value and the RMS value. There are relevant crest factors in collisions.

4.4.2 Frequency-domain chatter indicators

Changing the point of view of the signal analysis from time-domain to frequency-domain does not detract and does not add anything, but it is just a different way to represent the data. The FFT algorithm operates on a time history of finite length to calculate the Fourier transform. Fourier transform (FFT) gives the spectral content of the vibration signals allowing the identification of the dangerous vibration components.

Different synthetic features can be extracted by the spectrum of each vibration signal allowing the determination of the most promising index for the chatter monitoring. In tab. 4.5 is possible to see the frequency-domain

Table 4.5: Frequency-domain indicators.

N.	Name	Outputs	
6	Relative SEV[b]	$\frac{total\ sync.\ energy}{total\ energy}$	%
7	Relative maximum SEV	$\frac{max.\ sync.\ energy}{total\ energy}$	%
8	Absolute SEV	$total\ sync.\ energy$	m/s^2
9	Absolute maximum SEV	$max.\ sync.\ harmonic\ energy$	m/s^2
10	Relative maximum harmonic SEV	$\frac{max.\ sync.\ harmonic}{total\ sync.\ energy}$	%

[b] SEV: Synchronous Excitation Value.

chatter indicators proposed by *Engr.* Parenti, P. and *Engr.* Cassinari, A, who are working on the project to develop the EPC module.

The input for the calculation of chatter indicators in frequency-domain are the accelerometric signals and the wheel velocity. Most of these indicators refers to total energy as the integral of the FFT, while by synchronous energy they refer only to the integral of the bands of fig. 4.13 which are defined as multiple of the wheel speed expressed in Hz.

All the features captured by these indicators are important but some of them seem most prone to a quick identification of the chatter onset. In particular the *relative maximum SEV (SEV%)* is very sensitive in respect to chatter onset and it tends to increase rapidly when this condition is reached. For this reasons this main index is used by the EPC to determine the 'vibration process state': stable conditions are represented by low values of *SEV%* (< 20 %) while during chatter conditions this index increase significantly (up to 90 %). If chatter condition is maintained in the grinding process the waviness will certainly be present on the surface of the roll.

In fig. 4.13a the FFT synchronous bands for an in control pass is shown, highlighting the Max synchronous band on which indicates such as Relative Max SEV Absolute Max SEV and Relative Max harmonic SEV are based. In fig. 4.13b is possible to see a FFT of an out of control run (wheel speed = 10.5 Hz) that has a spike at the chatter frequency of $63Hz$ correctly identified by the band corresponding to 6times the wheel speed.

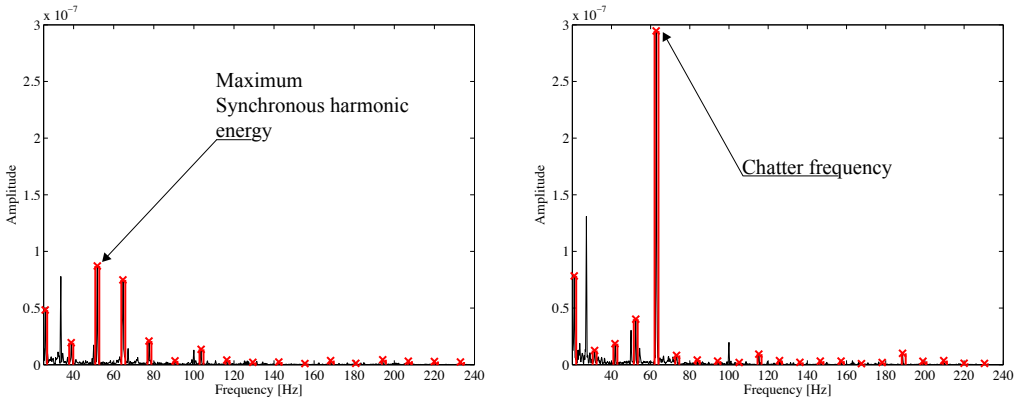

(a) In control pass - FFT spectrum.

(b) Out of control pass - FFT spectrum.

Figure 4.13: Fourier Spectrum and the extracted features that compose the synthetic indicators. Courtesy of *Engr.* Parenti, P. and *Engr.* Cassinari, A.

4.5 Data snooping of processed data

After having analyzed raw data of the test conducted, and calculated the indicators developed in sections 4.4.1 and 4.4.2, an analysis of the indicators is proposed. To develop a statistical process control on multiple indicators of this process it's important to identify if the proposed indicators are effectively capable of detecting the chatter phenomenon or they capture other sort of variations. The main issue is then to identify a set of these indicators that are robust to the process parameters but then are able to detect anomalous vibrations. A box plot analysis between the indicators calculated on the passes marked 'in control' and the indicators on the one 'out of control' is conducted to prove that the indicators detect a difference between these two groups. Then we will focus only on the 'in control' passes to see if the indicators calculated on good process conditions are statistically influenced by the modification of process parameters or not. This analysis is of great importance because if we realize a control chart on indicators that are greatly affected not only by the chatter presence but also by the variation of the process conditions, we would have a chart with a great number of false alarms.

The problem of the false alarms is one of the main cause of not adoption or dismiss of control charts for process monitoring because it would lead to a great number of process stops which translates in the increase of production costs. For this reason, one of the main issue that an SPC has to face is the problem of 'controlling' false alarms, which are in the industrial world of a great importance. An SPC built on indicators that changes mean or

variance during an in control phase is an SPC model that would not be used in industry; a much more appreciated model is one that is a little bit slower in the identification of out of control but much more reliable and robust during good process conditions.

4.5.1 Sensitivity of synthetic indicators to the chatter phenomenon

In this subsection we propose a preliminary analysis, carried out through the use of box-plots, which represent a sufficiently complete and concise description of the frequency distribution of the available data.

To verify that the indicators are sensitive to the two states of the process ('in control' and 'out of control'), two box-plots are plotted, one for each state of the process. This is done for each of the proposed indicators calculated on the three accelerometers. The box-plots displayed in this way indicate the relative variability of the entire sample defined 'in control' and 'out of control'.

The data used for this analysis are the results of the test described in tab. 4.3a and in tab. 4.3b. The fig. 4.14 shows the example for two time-domain indicators and the fig. 4.15 for two frequency-domain ones. All the others box-plots are shown in Appendix A.

This preliminary qualitative analysis shows a significant difference between the two types of process states. The two populations, in fact, seem to show significant qualitative differences for all five statistical values that the box-plots summarize.

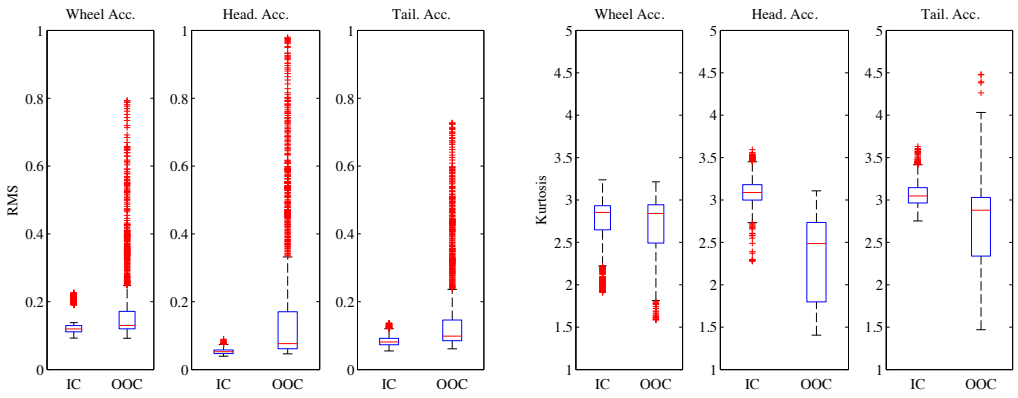

(a) RMS box-plot (b) KUR boxplot

Figure 4.14: Two examples of time-domain indicators box-plot

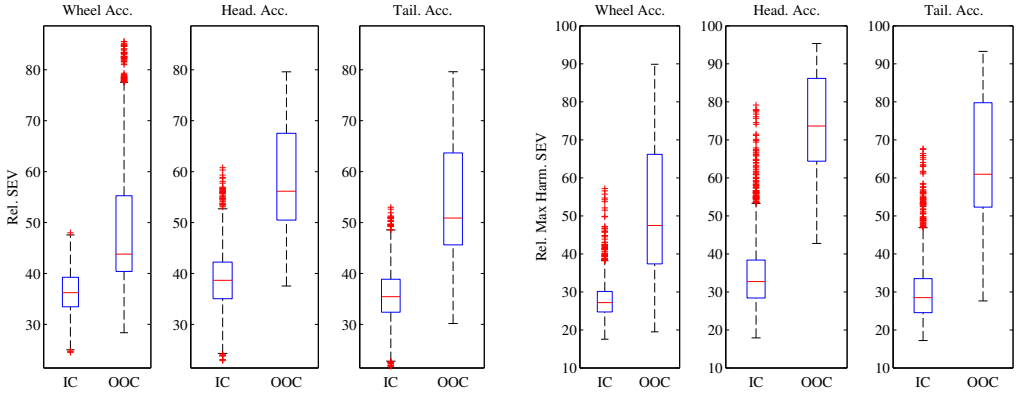

(a) Rel. SEV box-plot (b) Rel. Max Harm. SEV box-plot

Figure 4.15: Two examples of time-domain indicators box-plots

The main difference that is possible to see comparing the indicators is the presence of outliers: there are some indicators in the 'out of control' state that have many outliers points, and other indicators that do not present them; RMS, $P2P$, $Abs.\ SEV$ e $Abs.\ Max\ SEV$ are the most sensitive indicators to this phenomenon. The presence of outliers is probably due to the chatter phenomenon that, during the process, grows and amplifies exponentially with increasing of grinding operations. However, the other indicators are not exempt from this problem, which are present in a lower quantity and equally distributed in both states of the process. This could be due to some grinding operation with a wheel velocity that is 'border line' in the stability map of fig. 4.2. Probably, during these operations, higher vibration compared to the other 'in control' operations occurred, but the surface of the roll was categorized as 'in control' because the roll does not presented waviness on it. In the next subsection, we are going to investigate these problems of variability.

4.5.2 Sensitivity of synthetic indicators to process parameters

In this section, a qualitative analysis of the sensitivity of the indicators towards the process parameters is conducted. The test analysed are the one of tab. 4.3a, which are the test marked as 'in control'. It is important that the indicators calculated on good process conditions are not affected by the process parameters as said introduction of section 4.5. According to tab. 4.3a, the wheel speed and the infeeds have been changed while, as detailed in section 4.1, the roll speed has been kept constant to reduce the experimental

plan due to time constraints of machine availability. On empirical basis it has been proved that the main issues derive from wheel and infeed, and the roll speed affects the system stability in a much lower way. It will not be possible to investigate with a proper DoE the influence of the roll on the indicators but only wheel speed and indeed. As a qualitative analysis main effects plots and individual value plots are conducted on all the indicators proposed, and are included in Appendix B. The main effects plots show the sensitivity of indicators to wheel speed, infeed and location of the accelerometers. The individual value plots show the variability between and within the samples.

The first analysis that is proposed regards the comparison of the averages of each indicator calculated on the three accelerometers varying both speed and infeed parameters. It is observed from a first graphical analysis that all the indicators calculated on the wheel accelerometer are strongly affected by the grinding wheel speed variation, on the contrary the other two accelerometers are less affected by this parameter.

This is what we expected, and it is easy to explain: the wheel accelerometer is positioned very close to the wheel, exactly on the wheel carriage (see fig: 3.3) and therefore it is normal that most of the vibrations caused by a change in wheel speed affect the indicators levels. The other two accelerometers are placed far from the wheel carriage, and for this reason they do not seem to be very affected by this parameter. Moreover, as an additional proof, the wheel accelerometer appears to be the most sensitive, in fact, observing the level of indicators RMS and $P2P$, which are the only ones that share the measurement unit with the original signal, it is easy to see that it is higher when calculated the wheel accelerometer.

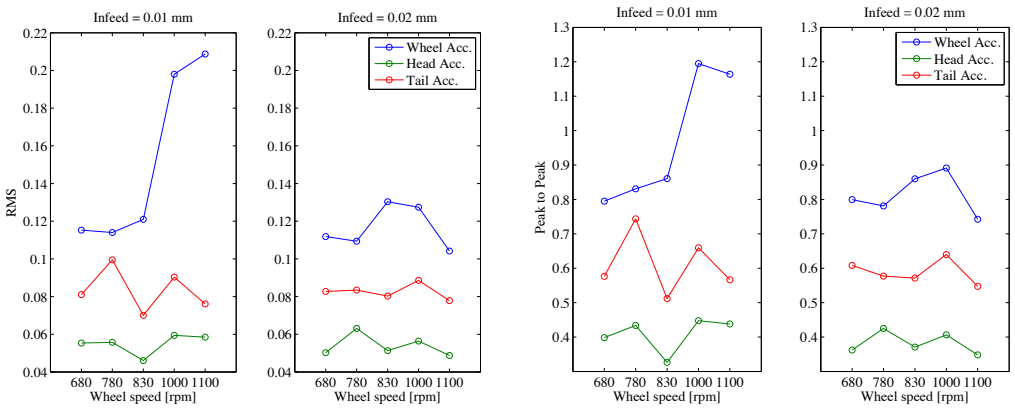

(a) RMS main effects plots

(b) P2P main effects plots

Figure 4.16: Main effects plots of RMS & Peak to Peak.

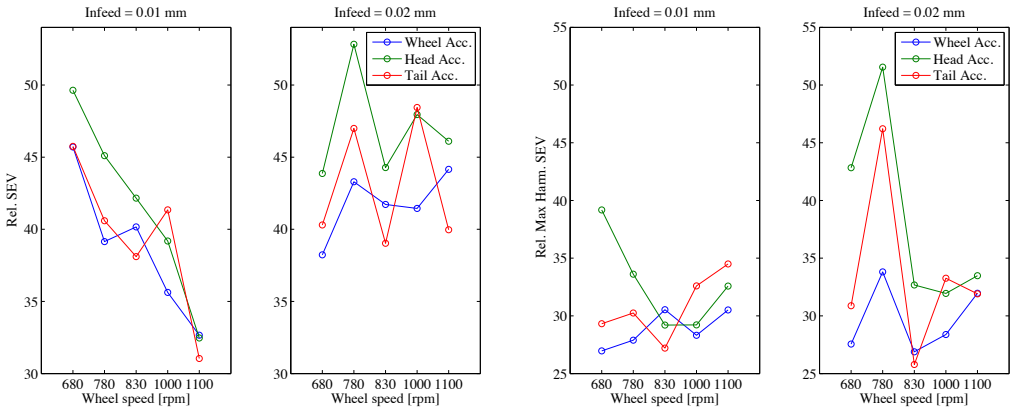

(a) Relative SEV (b) Relative Max Harm. SEV

Figure 4.17: Main effects plots of Relative SEV & Relative Max Harm. SEV.

Considering all the main effects plot is possible to see which are the indicators that are most sensitive to speed and infeed variations and then identify the most robust.

For the time-domain indicators (see fig. 4.16), it is possible to see that RMS, $P2P$ e $P2RMS$ calculated both on headstock and tailstock accelerometers seem to be the less sensitive to the process parameters and could be good candidates for an SPC model. The frequency-domain indicators, on the other hand, seem to be the most sensitive to process conditions, mainly due to their construction which is focused only on a specific range of frequencies. The frequency-domain indicators that are less affected by process parameters are the Relative SEV and the Relative Maximum Harmonic SEV, excluding the test with infeed 0.02 mm and wheel speed 780 rpm where the indicators level has increased even if on the roll no signs of chattering have been detected (see fig. 4.17). All the time-domain indicators, except from the skewness, when calculated on the wheel accelerometers show a different behavior whether the infeed is at 0.01 mm 0.02 mm. When the infeed is at 0.01 mm a dependency of the indicator towards the wheel speed is evident, on the other hand at 0.02 mm of infeed this dependency is less visible. This fact can be related to process, because when the infeed is at a low value, the contact between the wheel and the roll could be so small that the shapes of the vibrations change from speed to speed values. On the other hand the shapes of the vibration of captured by the indicators when the infeed is at 0.02 mm are not so different even if the wheel speed changes.

Even the frequency-domain indicators show, in some cases, a sort of linear dependency towards the wheel speed when the infeed is low and a different

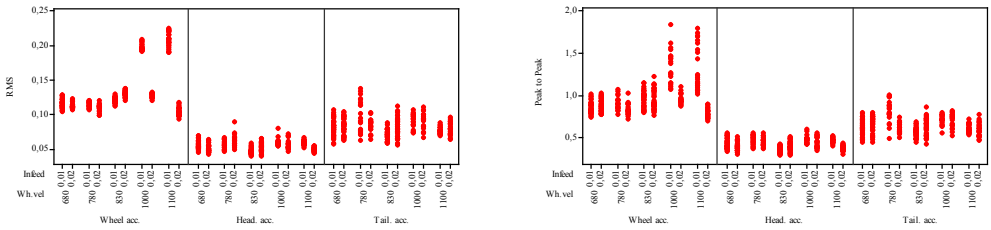

(a) RMS individual value plots

(b) P2P individual value plots

Figure 4.18: Individual value plots of RMS & Peak to Peak.

distribution when the infeed is high. Moreover with infeed 0.02 mm it is possible to see a strange behavior of all the indicators when the wheel speed is set to 780 rpm which suggest that maybe the process was going out of control.

The second type of graphs, individual value plots, is useful to analyze the variability of the samples at our disposal. In fig. 4.18, the individual value plot of the indicators RMS and $P2P$ are shown while fig. 4.19 displays the individual value plot of two frequency-domain indicators. The variability within the samples does not seem constant; however, from a brief analysis, it is not easy to identify a model underneath the behavior of the indicators when both speed and infeed are varied. In fact, for example, growth of variability, when increasing the speed or the infeed factors, it is not observed; sometimes the variability seems to grow with the infeed factor, sometimes the opposite happens. A chaotic behavior seems to be common to all these datas.

One of the main problems emerged from the box-plot analysis is the presence of numerous outliers, especially in some of the indicators calculated on the data defined in the control. Analyzing the individual value plot, we can identify the cause of what has been described.

The box-plot of the kurtosis indicator calculated on the wheel accelerometer shows many outliers relative to the lower tail of the box-plot. Looking at the individual value plot of wheel accelerometer, it is easy to see that there are two-speed wheel, with the same infeed, which have a mean value significantly lower than the other tests. The same is observed, on the contrary, in the box-plot of the RMS indicator (see fig. 4.18a) where the outliers are in the upper tail of the box-plot. Taking a look at the individual value plots, we can quickly see that the outliers are caused by the same tests that create outliers in the box-plot of the Kurtosis indicator. On the same parameters, a different phonemenon can be seen in the individual value plot of $P2P$ indicators in fig. 4.18b, where the variability of the indicator calculated on the

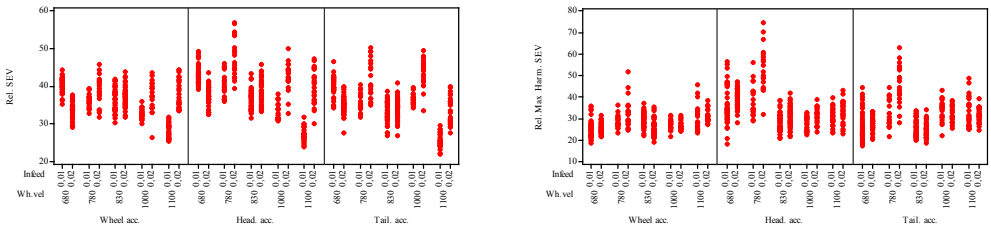

(a) Relative SEV

(b) Relative Max Harm. SEV

Figure 4.19: Individual value plots of Relative SEV & Relative Max Harm. SEV.

wheel accelerometer grows significantly only when the wheel speed is set to 1000 and 1100 *rpm* with an infeed of 0.01 *mm*. A second level of the speed factor that appears to be problematic, is 780 *rpm*; in correspondence of this level some indicators display outliers values which suggest that this test run is probably affected by an increase of chattering.

In conclusion, what emerges from these qualitative analysis is a quite strong dependance of the indicators from the wheel speed; instead the infeed factor appears more problematic to define. In some cases in fact it seems that the infeed affects the signals and sometimes it doesn't. As it is critical to select a subset of robust indicators we need to use an approach that is capable of combining in a robust way all these indicators. Through the vPCA approach we analyze the correlation between the different channels to fuse them appropriately. Combining the indicators in an appropriate way we should be able to design a control chart with control limits that are not sensible to process parameters variations, but sensitive to changes in acceleration caused by the chattering phenomenon.

Until now we have described in section 3.1 how we acquire the raw data from the on-line process and in section 4.4 how we summarize raw accelerometric data into a set of synthetic indicators. In section 2.2 and 2.3 we have detailed the statistical approach that we use to fuse the selected indicators into two statistics that we will monitor during the process. In chapter 5 we propose a selection of tests that show how the monitoring strategy has been applied in identifying the chatter phenomenon. We will test the robustness of the model against a phase II that includes both in & out of control samples. If appropriately estimated the empirical limits should have a rate of false alarms that is coherent to the target value with which they are designed, but they should also detect the samples in which the process has produced chatter marks on the roll.

Chapter 5

Results Analysis

In this chapter the application of the PCA technique, described in chapter 2, will be shown, following the methodology detailed in section 2.3. The available data are the accelerometric signals recorded during the grinding operations, on which the synthetic indicators, explained in sections 4.4.1 and 4.4.2, are calculated.

5.1 Assumptions

In this section, the assumptions used to perform the examples are summarized. All the examples are organized as follow:

1. system training on two 'in control' datasets;
2. system testing on two other datasets:
   (a) first set: 'in control', where the surface of the roll has been judged acceptable;
   (b) second set: 'out of control', where chatter marks are visible on the surface of the roll;

These examples are aimed at evaluating the control charts performances in terms of true and false alarms. In subsection 5.1.1 we will explain the input parameters for all the datasets used in Phase I and Phase II.

The previous analysis has shown, in section 4.5.2, that the time-domain indicators are generally more robust to the parameters variation than the frequency-domain ones. In spite of this, in order to perform a more complete comparison between time-domain and frequency-domain synthetic indicators, the same examples will be proposed performing the analysis with the use of the most robust indicators of both categories. In tab. 5.1 are listed, for each accelerometer, the indicators used to perform the PCA approach.

Table 5.1: For each accelerometer, the indicators used for PCA are summarized.

Accelerometer	**Time-domain ind.**	**Frequency-domain ind.**
Wheel	SKEW	Rel. Max. SEV Rel. Max. Harm. SEV
Headstock	P2P P2RMS	Rel. Max. SEV Rel. Max. Harm. SEV
Tailstock	P2P P2RMS	Rel. Max. SEV Rel. Max. Harm. SEV

The choice is made after the analysis proposed in chapter 4. In fact, the frequency-domain indicators that seem more stable are *Rel. SEV* and *Rel. Max Harm. SEV* of all three accelerometers. Instead, as regards the other group of indicators, these are not chosen equal for each indicator. For the wheel accelerometer, we have chosen only the $SKEW$ indicator, which is the only insensitive to the variation of the wheel speed. For the other two, the most robust indicators seem to be $P2P$ and $P2RMS$.

The accelerometers that we use are the wheelstock, the headstock and the tailstock ones, as they are the most sensitive to the process vibrations. To avoid excessive number of signals that the system has to manage, we decided to acquire only the *x-axis* signal because, as we have demonstrated in section 4.2, it turned out to be the most capable of providing more information about the ongoing process. All the indicators are calculated on a 5 s window with a 90% overlap, in order to have a frequency of 1 value every $0.5s$ but still referring to 5 seconds of data points. For this reason, the input matrix for vPCA method is composed by 5 indicators for the time-domain examples while by 6 indicators in the frequency-domain examples. On this matrix, the PCA will calculate the principal components (PC); then we will choose the number of principal components to reduce the size of the input matrix still explaining a good part of variability. These PC are then merged to obtain two statistics: T^2 and Q that are used to build the control charts. In the control charts, there will be two different control limits: the percentile control limit and the moving block bootstrap one. To calculate the control limits, we use $\alpha_{overall} = 1\%$. The procedure on which this analysis are based is analytically explained in section 2.2 and 2.3.

Table 5.2: Tests for phase I control charts.

	Test 1		**Test 2**	
	WH vel. $[rpm]$	**Infeed** $[mm]$	**WH vel.** $[rpm]$	**Infeed** $[mm]$
Phase I	680	0.02	680	0.02
	830	0.02	680	0.01

Table 5.3: Tests for phase II control charts.

	Test A		**Test B**	
	WH vel. $[rpm]$	**Infeed** $[mm]$	**WH vel.** $[rpm]$	**Infeed** $[mm]$
Phase II	830	0.01	1000	0.02
	970	0.02	910	0.01

5.1.1 Phase I & II tests

To verify that the control charts approach based on PCA is robust, we test two different phase I. As it is possible to see in tab. 5.2, every Test is composed by two different datasets, characterized by different input parameters. In fact, in Test 1 we have two different wheel speeds with the same infeed rate while in Test 2 there are two datasets with the same wheel speed but with a different infeed rate.

After calculating the control limits according to these two tests, the control charts are then evaluated on two other tests, which characteristics are summarized in tab. 5.3 (Test A & B).

Also these two tests are composed by two grinding operations: in both of them, the first is an operation with an in control wheel speed, while the second one has an out of control speed. In this way, with the first operation we can test if the system is robust to the variation of the input parameters while with the second one we can test if this approach is sensitive and responsive to the chatter phenomenon generation.

So, in the following sections we propose two examples with the use of the time-domain and frequency-domain synthetic indicators:

Example 1 : training on Test 1 and testing on Test A & B (subsection 5.2.2 and 5.2.3);

Example 2 : training on Test 2 and testing on Test A & B (subsection 5.3.2 and 5.3.3).

5.2 Testing the proposed approach on time-domain indicators

In this section we will show the results of control charts trained on Test 1 & 2 and tested on Test A & B for the PCA approach with time-domain synthetic indicators. Before showing the results, in the next subsection the two tests used for phase I are analyzed and compared.

5.2.1 Phase I

Phase I determines the number of principal components to be selected, and the coefficients of the A matrix; these are very important parameters that affect all the following analysis. There are many different approaches that can be used for the selection of the optimal number of components, e.g. Pareto chart, Laplace method and Kaiser's rule.

Joliffe [16] says that the most obvious criterion for choosing the number of PCs is the selection of the PCs number that explain a certain cumulative percentage of total variation of the PCs, usually between 70% and 90%. He also says that there is another approach, Kaiser's rule, which is based on the idea that the PCs with variance less than a threshold are not worth retaining. The threshold is the average value of the eigenvalues. In this work, the adopted criterion for PC retaining is the *Kaiser's rule*.

In tab. 5.4 are shown the variances for each PC. In these two tests, the eigenvalues average is always 1. It is possible to see that only the first two PCs have a variance > 1: in both cases the number of PCs chosen is 2.

Table 5.4: The variance explained for the two tests.

	Test 1	**Test 2**
	Var. Expl.	**Var. Expl.**
PC 1	1.55	1.38
PC 2	1.07	1.15
PC 3	0.98	0.96
PC 4	0.74	0.78
PC 5	0.67	0.72

In fig. 5.1 the Pareto charts are displayed. The charts shows the cumulative variance explained by the PCs. Choosing only two components means to explain only about 50% of the total variability for both tests; this is an important factor for the comparison between the tests. If we followed the Pareto rule, we would have chosen 4 PCs, which means retaining an higher

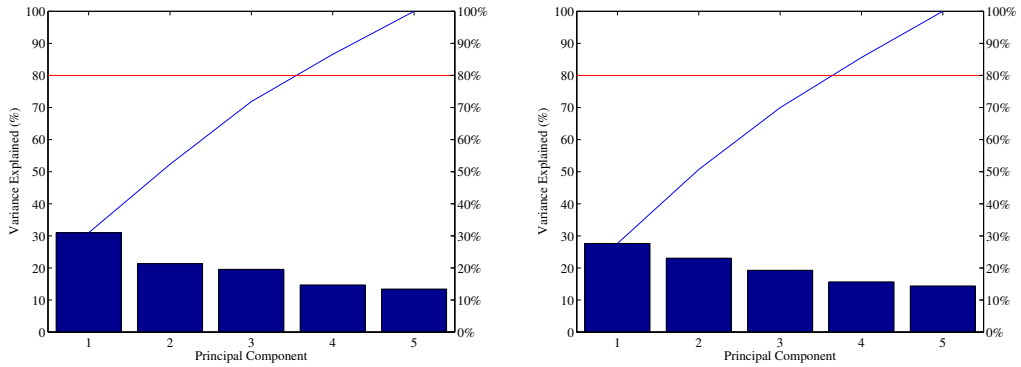

(a) Test 1 (b) Test 2

Figure 5.1: Time-domain indicators: Pareto charts of variance explained.

number of PCs that might lead to *overfit* the data. For these reasons, we use the Kaisen's rule, that retains always fewer components, remaining coherent to the previous choices.

To investigate on the meaning of the selected PCs, the barplots in fig. 5.2 are used. For every test, the two PCs seem to assume different meanings. In fact, in Test 1, the first PC averages the contribution of the five indicators. Indeed in Test 2 it is mainly influenced by the 2nd, 3th and 4th indicator ($P2P$ on headstock and tailstock accelerometers and $P2RMS$ on headstock accelerometer). The second PC of Test 1 contrasts the indicators 2 and 5 with, mainly, the first one. In Test 2, the second PC contrasts the indicators calculated on the wheel accelerometer with all the other ones.

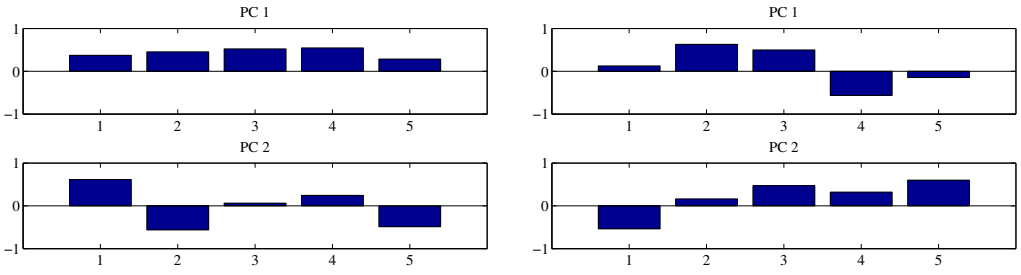

(a) Test 1 (b) Test 2

Figure 5.2: Time-domain indicators: barplots of main PCs.

After choosing the number of PCs, the control limits based on the percentile approach and the one on the moving block bootstrap approach are calculated. Tab. 5.5 shows the results in terms of false alarms percentage for Test 1 & 2. The results are divided in T^2 and Q. Then, an *overall* percent-

Table 5.5: False alarms percentage on phase I

	UCL type	T2 [%]	Q [%]	Overall [%]
Test 1	Percentile	0.57	0.57	1.14
	Moving Block Bootstrap	0.00	1.56	1.56
Test 2	Percentile	0.57	0.57	0.99
	Moving Block Bootstrap	0.00	0.43	0.43

age of false alarms is calculated, showing the number of samples identified as out of control by one or both the control charts. The overall rate of alarms indicates the performances of the charts.

Comparing the two control limits approaches, there is no evidence in assuming that one method always better performs than the other. This is due to the method used to calculate the moving block bootstrap limits. Indeed, extrapolating random samples on which calculating the limits, these will always be different, and never will be always lower or always higher than the percentile limit. For this reason, in the following examples we will report both the control limits to see how they behave varying the type of phase II dataset.

In the next two subsections we will see how the trained control charts behave with the two phase II example tests.

5.2.2 Phase II: example 1

In this first examples, we use Test 1 for training the control charts, that will be test on Test A & B.

The final output of the PCA approach is the T^2 and Q statistics, that are used to monitor the process. In fig. 5.3a and 5.3b there are the control charts for the two tests.

The control chart in fig. 5.3 (and all the other ones that will follow) is divided into three 'section': the first one is the phase I, where the Upper Control Limits are calculated; the second one is the first part of phase II (from now on, it will be called *'in control' phase II*), when a 'in control' wheel speed is used during the operation. In this section, we expect not to have alarms, because they would be false. Then, in the third section (from now on, it will be called *'out of control' phase II*), a grinding operation with an 'out of control' wheel speed is tested. In this last phase, it is easy to see that, after an initial stable phase, both T^2 and Q statistics begin to grow,

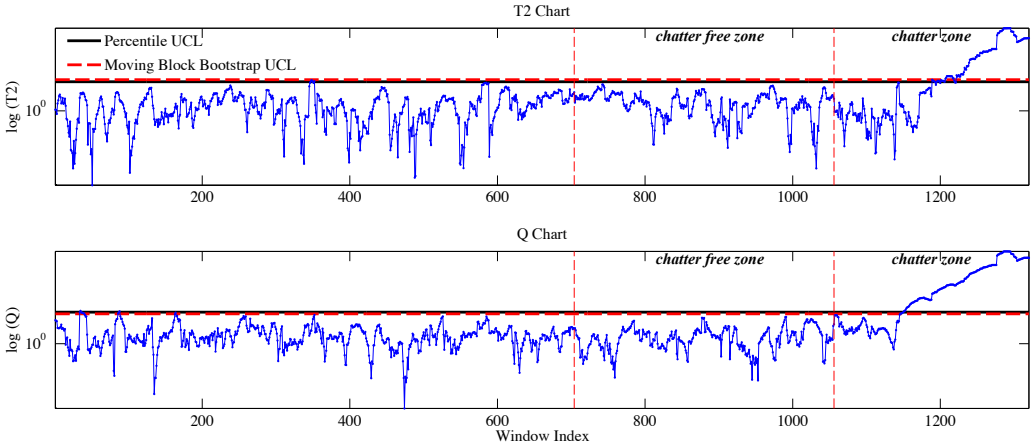

(a) Example 1-A.

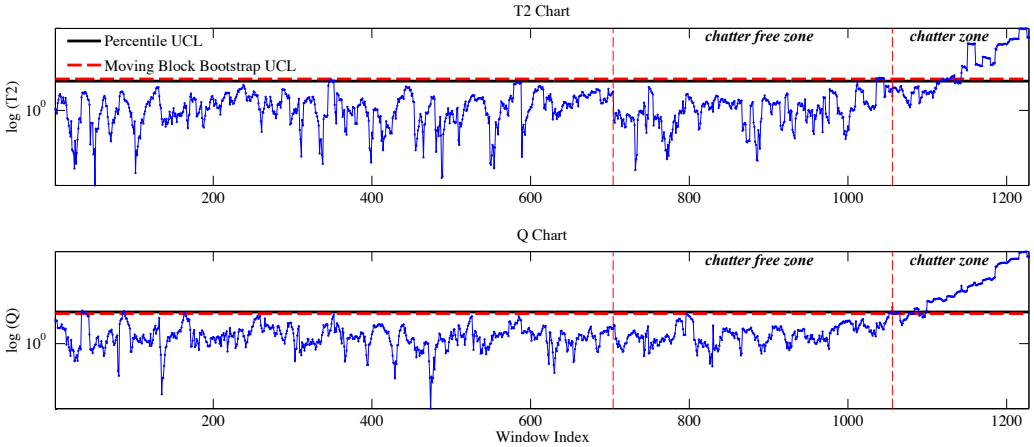

(b) Example 1-B.

Figure 5.3: Example 1: control charts.

exceeding the upper control limits, and continue to grow until the end of the test. This growth of T^2 and Q statistics is due to the chatter phenomenon, that, at the end of the test, has led to obtain waviness on the roll surface, that could be verified through the previously detailed analysis of section 4.3.

Both control charts seem to be robust to the variation of input; in fact, the chart is trained on two operations with 680 *rpm* and 830 *rpm* wheel speed, and then is tested on 830 *rpm* with another infeed rate (in the Test 1-A) and on 1000 *rpm* (in the Test 1-B). Fig. 5.3 shows that the control charts, in both the examples, don't have false alarms in the 'in control' phase II.

Moreover, both control charts seem to be sensitive to the chatter phenomenon that cause waviness on the roll (see 'out of control' phase II in fig. 5.3); if the approach would have been sensitive only to the 'bad' wheel speed,

Table 5.6: Percentage of alarms on **'in control' phase II** based on percentile and moving block bootstrap UCL.

	UCL Type	**T2** [%]	**Q** [%]	**Overall** [%]
Test 1-A	Percentile	0.00	0.00	0.00
	Moving Block Boot.	0.00	0.00	0.00
Test 1-B	Percentile	2.84	0.85	3.69
	Moving Block Boot.	2.84	1.42	4.26

the control chart had alarms since the beginning of the second part of phase II. Indeed, initially the charts do not have alarms because no chattering phenomenon has been developed yet. In fact chatter, as detailed in section 1.2, is a phenomenon that is not always evident at certain speeds. In fact, a single grinding pass at wheel speed categorized as 'out of control', it would not create waviness on the cylinder because the analyzed phenomenon takes time to develop, and only when the vibrations became significant, chatter creates waviness on the roll.

What can not be verified in this approach is the reactivity of the system as a function of the chatter creation. The grinding process is made on a high number of consecutive passes, and only at the end of the pass it was possible to verify the quality of the surface of the cylinder. On the other hand, stopping the process after each machining pass could not have lead to the waviness generation, because the vibrations would have been attenuated each time.

Tab. 5.6 summarizes the percentage of alarms for the 'in control' phase II of Test 1-A & 1-B. Test 1-A has a better performance than Test 1-B. In fact, this first test has 0% alarms while the second one appears to have a small percentage of alarms; this is lower in the percentile UCL than the moving block bootstrap UCL. Probably, the 1-B test is more affected by the high speed of the 'in control' phase II compared to the speed of phase I, and therefore is more sensitive at the parameters variation.

Tab 5.7 sums up the behavior of the same charts, when there is a test with a 'bad' wheel velocity as input. At the end of this operation, the roll surface presented waviness and both tests and both limits indicate the presence of chatter.

The first thing that is observed, analyzing the control charts, is a growing trend that starts in the second part of the Phase II. This is congruent with the chatter definition. In fact the chatter is defined as an increasing phenomenon,

Table 5.7: Percentage of alarms on **'out of control' phase II** based on percentile and moving block bootstrap UCL.

	UCL Type	**T2** [%]	**Q** [%]	**Overall** [%]
Test 1-A	Percentile	47.35	64.77	64.77
	Moving Block Boot.	42.05	66.29	66.29
Test 1-B	Percentile	60.47	80.23	80.23
	Moving Block Boot.	54.07	84.30	84.30

which develops after a certain period. The trend begins smooth but then grows faster both in Test 1-B than Test 1-A, where is visible observing the 'out of control' Phase II. The average time that the chatter phenomenon takes to grow may vary from wheel speed to wheel speed, and this is visible in the two proposed 'out of control' Phase II. The Test B takes less time to get 'out of control' compared to the results of test A.

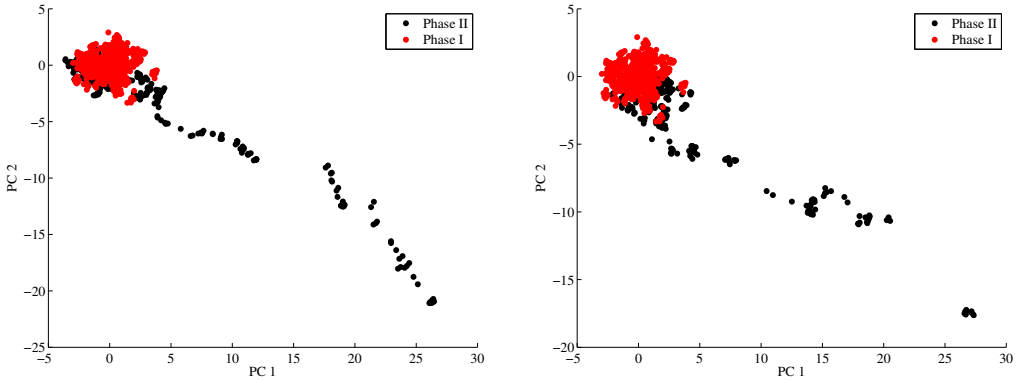

(a) Example 1-A. (b) Example 1-B.

Figure 5.4: Example 1: scatterplot of PC1 vs PC2.

In fig. 5.4 scatterplot of the PC1 vs. PC2 for each of the two tests is shown. It is easy to see that there are some values in phase II that have a completely different behavior compared to the phase I data. These data are the last values that exceed the control limit in the charts.

5.2.3 Phase II: example 2

The Example 2 is similar to the first one; compared with the previous one, only the phase I changes. In fact, in this case two operations with the same wheel speed (630 rpm) are used. This test might be more problematic than the previous one because, as we have seen, the indicators are not fully robust to the parameters variation. Training the phase I on a single speed could cause more false alarms than in the previous example in the 'in control' phase II.

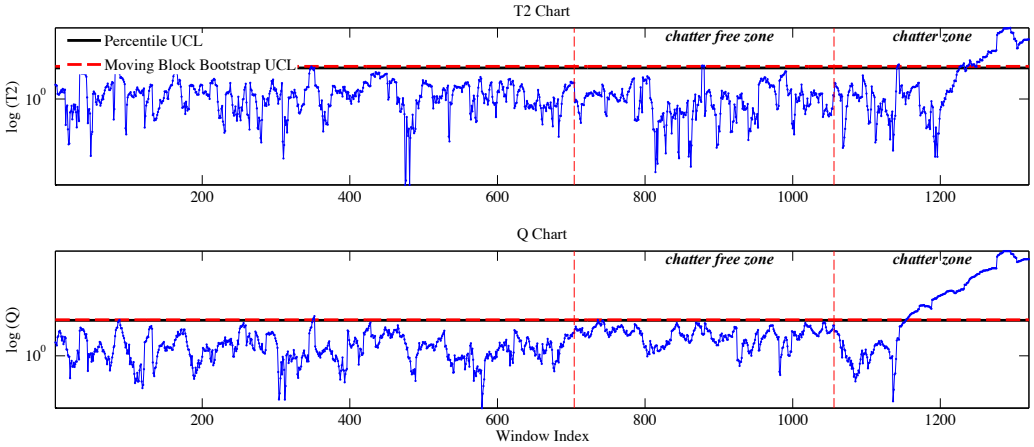

(a) Example 2-A.

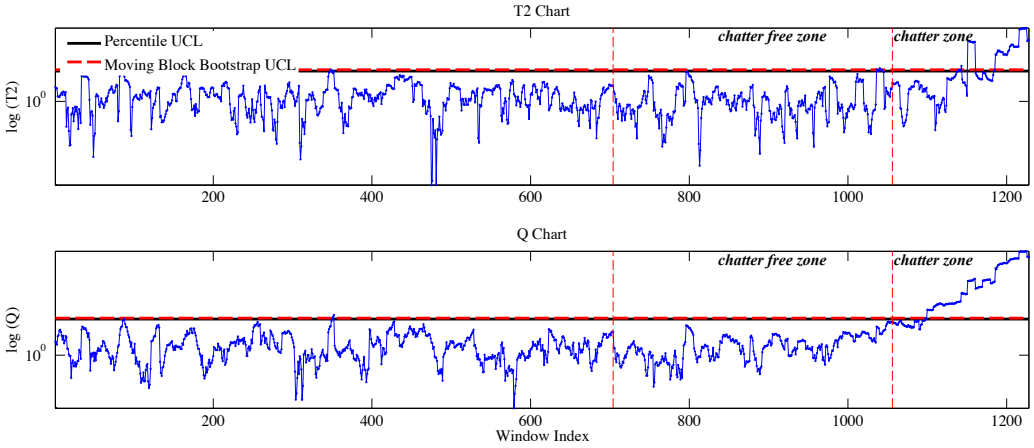

(b) Example 2-B.

Figure 5.5: Example 2: control charts.

The behavior of the two control charts, that is possible to see in fig. 5.5, appears the same as in Example 1, the opposite of what we could expect. In fact, both the charts work very well in the 'in control' phase II. The

Table 5.8: Percentage of alarms on **'in control' phase II** based on percentile and moving block bootstrap UCL.

	UCL Type	**T2** [%]	**Q** [%]	**Overall** [%]
Test 2-A	Percentile	1.14	0.28	1.42
	Moving Block Boot.	0.85	0.00	0.85
Test 2-B	Percentile	2.27	0.00	2.27
	Moving Block Boot.	0.85	0.00	0.85

Table 5.9: Percentage of alarms on **'out of control' phase II** based on percentile and moving block bootstrap UCL.

	UCL Type	**T2** [%]	**Q** [%]	**Overall** [%]
Test 2-A	Percentile	35.98	63.26	64.39
	Moving Block Boot.	34.09	63.26	64.02
Test 2-B	Percentile	34.30	75.58	75.58
	Moving Block Boot.	31.40	75.58	75.58

confirmation is given in tab. 5.8, where the percentage of false alarms are shown.

Compared to the previous case (Example 1 in subsection 5.2.2), false alarms are evenly distributed on both tests. In fact, both of them present alarms in a very low percentage. In this case, the moving block bootstrap limits seem to better perform than the percentile limits. However, it is important to remember that this is due by the random nature of the limits approach with which the moving block bootstrap one are calculated.

Observing the 'out of control' phase II, it is easy to see that even in this case, the charts seems to perform well. Test 2-A reports 65% of alarms, hoverer less than those indicated by Test 2-B (75%). Between T^2 and Q statistics, the second one appears to give a great number of alarms. This varies by the number of the few PCs which are chosen in the construction of the charts. In fact, Q statistics monitors the residuals which are the process features non included in the model.

At last, to make a total comparison, in fig. 5.6 the scatterplots of the first PCs are shown. The values of the PCs behave differently than Example 1. In fact in the first example when PC1 increases its values, also the PCs

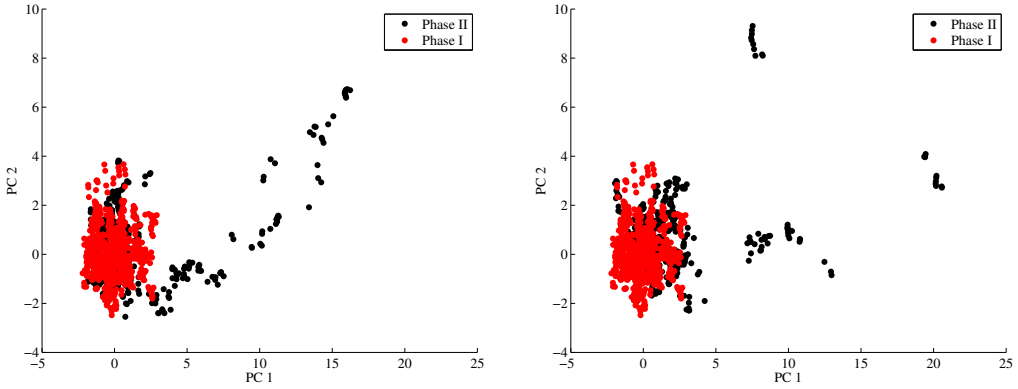

(a) Example 2-A. (b) Example 1-B.

Figure 5.6: Example 2: scatterplot of PC1 vs PC2.

does it; now we observe an opposite behavior. Moreover, there is not a linear trend, especially in Example 1-B, but the values are divided in subgroups instead of follow a trend line.

5.3 Testing the proposed approach on frequency-domain indicators

In this section we will show the results of control charts trained on Test 1& 2 and tested on Test A & B for the PCA approach with frequency-domain synthetic indicators. As in the time-domain analysis, in the next subsection the two tests used for phase I are analyzed and compared and then the results are shown.

5.3.1 Phase I

To maintain the same setting used in the previous examples, for the choice of the number of PCs, we will use Kaiser's Rule even with frequency-domain synthetic indicators. In tab. 5.10 the variances for each PC are shown.

Table 5.10: Frequency-domain indicators: Phase I. The variance explained for the two tests.

	Test 1		**Test 2**	
	Var.	**Expl.**	**Var.**	**Expl.**
PC 1	2.97		4.44	
PC 2	2.08		0.83	
PC 3	0.60		0.39	
PC 4	0.29		0.30	
PC 5	0.04		0.02	
PC 6	0.03		0.01	

The eigenvalues average, for both tests, is 1. Kaiser's rule suggest to choose 2 PCs for Test 1, and only 1 PC for Test 2. In fig. 5.7 is possible to see the percentage of explained variance, increasing the number of components. To compare the number of false and true alarms, it should be better to have a number of components that explain the same variability. For this reason, also for Test 2, we choose 2 PCs.

Fig. 5.8 shows the barplots of the first two components. The first PC of test 1 is more influenced by the last four indicators (calculated on headstock and tailstock accelerometers), that are positively weighted than the others (calculated on wheel accelerometer). In Test 2, the first PC averages the contribution of the six indicators. In both tests, PC2 is mainly influenced by the first two indicators.

To complete the analysis of phase I dataset, in tab. 5.11 the results in terms of false alarms are shown. Even in this case, the results are divided

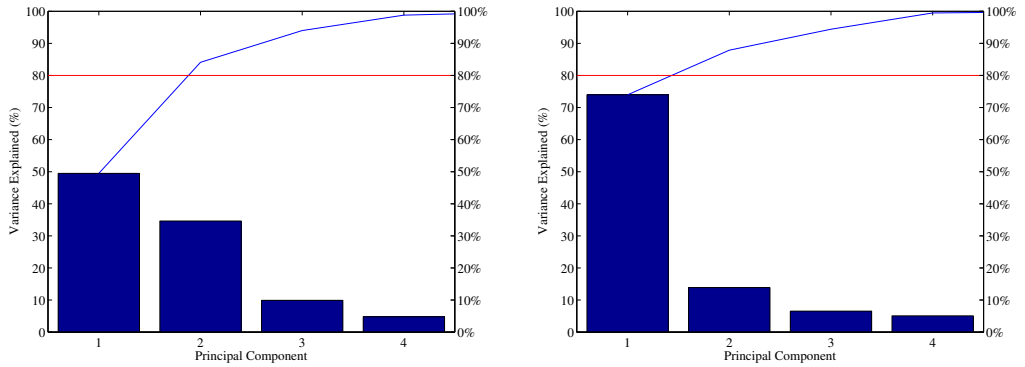

(a) Test 1 (b) Test 2

Figure 5.7: Frequency-domain indicators: Pareto charts of variance explained.

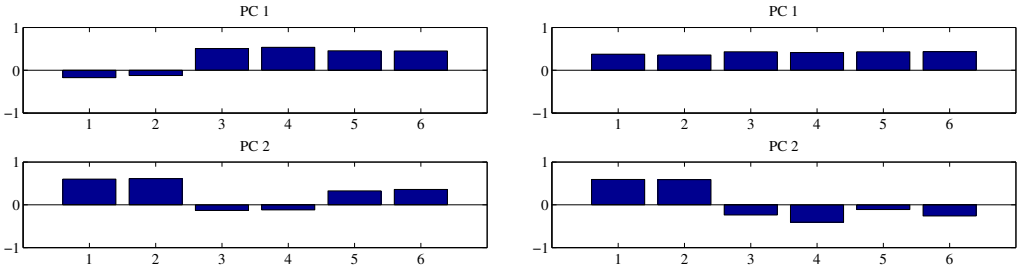

(a) Test 1 (b) Test 2

Figure 5.8: Frequency-domain indicators: barplots of main PCs.

into the two statistics T^2 and Q, and then summarized into the overall false alarms percentage.

The behavior of the two test are very similar in phase I. In fact, the false alarm rates are the same for the two test using the percentile approach to build the limits, and very similar when the limits are based on the moving block bootstrap approach. This again confirm the fact that the two limits are almost equal. Before drawing any conclusions, let's see how the control charts conduct the analysis in phase II.

5.3.2 Phase II: example 1

The same Example 1 proposed in section 5.2.2 is now repeated with the use of the PCA approach based on frequency-domain synthetic indicators. The procedure is the same: the phase I (Test 1) is used to training the charts, that are then tested on Test A & B. In fig. 5.9 the charts for these two

Table 5.11: False alarms percentage on phase I: frequency-domain indicators.

	UCL Type	T2 [%]	Q [%]	Overall [%]
Test 1	Percentile	0.57	0.57	1.14
	Moving Block Bootstrap	0.00	0.57	0.57
Test 2	Percentile	0.57	0.57	1.14
	Moving Block Bootstrap	0.00	0.14	0.14

Examples are shown.

It can be immediately seen several differences compared with the same case in time-domain. The differences are both in the 'in control' phase II and in the 'out of control' phase II.

Regarding to the 'in control' phase II, the Test 1-A doesn't have false alarms in the Q chart, but seems to have numerous false alarms in the T^2 statistics. This is confirmed by the alarms rates that are obtained, visible in tab. 5.12. The situation that exists in Test 1-B is totally reversed, but much more serious. The T^2 statistics has fewer false alarms compared to the Q statistic, but both are greater than in the Test 1-A. Indeed, globally there is a false alarms rate of 66%. These results are definitely influenced by the input parameters of the machine. Furthermore, in the 'in control' phase II of Test 1-B seems that the frequency-domain indicators assume a particular behavior that the time-domain indicators do not capture.

Indeed, looking at the 'out of control' phase II, a more rapid reactivity of the system than the same tests based on time-domain indicators is observed. This, however, is most likely caused by frequency-domain indicators, that have a higher sensitivity to the variation of the input parameters. However, even in this second part the two tests shows different results. In fact, the control charts of the Test 1-B have 100% of alarms for both statistics, in both of the UCL types (see tab. 5.13). Indeed, the control charts based on Test 1-A display less alarms in the Q chart. However, the overall alarms are very similar. This is due, at least in a part, to the sensitivity of the indicators to the wheel speed variation, as previously observed. This phenomenon with the frequency-based indicators is much stronger, but, according to the analysis of section 4.5.2, we were expecting this behavior.

In fig. 5.10 the scatterplots of the two PCs are displayed. The main trend of phase II data is the opposite than what it was observed in Example 1 with the time-domain indicators. Moreover, the dispersion of the phase I data appears to be very different. In fact, in the other case, the phase I data were

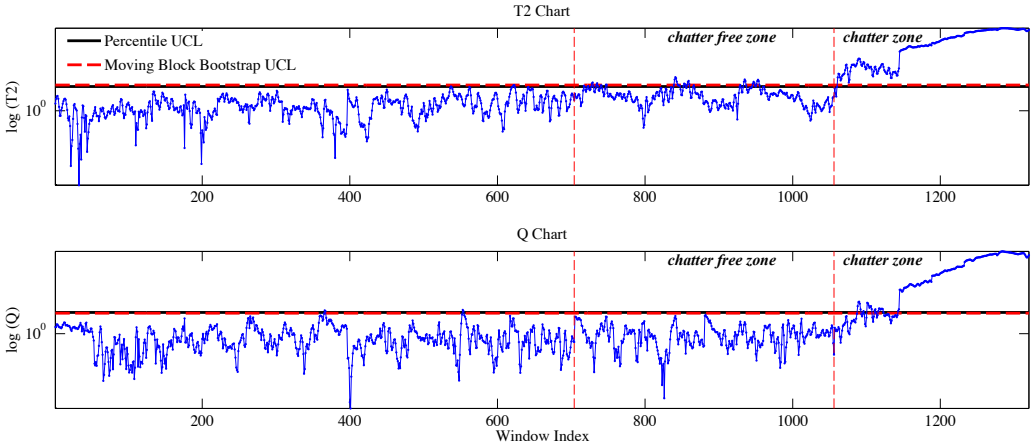

(a) Example 1-A.

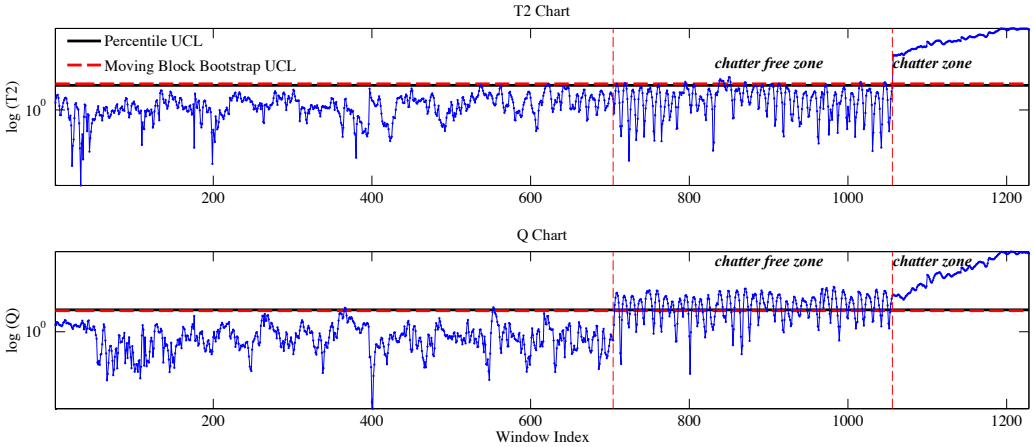

(b) Example 1-B.

Figure 5.9: Example 1: control charts.

uniformly spread around a value; in this case, two different components can be observed, a vertical and a horizontal one.

Table 5.12: Percentage of alarms on **'in control' phase II** based on percentile and moving block bootstrap UCL.

	UCL Type	**T2** [%]	**Q** [%]	**Overall** [%]
Test 1-A	Percentile	12.50	0.00	12.50
	Moving Block Boot.	8.24	0.00	8.24
Test 1-B	Percentile	10.23	65.34	65.91
	Moving Block Boot.	6.53	67.61	68.18

Table 5.13: Percentage of alarms on **'out of control' phase II** based on percentile and moving block bootstrap UCL.

	UCL Type	**T2** [%]	**Q** [%]	**Overall** [%]
Test 1-A	Percentile	98.48	76.14	98.48
	Moving Block Boot.	98.48	76.89	98.48
Test 1-B	Percentile	100.00	100.00	100.00
	Moving Block Boot.	100.00	100.00	100.00

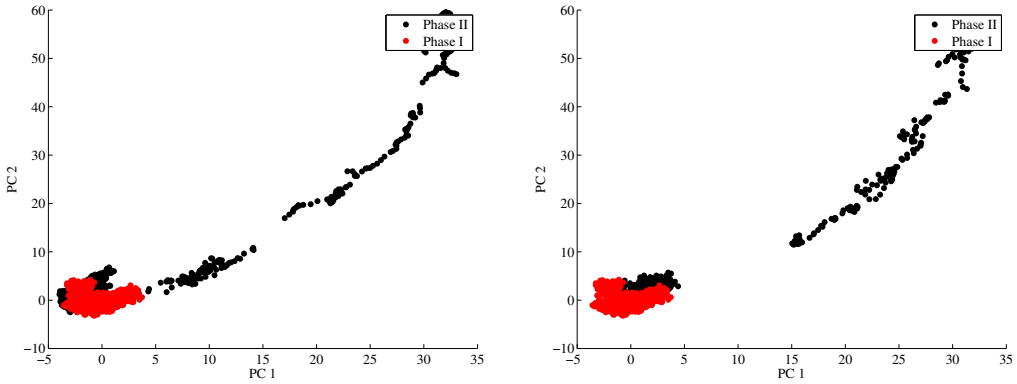

(a) Example 1-A. (b) Example 1-B.

Figure 5.10: Example 1: scatterplot of PC1 vs PC2.

5.3.3 Phase II: example 2

In the previous example, it was observed that the PCA approach with the frequency-domain synthetic indicators does not perform in a satisfactory way. Now, we expect even worse performances, because, to follow the pattern used for the time-domain indicators, the next control charts will be trained on a single wheel speed, and then they will be tested on two different velocities.

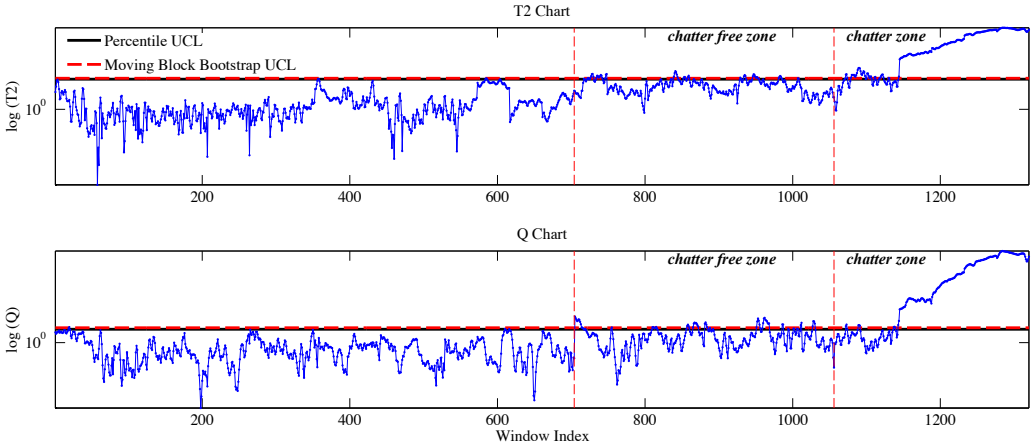

(a) Example 2-A.

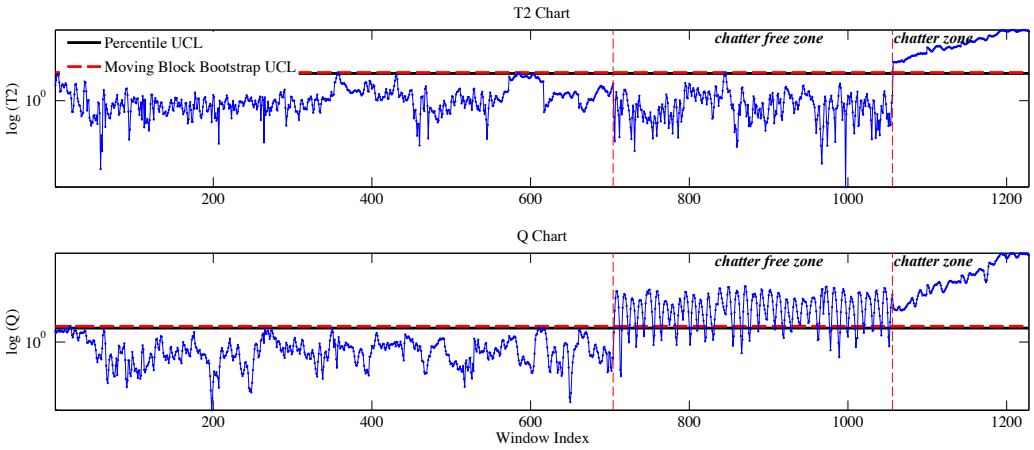

(b) Example 2-B.

Figure 5.11: Example 2: control charts.

Fig. 5.11 displays the output of these tests in terms of control charts. At first sight, the two control charts appear to behave very similar to the previous test. In fact, both systems in the 'in control' phase II have numerous alarms, which considerably increase in the 'out of control' phase II. Once again, to compare in a quantitative way what has been said, tab. 5.14 and

Table 5.14: Percentage of alarms on **'in control' phase II** based on percentile and moving block bootstrap UCL.

	UCL Type	**T2** [%]	**Q** [%]	**Overall** [%]
Test 2-A	Percentile	16.48	19.32	33.24
	Moving Block Boot.	12.22	15.06	26.14
Test 2-B	Percentile	0.28	82.95	82.95
	Moving Block Boot.	0.00	82.10	82.10

Table 5.15: Percentage of alarms on **'out of control' phase II** based on percentile and moving block bootstrap UCL.

	UCL Type	**T2** [%]	**Q** [%]	**Overall** [%]
Test 2-A	Percentile	83.33	70.45	84.85
	Moving Block Boot.	81.44	70.45	82.95
Test 2-B	Percentile	100.00	100.00	100.00
	Moving Block Boot.	100.00	100.00	100.00

5.15 summarize the percentage of alarms obtained in the first part and the second parts of phase II.

The performances of the control charts for the 'in control' phase II are much worse than the previous example. In fact, in Test 1-A there is, on average, 10% of false alarms. Now the alarms are more than doubled, reaching 30%. The same increasing trend is observed in Test B, that passes from 66% to 82% of false alarms.

Indeed, analyzing the 'out of control' phase II, it is possible to see that Test 2-A, with 83%, on average, of alarms is less sensitive than Test 1-A (98% of alarms). Test B performs equally varying the phase I test.

Fig. 5.12 shows the scatterplots for both tests. The main trend is always the same, and shows how some of the data are correlated: increasing the PC 1 values, also the PC 2 values increase. In addition, we observe a particular tendency in the 'in control' phase II, which is divided into two different components and does not appear to be uniformly distributed.

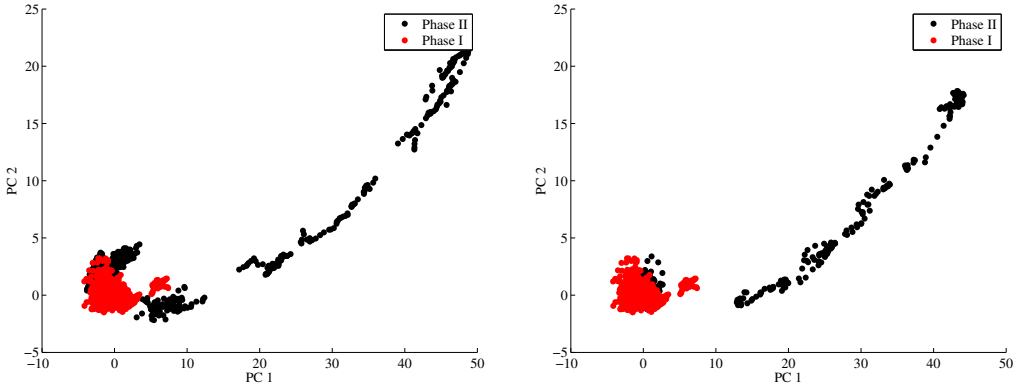

(a) Example 2-A.

(b) Example 2-B.

Figure 5.12: Example 2: scatterplot of PC1 vs PC2.

In the proposed examples of the monitoring approach, we have observed that the model, based on the fusion of time-domain indicators, is more robust than the one constructed with the frequency-domain indicators. Frequency domain indicators proved to be much more sensible both to the chatter phenomenon and to the variation of process parameters. The sensitivity to the chatter phenomenon makes them faster in recognizing process deviations, but, on the other hand, their dependency on the process parameters produces a great number of false alarms. For an industrial application we suggest then the use of a set of indicators that might not produce an excessive number of false alarms even if this mean a small delay in the process deviation detection. A further study that can be considered in future works might be an approach that is able to discriminate whether the shift of the indicators is due to the variation of the parameters or due to out of control conditions.

Chapter 6

Final Remarks

In this chapter a brief review of a further approach which could be used in the analysis of this type of data is proposed. The methodology being tested is another different development of the traditional PCA approach, which is called *Multichannel Singular Spectrum Analysis*. The MSSA is an approach useful for data where the absence of autocorrelation hypothesis is violated. In fact, the traditional PCA is based on the assumption of temporal independence of the data, although it is often applied for the time series analysis. The MSSA is the natural extension of the PCA to analyze temporally dependent data streams (i.e. autocorrelated data). For this reason we believe that it is interesting to apply it to out datasets.

The MSSA is the extension of the *Singular Spectrum Analysis* approach to the multivariate case. The SSA is an approach useful to analyze the autocorrelation in a series and the MSSA is used when there are several time series to analyze. The basic idea in SSA is simple: a principal component analysis is done with the variables analyzed being lagged versions of a single time series variable [16].

Monitoring a signal means, most of the times, analyzing time series that usually present autocorrelation phenomena and non stationary behavior. Specifically in this work synthetic indicators with overlapped windows are calculated on the raw accelerometric data, and this procedure creates further correlation in the data. The MSSA method will consider not only the covariance between the variables at the same time instant, but also the covariance in different time instances, thus it could be an appropriate tool for this kind of application.

In the next section we will briefly explain the basis of the MSSA approach; then, we will propose an example of its application on a dataset used in the previous chapter.

6.1 Theoretical framework

The idea of the SSA and then its multivariate extension MSSA is to lag the variable observed and study the space-time correlation. If we have N observations of p variables, the MSSA applies a technique similar to the principal component analysis on a matrix of $N' \times p'$ variables. This new matrix is obtained reorganizing the input data, where $N' = N - m + 1$ and $p' = mp$. We refer to m as the maximum lag introduced constructing the new input matrix.

The *k-th* row of the matrix will be:

$$X_k = [X_{k,1}, X_{k+1,1}, \ldots, X_{k+m-1,1}, X_{k,2}, X_{k+1,2}, \ldots, X_{k+m-1,2}, \ldots \\ \ldots, X_{k,p}, X_{k+1,p}, \ldots, X_{k+m-1,p}]$$

where the first $k+m-1$ columns represents the values of the first variable lagged m times; then there are the same values of the second variable and so on, until the values for the last variable P. Essentially, what is done is a vectorization and a time lagging of the input variables. Monitoring multi-channel signals, MSSA approach can be seen as an extension of the vPCA, to consider the time dependance of the monitored variables.

The variance-covariance matrix is larger then in the previous approach and assumes the form of:

$$\mathbf{S} = \begin{bmatrix} S_{1,1} & S_{1,2} & \ldots & S_{1,p'} \\ S_{2,1} & S_{2,2} & \ldots & S_{2,p'} \\ \vdots & \vdots & \ddots & \vdots \\ S_{p',1} & S_{p',2} & \ldots & S_{p',p'} \end{bmatrix}$$

where S_{kk} is a $m \times m$ variance-covariance matrix at different lag for the k-th variable and S_{kl}, with $k \neq l$ has the $(i,j)^{th}$ element equivalent to the covariance between the k-th and l-th variable at lag $|i-j|$.

For a more exhaustive description of the method, we refer to Joliffe [16] for an introduction and to [26, 30] for specific literature.

6.2 An example of the MSSA application

In this section we propose an example of the MSSA application, that could be a future development for this kind of work. We choose to show one of the examples tested for the vPCA, in particular the first one. The input working parameter are summarized in tab 6.1. This choice is made in order to compare the vPCA approach and the MSSA.

Table 6.1: Input parameters for Test 1-A.

	WH vel. $[rpm]$	**Infeed** $[mm]$
Phase I	680	0.02
	830	0.02
Phase II	830	0.01
	970	0.02

We choose to use the same time-domain indicators with the same assumptions adopted in the Example 1 shown in subsection 5.2.2.

The MSSA method is suitable for modeling multivariate time series for few variables. A common practice is to apply the MSSA only at the first PCs of the multivariate process, as said in Joliffe [16] and described by Plaut and Vautard [26].

The initial input matrix is constituted by 5 columns, each one for an indicator. Peak to peak and Peak to RMS are calculated on the head and tail stock channels, while Skewness is calculated on the wheel channel. On this matrix, the PCA approach previously used is performed. Similarly, from 5 PCs we choose only the first two. The output form this first step is composed by two series that are the linear combination of the 5 input indicators. Hence these two series will be the input for the MSSA method which is the second step of the analysis that considers time dependency.

The first thing to choose is the number m, that represent the maximum lag introduced in the construction of the matrix. In this case, we set $m = 44$. In fact 44 is the average number of points that we have for a singular pass of a grinding operation. Consider $m = 44$ means that we can analyze the autocorrelation of the indicators within the entire pass.

The variability explained by the first two PCs of the MSSA is shown in fig. 6.1a. As it is possible to see, by choosing 4 PCs we can explain 70% of variability and 6 PCs are needed to explain 80% of variability. Fig. 6.1b displays the loadings for the first 4 PCs.

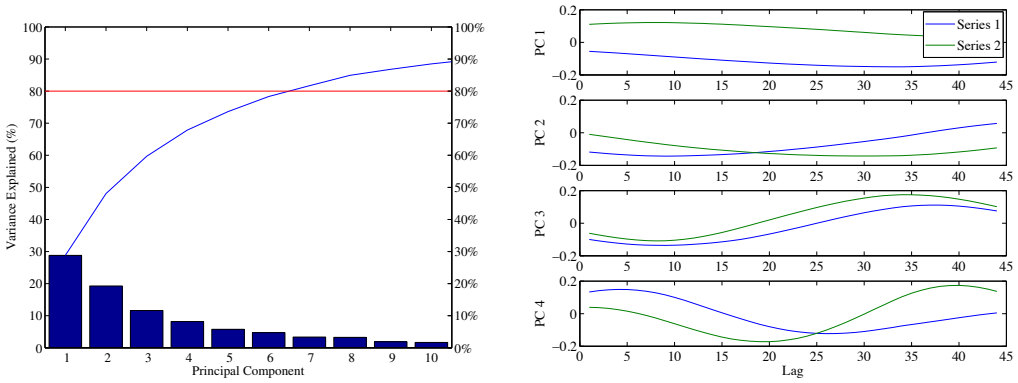

(a) Pareto Chart (b) Loadings

Figure 6.1: Time-domain indicators: Pareto charts of variance explained.

For both series, it seems that the first two PCs capture a very low frequency oscillations (almost constant), while, increasing the number of PCs, more higher frequency are considered. The 3rd and 4th PCs, however, still seem to capture long term behavior. For the next analysis, we choose 4 PCs, to be able to explain 70% of total variability.

For each input series, the MSSA calculates its reconstruction through the linear combination of the chosen PCs. In fig. 6.2 are displayed the output of the MSSa approach compared with the input series. Both series seem to capture an oscillating behavior between different passes, while filtering out the oscillating components within each pass.

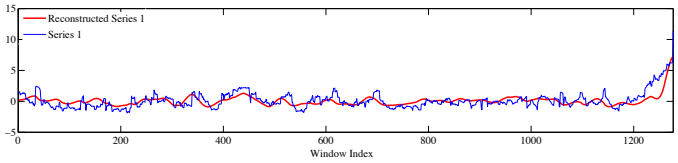

(a) Reconstructed series 1

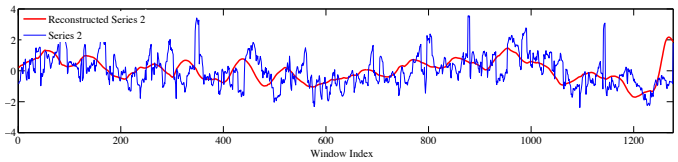

(b) Reconstructed series 2

Figure 6.2: Reconstructed series.

The T^2 and Q statistics for the Test 1-A are calculated on the first 4 PCs of the MSSA and are displayed in fig. 6.3. As we noted in the previ-

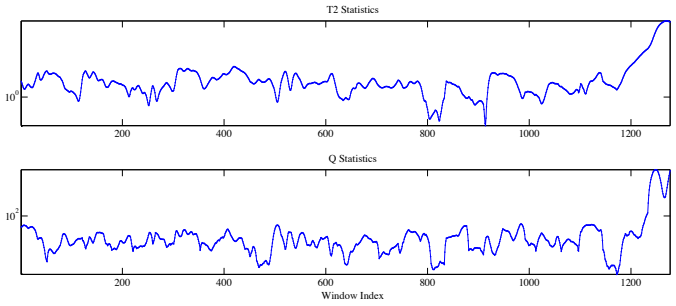

Figure 6.3: Output of the MSSA approach.

ous graph, both statistics are smoothed and cyclical compared to the initial series. In fact, by definition of the MSSA approach, the statistics are autocorrelated.The violation of the hypothesis of autocorrelation absence does not allow the application of traditional multivariate tools to monitor the characteristic. Consequently, it is necessary to use a control chart robust to this violation. An easy-to-use method that attempts to solves this problem is the EWMA (Exponentially Weighted Moving Average) control chart for autocorrelated data, as is proposed in [23].

The control chart follows this simple principle: the EWMA is the best predictor for a first order process integrated and with a moving average:

$$x_t = x_{t-1} + \varepsilon_t - \theta\varepsilon_{t-1}.$$

If we call $\lambda = 1 - \theta$, where θ is a model parameter and ε_t is a random component normally and independently distributed with mean and standard deviation σ.

The prediction based on EWMA for the $t + 1$ observation is given by:

$$\hat{x}_{t+1} = z_t = \lambda x_t + (1 - \lambda) z_{t-1}$$

The prediction error one-step-ahead will be:

$$e_t = x_t - \hat{x}_t$$

that it will be independent and identically distributed if the below model is correct.

In fig. 6.4 are displayed the control charts based on the e_t residuals of the EWMA calculated with a $\lambda = 0.2$

Due to non-normality of the e_t statistics and still presence of autocorrelation that the EWMA model has not been able to fully reduce, empirical

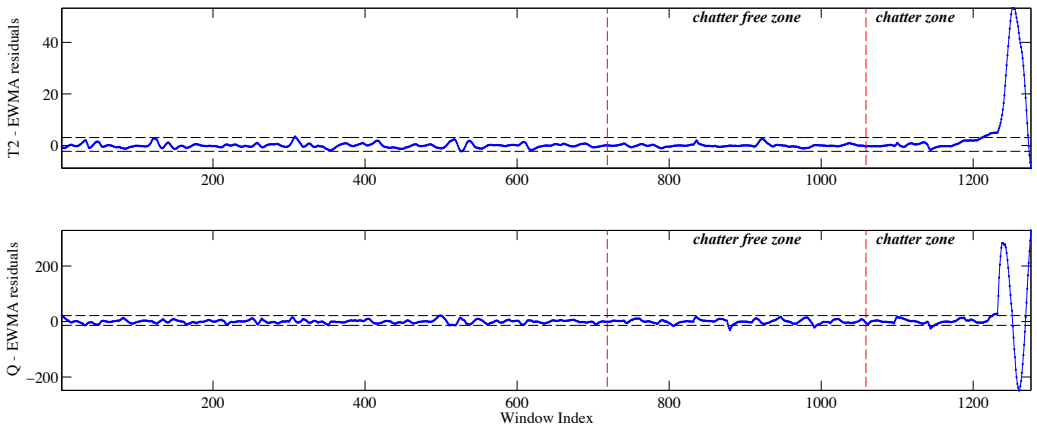

Figure 6.4: EWMA residuals charts on T^2 and Q with empirical limits.

limits have been considered to deal with these problems. Even if the charts seem to identify the development of chattering, there is still some research to do in order to conduct these analysis in accordance to the model hypothesis.

Conclusions

This work summarized the results of the development of an *in-process* quality monitoring approach for chatter identification. This study was part of a research project that involved a world-leader producer of grinding systems for rolls. The main aim of the research project was to develop an innovative software aimed at controlling the grinding process to avoid chatter occurrences, which result is a bad quality of the surface of the ground rolls.

Our assignment in this project involved the development of a methodology for monitoring process vibrations. The proposed framework consisted in designing a multivariate control chart based on an extension of the principal component analysis technique. For this purpose, a statistical approach for multi-sensor data fusion, based on the use of PCA, has been proposed. The idea of sensor fusion comes from the assumption that the sensitivity of signals that are acquired from different drives may change depending on several process factors. For this reason the integrated monitoring of multiple signals with multivariate techniques allows capturing correlation among different sources, leading to a more effective process monitoring during different operative conditions.

Along this analysis important issues have been faced with, such as the big amount of data coming from the accelerometers, the time-varying nature of grinding processes, the modification of the wheel geometry, the change of cutting conditions and other working parameters.

To deal with the high frequency rate of the signals and their noisy nature, it has been proposed to work with a set of indicators developed both in the time and frequency domain. The use of a subset of indicators has helped not only to reduce outliers in the raw data but also to capture different features of the process. However great effort has been done in finding indicators robust to the variation of process parameters but sensible to the chatter phenomenon. An experimental plan has been used to investigate the dependency of parameters, such as wheel speed and infeed rate, on the indicators responsiveness.

PCA has proved to be an appropriate methodology to investigate correlations between signals pattern on which a robust monitoring process can be

built.

Furthermore to face the time-varying nature of the grinding process, which involves the presence of autocorrelation and non-normality across the data, empirical bootstrap-based limits has been used to conduct the analysis. Further extensions of the proposed approach have been considered as future developments in order to consider the oscillating nature and time dependency of these kinds of process. Multichannel Singular Spectrum Analysis (MSSA), coupled with the Principal Component Analysis (PCA) seems to be a promising joint for a deeper and more complex analysis.

However, the developed framework has somehow reached the goal of multi-sensor data fusion for process monitoring, extracting knowledge about the working conditions of the machine and the quality and stability of the process, performing better than what could be done with a single signal.

The use of statistical methods for data fusion and multivariate control charts, adopted to monitor the process, consist in an improvement of the monitoring approach currently used, which relies on subjective analysis of process outputs and post-process inspection of the final workpiece. Presently the quality of the final product depends on the ability of the operator to perform a correct analysis of the working conditions, understanding whether the final product will meet its specifications or not. If the operator is not able to detect the presence of process abnormalities, the final product's characteristics might result out of the specification limits thus meaning the rework of the workpiece. We believe that keeping the process between control limits by monitoring its behavior can reduce wastes of time and resources. The benefits of our approach have to be found in the objective and quantitative analysis performed and the lower request of skilled supervision.

Furthermore, the innovation of this work consists in using statistical methods for the roll grinding process characterization, which don't use neither black box methods nor specific physical models that require proper training or evaluation on the single machine as proposed in the reviewed literature. The approach is not computationally intensive and the control charts for monitoring require only a set of stable working conditions to perform further analysis. For these reasons we believe that it can be easily integrated on-line in the machine control unit without great efforts. Further improvements for this framework can be represented by the adoption of new indicators that are yet more robust and specific for the grinding process. Statistical tools, such as the MSSA, may represent future developments to deal with space-time correlation of the different machine signals which can lead to even more robust analysis. An important challenge, that should be faced for an efficient industrial application, is the reduction of false alarms while keeping the same reactivity of the system to the process instability.

Appendix A

Sensitivity of indicators to chatter

In this appendix we report all the box-plots used for the preliminary analysis of synthetic indicators. The signals used for the box-plots calculations are the same for all the indicators. In fig. 4.14 and 4.15 are shown the time-domain indicators and in fig. A.3 the frequency-domain ones. A summary analysis of these box-plots is described in subsection 4.5.1.

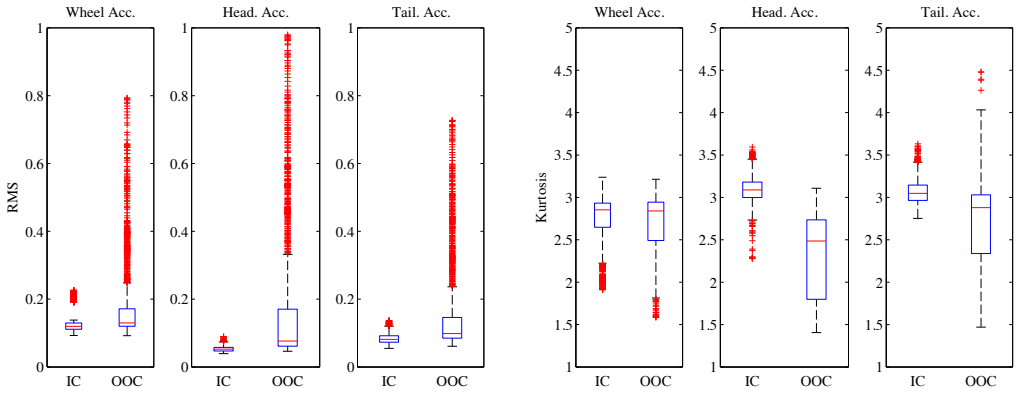

(a) RMS box-plot (b) KUR box-plot

Figure A.1: Box-plots of time-domain indicators: RMS & KUR.

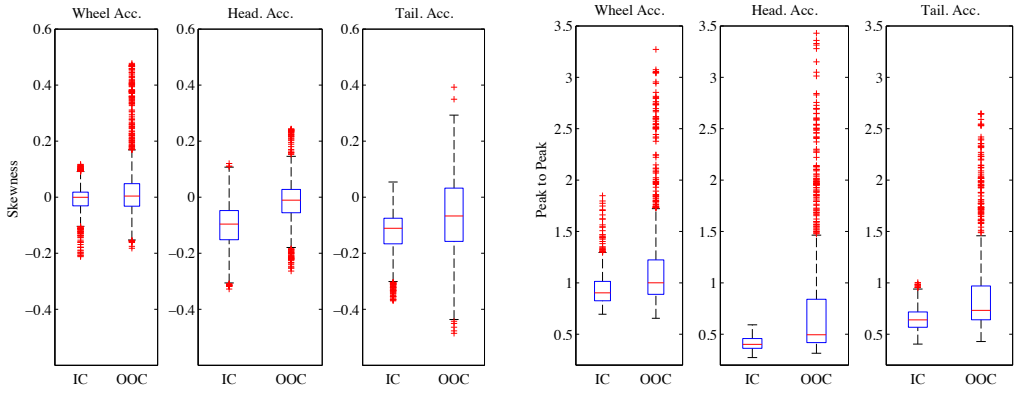

(a) SKEW box-plot

(b) P2P box-plot

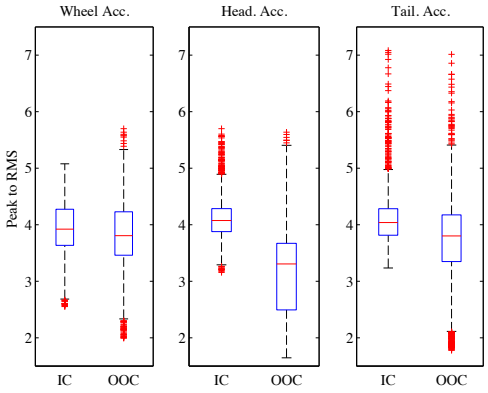

(c) P2RMS box-plot

Figure A.2: Box-plots of time-domain indicators: SKEW, P2P & P2RMS.

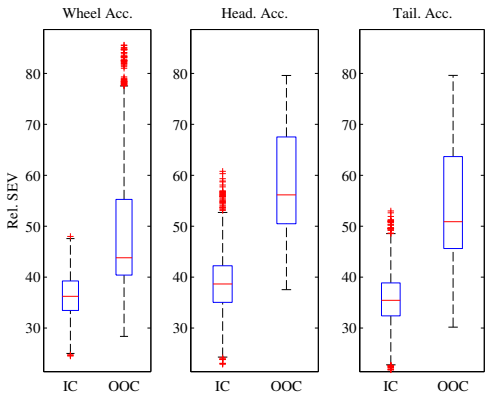

(a) Rel. SEV box-plot

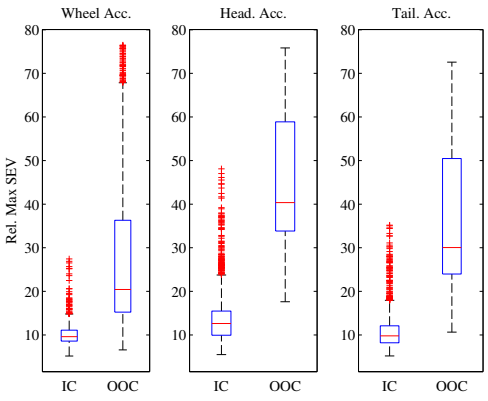

(b) Rel. Max SEV box-plot

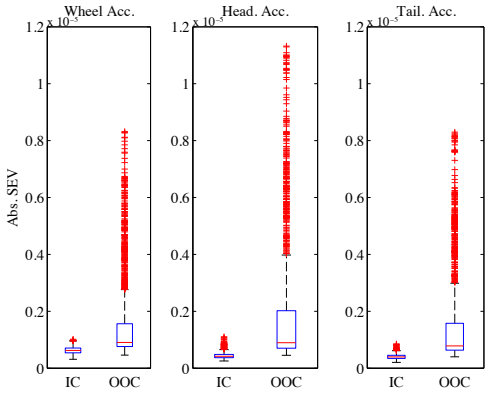

(c) Abs. SEV box-plot

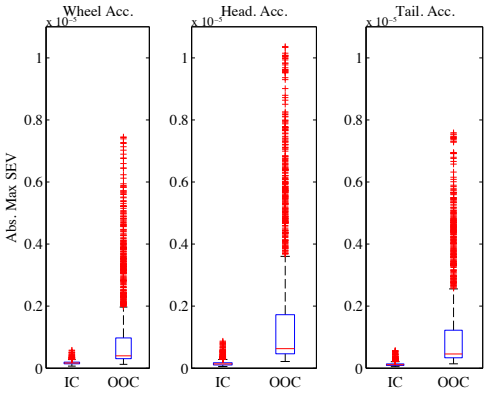

(d) Abs. Max SEV box-plot

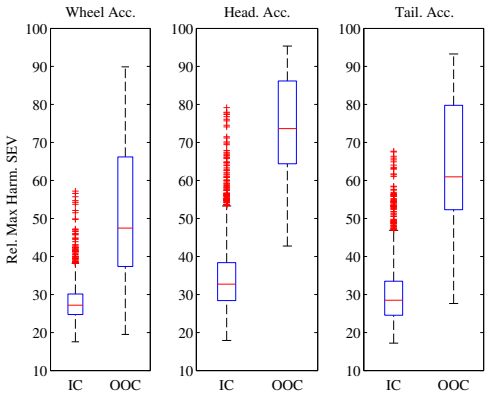

(e) Rel. Max Harm SEV box-plot

Figure A.3: Box-plots of frequency-domain indicators.

Appendix B

Sensitivity of indicators to process parameters

The main effects and individual value plots used for the preliminary analysis of indicators (see subsection 4.5.2) are reported. In fig. B.1 and B.2 are shown the time-domain indicators, in fig. B.3 and B.4 the frequency-domain ones.

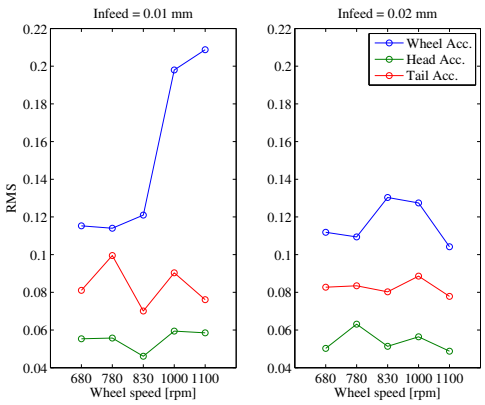

(a) RMS main effect plot

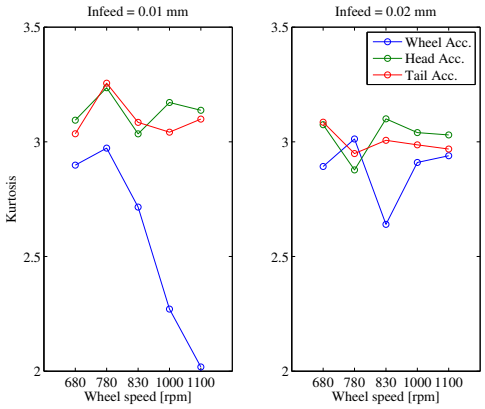

(b) KUR main effect plot

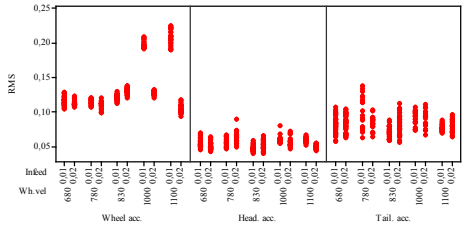

(c) RMS individual value plot

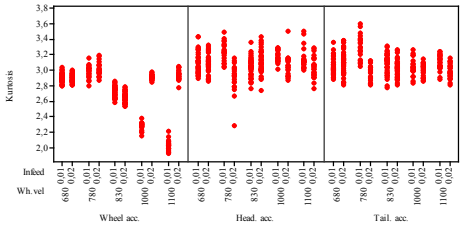

(d) KUR individual value plot

Figure B.1: Datasnooping RMS & KUR.

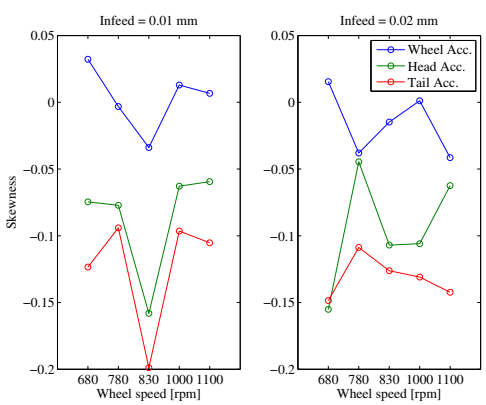

(a) SKEW main effect plot

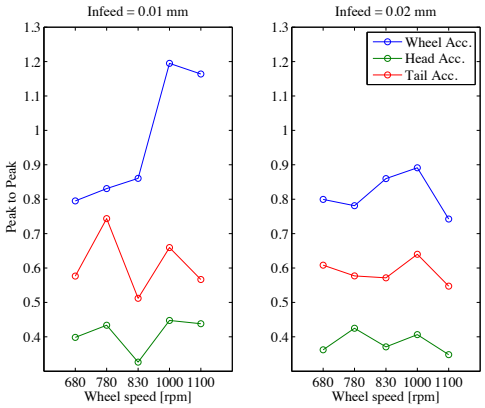

(b) P2P main effect plot

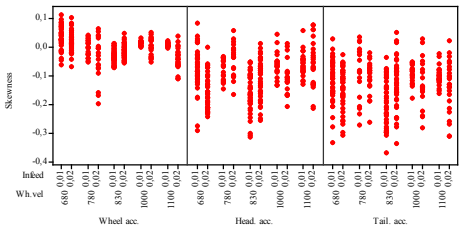

(c) SKEW individual value plot

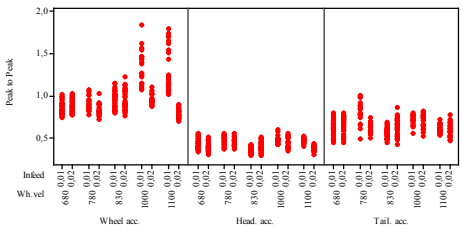

(d) P2P individual value plot

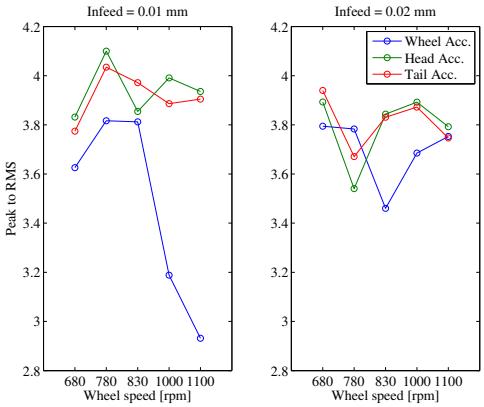

(e) P2RMS main effect plot

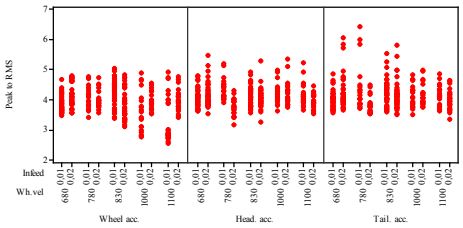

(f) P2RMS individual value plot

Figure B.2: Datasnooping SKEW, P2P & P2RMS.

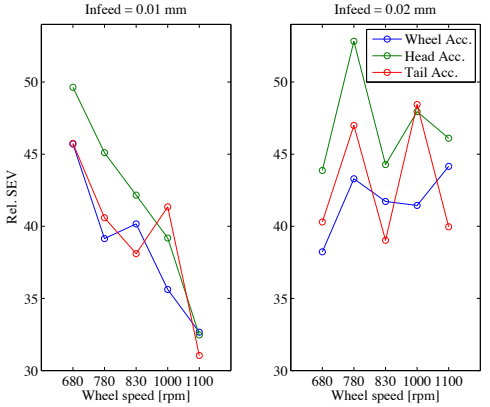

(a) Rel. SEV main effect plot

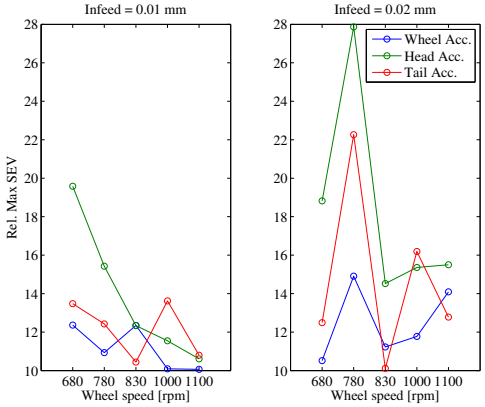

(b) Rel. Max. SEV main effect plot

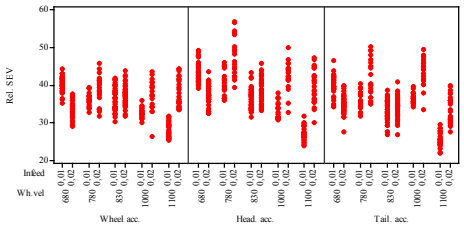

(c) Rel. SEV individual value plot

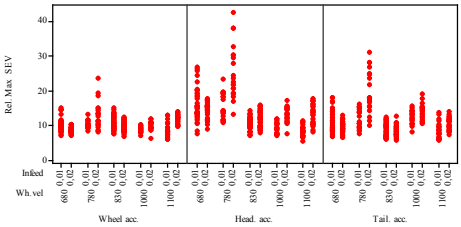

(d) Rel. Max. SEV individual value plot

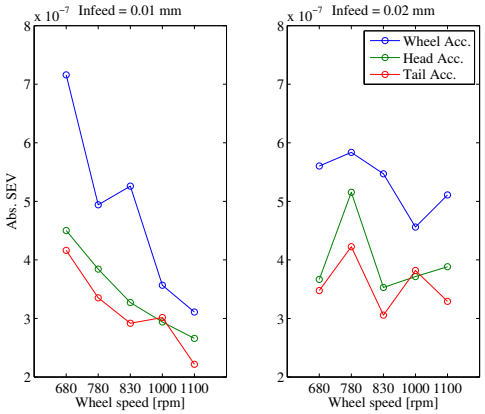

(e) Abs. SEV main effect plot

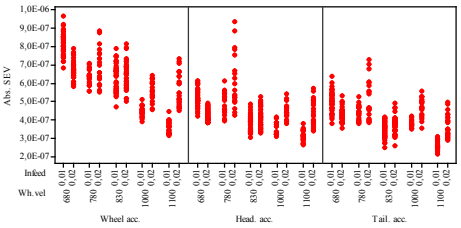

(f) Abs. SEV individual value plot

Figure B.3: Datasnooping Rel. SEV, Rel. Max. SEV & Abs. SEV.

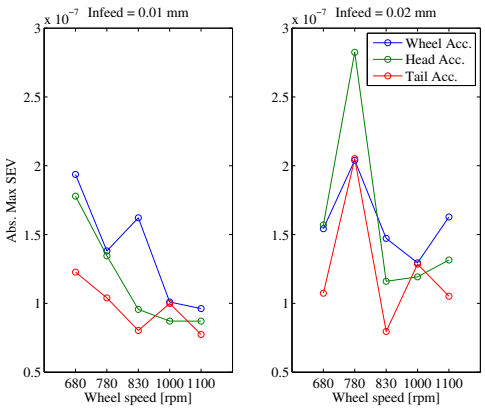

(a) Abs. max. SEV main effect plot

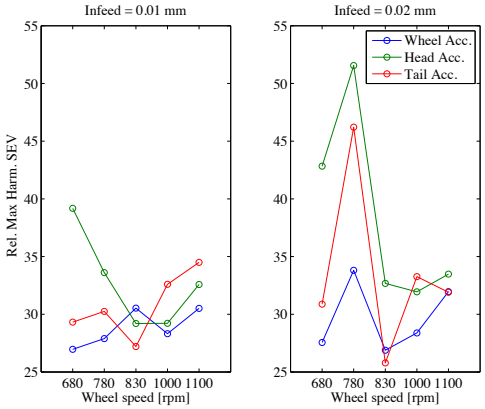

(b) Rel. max. harm. SEV main effect plot

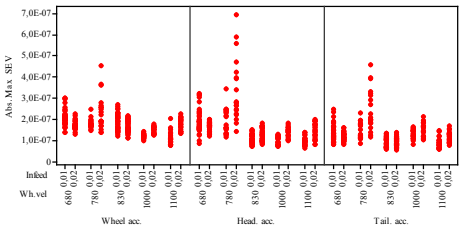

(c) Abs. max. SEV individual value plot

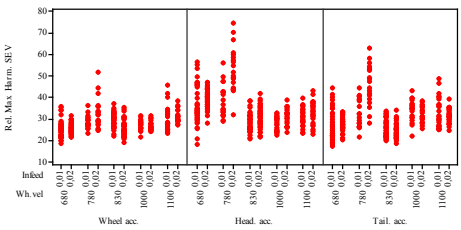

(d) Rel. max. harm. SEV individual value plot

Figure B.4: Datasnooping Abs. max. SEV & Rel. max. harm. SEV.

Bibliography

[1] P. R. Aguiar, P. J. A. Serni, F. R. L. Dotto, and E. C. Bianchi, "In-process grinding monitoring through acoustic emission," *Journal of the Brazilian Society of Mechanical Sciences and Engineering*, vol. XXVIII, no. 1, January – March 2006.

[2] Y. Altintas, *Manufacturing automation: metal cutting mechanics, machine tool vibrations, and CNC design.* Cambridge University Press, 2000.

[3] M. C. Carnero, R. Gonzalez-Palma, D. Almorza, P. Mayorga, and C. Lopez-Escobar, "Statistical quality control through overall vibration analysis," *Mechanical Systems and Signal Processing*, vol. 24, pp. 1138–1160, 2010.

[4] C. D. Caterina, "Metodi bootstrap per serie storiche," Master's thesis, Università degli Studi di Padova, 2010–2011.

[5] B. M. Colosimo and M. Pacella, "On the use of principal component analysis for identifying and monitoring geometric profiles," *Quality and Reliability Engineering International*, vol. 23, no. 6, pp. 707–725, October 2007.

[6] B. M. Colosimo, Q. Semeraro, and M. Pacella, "Statistical process control for geometric specifications: On the monitoring of roundness profiles," *Journal of Quality Technology*, vol. 40, no. 1, 2008.

[7] J. C. Fu, C. A. Troy, and K. Morit, "Chatter classification by entropy functions and. morphological processing in cylindrical traverse grinding," *Precision Engineering*, vol. 18, pp. 110–117, 1996.

[8] O. Gonzalez-Brambila, E. Rubioa, J. C. Jauregui, and G. Herrera-Ruizb, "Chattering detection in cylindrical grinding processes using the wavelet transform," *International Journal of Machine Tools and Manufacture*, vol. 46, pp. 1934–1938, 2006.

[9] J. Gradišek, A. Baus, E. Govekar, F. Klocke, and I. Grabec, "Automatic chatter detection in grinding," *International Journal of Machine Tools and Manufacture*, vol. 43, no. 14, pp. 1397–1403, 2003.

[10] M. Grasso, P. Albertelli, and B. Colosimo, "An adaptive spc approach for multi-sensor fusion and monitoring of time-varying processes," *Procedia CIRP*, vol. 12, pp. 61–66, 2013.

[11] M. Grasso, B. Colosimo, and G. Moroni, "The use of adaptive pca-based condition monitoring methods in machining processes," *Proceedings of the ASME 2012 11th Biennial Conference On Engineering Systems Design And Analysis*, vol. 4, pp. 133–140, 2012.

[12] W. Hardle, J. Horowitx, and J. Kreiss, "Bootstrap methods for time series," *International Statistical Review*, vol. 71, no. 2, pp. 435–459, 2003.

[13] I. Inasaki, "Sensor fusion for monitoring and controlling grinding processes," *The International Journal of Advanced Manufacturing Technology*, vol. 15, no. 10, pp. 730–736, 1999.

[14] I. Inasaki, B. Karpuschewski, and H.-S. Lee, "Grinding chatter – origin and suppression," *Cirp Annals-manufacturing Technology*, vol. 50, pp. 515–534, 2001.

[15] R. Johnson and D. W. Wichern, *Applied Multivariate Statistical Analysis*, 6th ed. Pearson Education, 2007.

[16] I. T. Joliffe, *Principal Component Analysis*, 2nd ed. Springer, 2002.

[17] S. Kalpakjian and S. R. Schmid, *Manufacturing Engineering and Technology*, 6th ed. Pearson - Prentice Hall, 2009.

[18] B. Karpuschewski, M. Wehmeier, and I. Inasaki, "Grinding monitoring system based on power and acoustic emission sensors," *CIRP Annals - Manufacturing Technology*, vol. 49, no. 1, pp. 235–240, 2000.

[19] B. Khaleghi, A. Khamis, F. O. Karray, and S. N. Razavi, "Multisensor data fusion: A review of the state-of-the-art," *Information Fusion*, vol. 14, pp. 28–44, 2013.

[20] E. Kuljanic, G. Totis, and M. Sortino, "Development of an intelligent multisensor chatter detection system in milling," *Mechanical Systems and Signal Processing*, pp. 1704–1718, 2009.

[21] H. R. Kunsch, "The jackknife and the bootstrap for general stationary observations," *The Annals of Statistics*, vol. 17, no. 3, pp. 1217–1241, 1989.

[22] S. N. Lahiri, "Theoretical comparison of block bootstrap methods," *The Annals of Statistics*, vol. 27, no. 1, pp. 386–404, 1999.

[23] D. C. Montgomery, *Introduction to Statistical Quality Control*, 6th ed. McGraw-Hill, 2009.

[24] P. Nomikos and J. F. Macgregor, "Multivariate spc charts for monitoring batch processes," *Technometrics*, vol. 37, no. 1, pp. 41–59, February 1995.

[25] P. Phaladiganon, S. B. Kim, V. C. P. Chen, J.-G. Baek, and S.-K. Park, "Bootstrap-based t2 multivariate control charts," *Communications in Statistics - Simulation and Computation*, vol. 40, no. 5, pp. 645–662, 2011.

[26] G. Plaut and R. Vautard, "Spells of low-frequency oscillations and weather regimes in the northern hemisphere," *Journal of the Atmospheric Sciences*, vol. 51, no. 2, pp. 210–236, 1994.

[27] B. K. N. Rao, *Handbook of Condition Monitoring*. Elsevier Science Ltd., 1996.

[28] W. B. Rowe, *Principles of Modern Grinding Technology*. William Andrew, 2009.

[29] H. Tönshoff, T. Friemuth, and J. Becker, "Process monitoring in grinding," *CIRP Annals - Manufacturing Technology*, vol. 51, no. 2, pp. 551–571, 2002.

[30] R. Vautard, P. You, and M. Ghil, "Singular-spectrum analysis: A toolkit for short, noisy chaotic signals," *Physica D*, vol. 58, pp. 95–126, 1992.

[31] Z. Yao, D. Mei, and Z. Chen, "On-line chatter detection and identification based on wavelet and support vector machine," *Journal of Materials Processing Technology*, vol. 210, pp. 713–719, 2010.